

Deep Europe today: geophysical synthesis of the upper mantle structure and lithospheric processes over 3.5 Ga

IRINA M. ARTEMIEVA^{1,2}, HANS THYBO² & MIKHAIL K. KABAN³

¹US Geological Survey, Menlo Park, CA 94025, USA (e-mail: irina@geol.ku.dk)

²Geological Institute, University of Copenhagen, Copenhagen, Denmark DK-1350

³GFZ, Potsdam, Germany D-14473

Abstract: We present a summary of geophysical models of the subcrustal lithosphere of Europe. This includes the results from seismic (reflection and refraction profiles, P- and S-wave tomography, mantle anisotropy), gravity, thermal, electromagnetic, elastic and petrological studies of the lithospheric mantle. We discuss major tectonic processes as reflected in the lithospheric structure of Europe, from Precambrian terrane accretion and subduction to Phanerozoic rifting, volcanism, subduction and continent–continent collision. The differences in the lithospheric structure of Precambrian and Phanerozoic Europe, as illustrated by a comparative analysis of different geophysical data, are shown to have both a compositional and a thermal origin. We propose an integrated model of physical properties of the European subcrustal lithosphere, with emphasis on the depth intervals around 150 and 250 km. At these depths, seismic velocity models, constrained by body- and surface-wave continent-scale tomography, are compared with mantle temperatures and mantle gravity anomalies. This comparison provides a framework for discussion of the physical or chemical origin of the major lithospheric anomalies and their relation to large-scale tectonic processes, which have formed the present lithosphere of Europe.

‘Evidence obtained under different experimental conditions cannot be comprehended within a single picture, but must be regarded as complementary in the sense that only the totality of the phenomena exhausts the possible information about the objects.’

Niels Bohr

‘One cannot embrace the non-embraceable.’

Kozma Prutkov

The European continent comprises tectonic structures ranging in age from Archaean to Cenozoic. A great variety of past and present tectonic regimes within the European continent provides a unique opportunity to analyse the effects of processes related to plate tectonics (e.g. continent–continent or continent–ocean collisions, leading to formation of continental orogens and subduction zones) and mantle dynamics (manifesting itself in magmatism, continental rifting and formation of large sedimentary basins) on lithospheric structure.

The Precambrian part of the continent is formed by the East European craton (EEC) that crops out in the Baltic and Ukrainian shields and underlies the Archaean–early Proterozoic East European Platform (EEP) (Fig. 1). The EEP is crossed by a craton-scale system of mid–late Proterozoic rifts in its central part (Gorbatshev & Bogdanova 1993) and Palaeozoic rifts in its southern parts, perhaps of plume origin (Lobkovsky *et al.* 1996). A unique feature of the EEP is the existence of a thick (typically *c.* 2–4 km, although locally 20 km thick) sedimentary cover over most of the platform (e.g. Nalivkin 1976; Khain 1985). Rapid subsidence of the EEP in the Palaeozoic was associated with subduction during the formation of the Uralides orogen (Mitrovica *et al.* 1996). The fundamental lithospheric boundary in Europe, the Trans-European Suture Zone (TESZ), which was first discovered from geological, palaeontological and magnetic data by W. K. de Teisseyre and A. J. H. Tornquist (Teisseyre 1903; Tornquist 1908), separates the Precambrian lithosphere of the EEC from the Phanerozoic lithosphere of Western Europe. Recent seismic reflection/refraction and tomography studies show a dramatic change in all lithospheric properties across the TESZ (e.g. Zielhuis & Nolet 1994; Arlitt 1999; Sroda *et al.* 1999; Villaseñor *et al.* 2001). The Phanerozoic part of Europe includes a mosaic of tectonic structures, such as Caledonian, Hercynian (Variscan) and Uralides Palaeozoic orogens, Mesozoic rifts, areas of Cenozoic rifting and tectonomagmatic activity (the Central European Rift System), and Cenozoic collisional

orogens often associated with subducting lithospheric slabs (e.g. the Alps, the Pyrenees, the Carpathians).

The goal of this paper is to present a comparative overview of lithospheric structure of the major tectonic provinces of Europe, in an attempt to distinguish the effects of the tectonic evolution of the continent from the Archaean to the present. The results of numerous recent multi-disciplinary international projects in European Earth sciences, the largest of which are the European Geotraverse (EGT) (Blundell *et al.* 1992) and the EUROPROBE programme (Gee & Zeyen 1996; Gee & Artemieva 2001), form the basis of this paper. The extensive set of geophysical information available for Europe does not permit even simple listing of the key publications. With the goal of summarizing the present knowledge on the European lithosphere on a continent scale, we have deliberately omitted local details. The comprehensive analysis of various geophysical data accumulated by the EUROPROBE research during the past decade is presented in the subsequent papers in this book.

With rare exceptions, the lithospheric mantle is inaccessible for direct studies. Images of the upper mantle structure provided by remote geophysical sampling are non-unique, and different techniques measure variations in different properties of the mantle (e.g. density, elastic moduli and conductivity, which are related to variations in composition, structure, mineral alignment, and fluid and thermal regime). Geophysical data obtained by different methods are, to some degree, complementary, such that integrated interpretations of different data types may provide a comprehensive picture of the physical properties of the lithospheric mantle. We combine the highlights of recent achievements in different disciplines of geosciences to provide the reader with comparative and diverse information on the upper mantle structure of the major tectonic structures of the continent. Numerous recent seismological surveys of the deep European lithosphere include a set of continent-scale seismic tomography models. Comparison of these models with thermal and gravity models for Europe permits us to constrain an integrated model of the European lithospheric mantle, which reflects diversity in both its structure and composition.

Precambrian lithosphere of Europe

The oldest crust within the European continent (in the Ukrainian Shield, Stepanyuk *et al.* 1998) is *c.* 3.6 Ga old and thus is one of

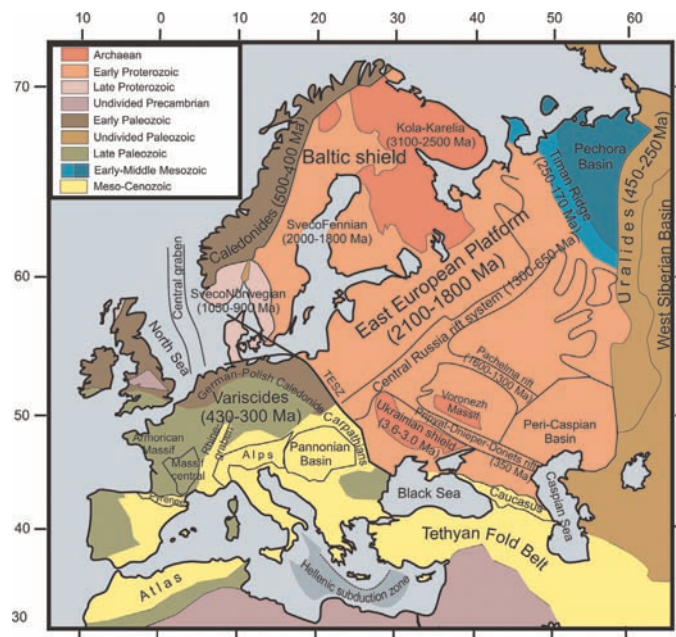


Fig. 1. Simplified tectonic map of Europe. TESZ, Trans-European Suture Zone.

the oldest known on the planet. The oldest crust of the Baltic Shield and the EEP is younger, 3.0–3.1 Ga and 1.8–2.1 Ga, respectively (Fig. 1). The basement of the EEP is buried under a thick cover of Proterozoic and Phanerozoic sediments, which complicates dating of the basement rocks. Petrological studies of mantle xenoliths from Precambrian cratons of the world suggest that the crust and the entire lithospheric mantle of the cratons were formed simultaneously and remained attached ever since (Carlson *et al.* 1994; Pearson *et al.* 1999). Therefore, one may expect that the lithospheric mantle of a large part of the continent, from the Urals in the east to the TESZ in the west, also has Archaean–Proterozoic ages. Knowledge of the ages of the subcrustal lithosphere is important for interpretations of seismic and gravity data, as petrological studies of mantle xenoliths indicate that cratonic lithosphere has a unique composition, depleted in basaltic components. The highest depletion is found globally in the Archaean roots and it decreases in Proterozoic and Phanerozoic lithosphere (Griffin *et al.* 1998). Low iron content in the Archaean lithospheric mantle has important geophysical consequences: it implies higher (by 3–5%) seismic velocities and lower (by *c.* 1.5%) density than in the Phanerozoic mantle (Jordan 1988; Poudjom Djomani *et al.* 1999, 2001; Deschamps *et al.* 2002). On the other hand, Archaean cratons have the lowest average values of surface heat flow measured on the continents (Nyblade & Pollack 1993). Low temperatures in Archaean lithospheric roots (Pollack & Chapman 1977; Artemieva & Mooney 2001) essentially compensate for the effect of the depleted composition on densities (Jordan 1988) and thus mask gravity anomalies produced by compositional variations in the mantle. However, low temperatures in cratonic lithosphere enhance the effect of depletion on seismic velocities. High mantle velocities, as observed in the EEC, are often interpreted in terms of ‘hot’ or ‘cold’ regions, but their origin can be both compositional and thermal. For example, a 1% velocity increase can be caused either by 4% Fe depletion or by 100–150 °C temperature decrease in the mantle (Nolet & Zielhuis 1994; Deschamps *et al.* 2002). We present seismic and gravity models for Precambrian Europe and compare them with thermal models to distinguish structural and compositional variations in the lithospheric mantle.

Baltic Shield

Seismic data. Most of the data on the lithospheric structure of the EEC come from the Baltic Shield, for which interpretations of seismic reflection/refraction profiles, regional upper mantle seismic tomography, electromagnetic, xenolith, thermal and elastic data became available over recent decades. This extensive dataset provides important information on the lithospheric evolution of the Baltic Shield since the Archaean and reveals the presence of a thick lithospheric keel beneath it. A 180–230 km thick lithosphere has been interpreted from explosion P-wave data along the long-range refraction FENNOLORA profile in the northern part of the Baltic Shield (Guggisberg & Berthelsen 1987). The existence of a high-velocity upper mantle down to 200–250 km beneath most of the EEC, including the Baltic Shield, is supported by regional dispersion analysis of long-period Rayleigh waves and by large-scale P- and S-wave seismic tomography models (Calcagnile 1982, 1991; Bijwaard & Spakman 2000; Shapiro & Ritzwoller 2002; Boschi *et al.* 2004) (Fig. 2). However, most surface-wave models lose resolution at depths below *c.* 200–250 km and cannot provide reliable constraints on mantle structure below this depth (e.g. Panza *et al.* 1986).

Some regional high-resolution P-wave tomography models have been interpreted as indicators of the existence of high seismic velocities (+2% anomaly compared with the global continental model *iasp91*, Kennett & Engdahl 1991) down to 250 ± 50 km under the Baltic Shield of Finland (Bock *et al.* 2001; Sandoval *et al.* 2004). The region with the thickest lithospheric keel is located at the suture between the Archaean and early Proterozoic provinces, and spatially coincides with the anomalously thick crust that has formed during Palaeoproterozoic accretion of Svecofennian terranes to the Archaean Karelian block (Korja *et al.* 1993). The small size of the region (*c.* 200 km × 300 km), where both the crust and the lithosphere have anomalous thicknesses, suggests that both crustal and lithospheric roots could have been formed during the same tectonic event and may represent a unique preserved remnant of an ancient subduction zone. This hypothesis is supported by xenolith data that indicate a compositionally stratified mantle in the region (Peltonen *et al.* 1999), and by an eastward-dipping high-velocity anomaly in the mantle beneath the Archaean–Proterozoic suture (Sandoval *et al.* 2004). The geographical distribution of mid-Proterozoic rapakivi granite intrusions at the western and southern sides of the anomalous region of thick lithosphere suggests a deflection of ascending magmas by the pre-existing lithospheric keel. This deflection of mantle heat and magma could have assisted the survival of this thick keel during the mid-Proterozoic tectonothermal activity in the region, which ‘embraces’ the anomalous region of thick lithosphere and led to the formation of the Baltic–Bothnian Sea basin.

A layer with reduced seismic velocities (*c.* 8.1 km s^{-1} for the mean model) has been identified at the depth range of 100–160 km within the high-velocity (8.6 km s^{-1} at 100 km depth) lithospheric mantle of the Baltic Shield (Perchuc & Thybo 1996). Similar seismic velocity structure has been revealed for the Archaean part of the Karelian province in a recent surface-wave based seismic tomography survey (Bruneton *et al.* 2004), similar to recent results from the Canadian Shield and Greenland (Darbyshire 2005). Tomographic inversion for velocities in the upper mantle in the Baltic Shield, based on the FENNOLORA data, suggests that the 100–160 km depth interval is also characterized by very small S-wave velocities, corresponding to a much more pronounced reduction in velocity for S waves than for P waves (Abramovitz *et al.* 2002). The nature of the reduced-velocity zone is still debated. Alternative interpretations include (1) regional metasomatism (Bruneton *et al.* 2004); (2) the presence of pockets of small-percentage melting or fluids (Perchuc & Thybo 1996), probably associated with ancient subduction zones

(although the layer may be at supersolidus temperatures; Abramovitz *et al.* 2002); (3) petrological heterogeneities in the lithosphere (e.g. a compositional boundary from a highly depleted upper lithosphere to a less depleted lower lithosphere can produce a seismic pattern similar to the top of a low-velocity zone; Artemieva 2003).

However, neither the existing seismic models nor petrographic data on mantle xenoliths (Kukkonen & Peltonen 1999) require the presence of asthenospheric material in the upper 250–300 km beneath the Archaean–early Proterozoic part of the Baltic Shield. This conclusion is supported by electromagnetic studies in the region (Korja 1990), in which no highly conductive asthenospheric layer has been identified beneath the Finnish part of the Baltic Shield. Earlier interpretations of a high-conductivity layer below 100–130 km depth (e.g. Jones 1982, 1984) should be considered with caution, as they did not account for high-latitude ($>60^\circ$) distortions of the magnetic field (Osipova *et al.* 1989).

Seismic evidence for Precambrian plate tectonics. At present, Precambrian plate tectonic processes are reliably identified only from deep mantle reflectors and associated structures in active seismic reflection surveys. Teleseismic tomography cannot resolve small velocity contrasts (e.g. $<1\%$) in the lithospheric mantle beneath Archaean and Proterozoic terranes (e.g. Poupinet *et al.* 1997; Sandoval *et al.* 2004). With the exception of the Archaean–Proterozoic suture in the Baltic Shield (as discussed in the previous section) and the Southern Baltic Sea (Abramovitz *et al.* 1997), neither the anomalous crustal structure typical for modern collisional orogens, nor a linear high-velocity seismic anomaly in the mantle (which might indicate the presence of a subducting slab) is documented for Proterozoic collisional structures. The only robust dipping high-velocity ‘slab’ anomaly in a cratonic root has been distinguished recently in P- and S-seismic tomography studies along the Western Superior Transect (Canada) down to *c.* 660 km depth (Sol *et al.* 2002). Otherwise, the oldest slab of subducted lithosphere individually recognized in the mantle from teleseismic tomographic data is Jurassic in age (van der Voo *et al.* 1999). Well-documented evidence for Precambrian plate tectonic processes was first presented by the BABEL Working Group (1989) for the Baltic Shield. Older relict (2.7–2.8 Ga) subduction has been imaged in seismic reflection studies by the Canadian LITHOPROBE programme in the Superior province (e.g. Calvert *et al.* 1995; Clowes *et al.* 1996) and in the Slave craton (Bostok 1998; Cook *et al.* 1998, 1999; Aulbach *et al.* 2001). Analogy between the observed reflection geometries and modern subduction zones allows interpretations of seismic images as ancient subduction of former oceanic crust (van der Velden & Cook 1999). Dipping mantle reflectors are of a particular importance, as they are interpreted as relict subduction zones.

Two large-scale high-resolution marine seismic reflection experiments in the Baltic Shield (BABEL in the Bothnian Gulf and ‘Mobil Search’ in the Skagerrak between Norway and Denmark) have found evidence for sets of dipping mantle reflectors, which provide new insights into Precambrian tectonic processes. Distinct, dipping sub-Moho reflections have been identified at 40–110 km depths (BABEL Working Group 1990, 1993; Lie *et al.* 1990). Dipping at a 15–35° angle, these reflections can be traced laterally over distances of up to 100 km, and in two out of three occurrences they are accompanied by a sharp 5–7 km offset of Moho. By analogy between the reflectivity patterns in the Baltic Shield and Cenozoic (e.g. the Alps and the Pyrenees) and Palaeozoic (the Caledonides and the Appalachians) orogens, these mantle reflectors are interpreted as relics of Proterozoic (0.9–1.2 Ga and 1.8–1.9 Ga) tectonic processes related to Svecofennian and Sveconorwegian plate convergence, subduction and accretion of terranes onto the Archaean nucleus of the Baltic Shield (BABEL Working Group 1990, 1993b).

This tectonic interpretation is supported by Sm–Nd isotopic data from the exposed volcanic arc complex in the Baltic Shield (Öhlander *et al.* 1993). Recent analysis of lithospheric-scale seismic data from 1.90–1.85 Ga subduction zones at the Slave and Baltic cratonic margins (Snyder 2002) reveals strong similarity between them and modern tectonic analogues.

Thermal and xenolith data. Surface heat-flow values within the Baltic Shield are close to the global average for Precambrian cratons, 30–50 mW m⁻² (Nyblade & Pollack 1993), although extremely low values (20–30 mW m⁻²) have been reported for the southern part of the Finnish–Karelian province (Balling 1995; Kukkonen & Joeleht 1996) (Fig. 3). Several thermal models for the upper mantle of the Baltic Shield indicate that variations in the surface heat flow largely result from heterogeneous heat production in the crust (Pinet & Jaupart 1987; Kukkonen 1998). Estimates of Moho temperatures vary from 350 °C to 600 °C (Balling 1995; Kukkonen & Joeleht 1996; Pasquale *et al.* 2001; Artemieva 2003); large scatter comes not only from different model constraints but also from a highly heterogeneous crustal structure, varying in thickness from *c.* 30 km in the Caledonides to *c.* 60 km at the Archaean–Proterozoic suture in southern Finland.

Thermal models suggest that in the Archaean–early Proterozoic part of the Baltic Shield the thickness of the thermal boundary layer with predominantly conductive heat transfer (thermal lithosphere) is in the range from 200 to 280 km (Pasquale *et al.* 2001; Artemieva 2003). These values are in agreement with regional seismic tomography models, in which no low-velocity layer has been found down to a 250–300 km depth (Fig. 4).

However, a direct quantitative comparison of lithospheric thickness constrained by diverse techniques is inadequate, as they measure different physical properties of the upper mantle (Artemieva & Mooney 2002). For example, the difference between ‘seismic’ lithosphere (defined as the seismic high-velocity region on the top of the mantle) and ‘thermal’ lithosphere (defined as the depth at which the geotherm intersects the mantle adiabat or becomes supersolidus) can be up to several tens of kilometres (Jaupart & Mareschal 1999); this difference approximately corresponds to the thickness of the transition zone between purely conductive and purely convective heat transfer. In tomography studies, where seismic lithosphere is considered as the layer above the convecting mantle, its base is defined either as a zone of high velocity gradient or the bottom of a layer with positive velocity anomalies. However, seismic tomography and seismic refraction models would not necessarily indicate the same depth to the base of the lithosphere. In seismic reflection surveys, strong mantle reflectors are often interpreted as the base of the seismic lithosphere, as it is assumed that they originate at the transition from the lithosphere to a zone of partial melt (Lie *et al.* 1990). Furthermore, the base of the seismic lithosphere should be a diffuse boundary if the decrease of the seismic velocities associated with the lithospheric base is caused by high-temperature relaxation or by partial melting (Anderson 1989).

Xenolith geotherms for mantle-derived peridotites from kimberlite pipes of the Finnish part of the Baltic Shield and the Arkhangelsk region confirm low mantle temperatures (Kukkonen & Peltonen 1999; Kukkonen *et al.* 2003; Malkovets *et al.* 2003) (see Fig. 6). Peridotites from Finnish xenoliths suggest that lithospheric mantle extends down to at least 240 km depth (the depth from which the deepest xenoliths originated) (Kukkonen & Peltonen 1999) as the peridotites show no variations in texture or composition that could be interpreted as indicators of the transition zone from conductive to convective heat transfer. For example, high-temperature sheared peridotites are absent even in the deepest sampled part of the lithospheric column.

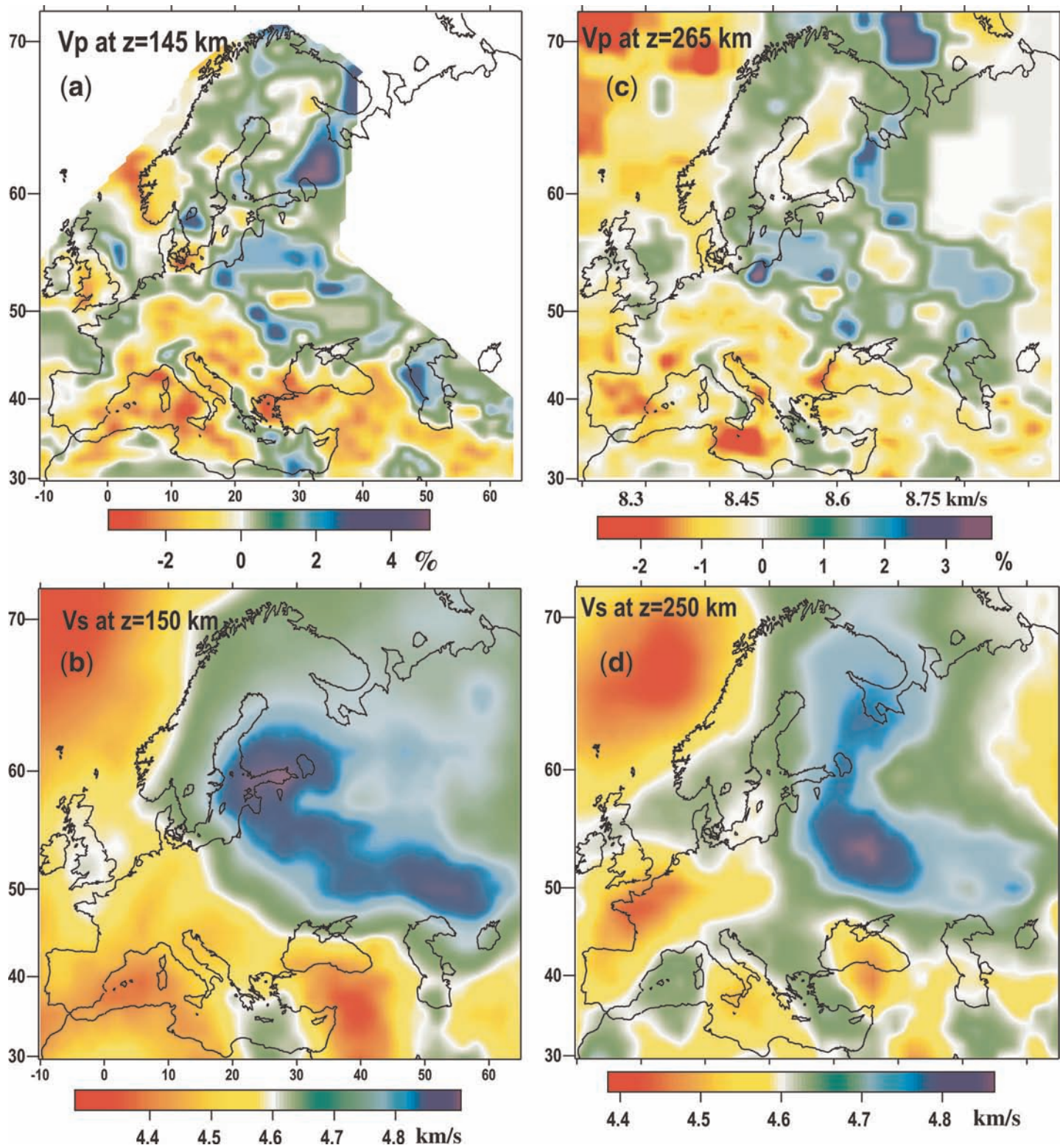


Fig. 2. Cross-section of the European lithosphere at depths of 150 km and 250 km. Most of the Precambrian part of the continent has high seismic velocities and low attenuation, at least partly caused by low mantle temperatures. In contrast, Phanerozoic Europe is characterized by low seismic velocities, high attenuation and high temperatures. (a) P-wave velocity perturbations with respect to the *ak135* model (based on the tomography model of Bijwaard & Spakman (2000), smoothed by Gaussian filtering). The lateral resolution of the model is very uneven. High resolution (*c.* 100 km) is achieved for regions with a good coverage of events and stations (Southern and Western Europe). For the EEP the lateral resolution is very low (500–1000 km) and this region is shown white. The vertical resolution of P-wave tomography models is poor, as body waves sample the entire mantle with almost vertical propagation. Most of the anomalies seen in the map propagate to deeper levels (see. (c)). (b) Rayleigh-wave phase velocities (based on the global model of Shapiro & Ritzwoller 2002). The vertical resolution is 50–100 km for the upper 250 km and coverage disappears at deeper levels; the lateral resolution does not exceed 500–1000 km. (c) As (a) for 265 km depth (based on the model of Bijwaard & Spakman 2000). The low lateral resolution for the eastern Baltic Shield and EEP, should be noted. (d) As (b) for 250 km depth (based on the global model of Shapiro & Ritzwoller 2002). The surface wave inversion loses resolution below depths of *c.* 250 km.

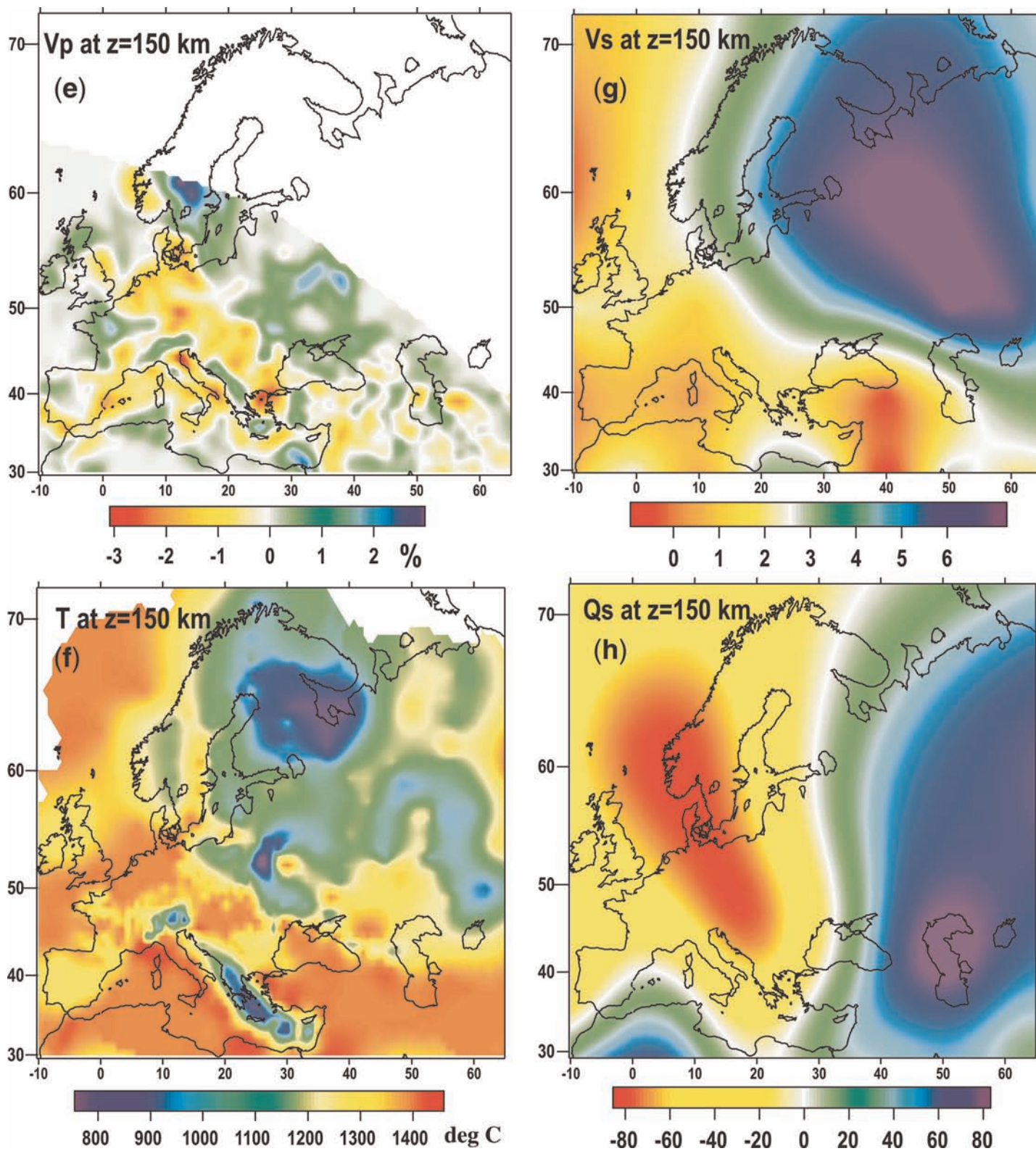


Fig. 2. *Continued.* (e) P-wave velocity perturbations with respect to the *sp6* reference model (based on the tomography model of Piromallo & Morelli (2003), defined over the equi-spaced nodes with 0.5° spacing). The model has been smoothed by Gaussian filtering. Vertical resolution is low compared with surface-wave tomography. The model resolves similar features in the upper mantle as the model of Bijwaard & Spakman (2000). (f) Mantle temperatures (in $^\circ\text{C}$) at 150 km depth (Artemieva 2003, complemented by new data for Western Europe). Temperatures for the EEC are constrained by surface heat flow for steady-state conductive heat transfer; geotherms for Western Europe are constrained by lithospheric thickness data derived from different seismic models and assuming that 1300°C is reached at the lithospheric base. The uncertainty in temperatures is *c.* 10–15%, but for western Europe can be locally larger. Lateral resolution is *c.* 50–500 km. (g) Rayleigh-wave tomography for velocity model at 150 km depth (based on the model of Billien *et al.* 2000). The model is constrained effectively to 12th-degree spherical harmonics with a vertical resolution of *c.* 50–80 km at 150 km depth. (h) Rayleigh-wave tomography for inverse attenuation at 150 km depth (based on the model of Billien *et al.* 2000). The model is constrained effectively to 12th-degree spherical harmonics with a vertical resolution of *c.* 50–80 km at 150 km depth.



Fig. 3. Surface heat flow in Europe (after Pollack *et al.* 1993, updated for new heat-flow data); a low-pass filter has been applied to remove short-wavelength anomalies caused by shallow effects (e.g. heterogeneities in crustal heat production and conductivity). Stars show locations of mantle xenoliths discussed in the text.

East European Platform

Seismic data. The lithospheric mantle of the EEP is not studied as extensively as the upper mantle of the Baltic Shield. Continent-scale seismic tomography models (Fig. 2), especially for body waves, have insufficient resolution for the northeastern parts of the EEP as there are few seismic events and the distribution of stations is sparse. Regional electromagnetic models are limited to models of crustal conductivity. With rare exceptions, seismic reflection or refraction profiles do not image the lithosphere deeper than 50–60 km (Vinnik & Ryaboy 1981; Garetskii *et al.* 1990; Grad & Tripolsky 1995; Kostyuchenko *et al.* 1999; EUROBRIDGE Working Group & EUROBRIDGE'95 2001; Grad *et al.* 2002; Thybo *et al.* 2003). Weak mantle reflectivity along the profiles, which image the lithosphere of the EEP to a significant depth, suggests either that the entire cratonic root was formed in a fast thermal event in the Precambrian, or that pre-existing reflectivity has been erased by later tectonic processes. However, the lack of significant tectonic activity in most of the EEP since the Precambrian rules out the latter hypothesis.

Recent P- and S-wave tomography of the upper mantle of the entire EEP has demonstrated that it is characterized by constant shear velocities (4.65 km s^{-1}) in the depth range 100–250 km and radial anisotropy (*c.* 5%) down to a depth of 200–250 km, where the anisotropy decreases sharply to *c.* 2% (Matzel & Grand 2004). The depth of 250 km is interpreted as a transition from dislocation deformation to diffusion creep and thus may be considered as a rheological base of the EEP lithosphere. Seismic refraction data indicate that the lithosphere of the northern EEP (along the Peaceful Nuclear Explosion (PNE) profile Quartz) is *c.* 200 km thick (Mechie *et al.* 1993; Ryberg *et al.* 1996); the base of the lithosphere is likely to have a transitional character as no sharp velocity contrast was found at the inferred lithospheric base. Waveform inversion for the upper mantle

structure in the western part of the EEP along the 30°E meridian revealed similar values of lithospheric thickness, *c.* 200 km (Paulssen *et al.* 1999). These estimates of the seismic base of the lithosphere are, on the whole, in agreement with thermal estimates of the lithospheric thickness of the EEP, *c.* 170–200 km with small regional variations within the accuracy of the model (Artemieva 2003; Fig. 4c).

Similar to the Baltic Shield, a pronounced reduced-velocity channel at a depth of 105–130 km has been identified within the lithospheric mantle of the northeastern EEP along the PNE profile Quartz (Ryberg *et al.* 1996). According to travel-time inversion of seismic data along the PNE profiles Quartz and Kraton, this feature extends eastwards as a continuous layer for at least 3000 km into the West Siberian Basin and the Siberian Shield (Nielsen *et al.* 1999). Similar reduced-velocity layers have been reported earlier for other cratonic regions of the world (Grand & Helmberger 1984; LeFevre & Helmberger 1989; Pavlenkova *et al.* 1996; Darbyshire 2005) and suggest that it may be a global characteristic of Precambrian lithosphere (Thybo & Perchuc 1997; Thybo 2006). The proposed models for such a layer, with a relatively low seismic velocity within high-velocity cratonic root, include the presence of fluids, partial melts (or temperature close to the solidus), metasomatism, or compositional variations. For example, in North America, a low-velocity zone was found in an S-wave model but was not observed in a P-wave model, which suggests that it is an indicator of a partially molten zone (Rodgers & Bhattacharyya 2001).

Thermal data. The EEP is characterized by relatively homogeneous values of the surface heat flow ($35\text{--}45 \text{ mW m}^{-2}$, Fig. 3), that are within the range of the global average for the Archaean–early Proterozoic cratons of the world (Nyblade & Pollack 1993). Slightly higher values ($40\text{--}55 \text{ mW m}^{-2}$) have been measured in the southern parts of the platform although, locally, thermal anomalies can reach values as high as $70\text{--}90 \text{ mW m}^{-2}$ (i.e. in the Pripyat Trough). The transition to the Phanerozoic lithosphere of Western Europe is marked by a sharp step-like increase in surface heat flow by *c.* 20 mW m^{-2} (Fig. 3).

The thickness of the thermal lithosphere within the EEP has been estimated to be 170–200 km (Cermak 1982; Artemieva 2003; Majorowicz *et al.* 2003) (Fig. 4c). Surprisingly, the Ukrainian Shield, which is the oldest part of the European continent, has similar lithospheric thickness, 180–220 km (Kutas 1979). Such values have also been reported for the Archaean lithosphere of South Africa and Australia (Jaupart & Mareschal 1999; Artemieva & Mooney 2001). These cratons are among the oldest on the Earth: the major crust-forming events in the Kaapvaal, Zimbabwe, Indian and Pilbara cratons and the Greenland Shield occurred at *c.* 3.0–3.5 Ga, whereas in the East European, Siberian and North American cratons the major crust-forming events occurred significantly later, *c.* 1.8–2.5 Ga (Goodwin 1996). The large difference in lithospheric thickness of Precambrian regions, which were assembled into cratons at different times (Artemieva 2006), poses the question of whether different tectonic and/or mantle processes have operated in the early and late Archaean and led to the formation of cratons with significantly different lithospheric structures (Artemieva & Mooney 2002; Artemieva *et al.* 2002). As Re–Os isotope studies indicate similar geological ages (i.e. approximately the ages of crustal differentiation; Richardson *et al.* 1993) for all of the Archaean cratons, it is likely that anomalously thick lithospheric roots could have formed by different intensities of tectonic modification of pre-existing terranes during the cratonization stage and not as a result of different differentiation processes within the deep mantle.

Precambrian rifts within the EEP. Mantle processes have played an important role in the evolution of the continental lithosphere since

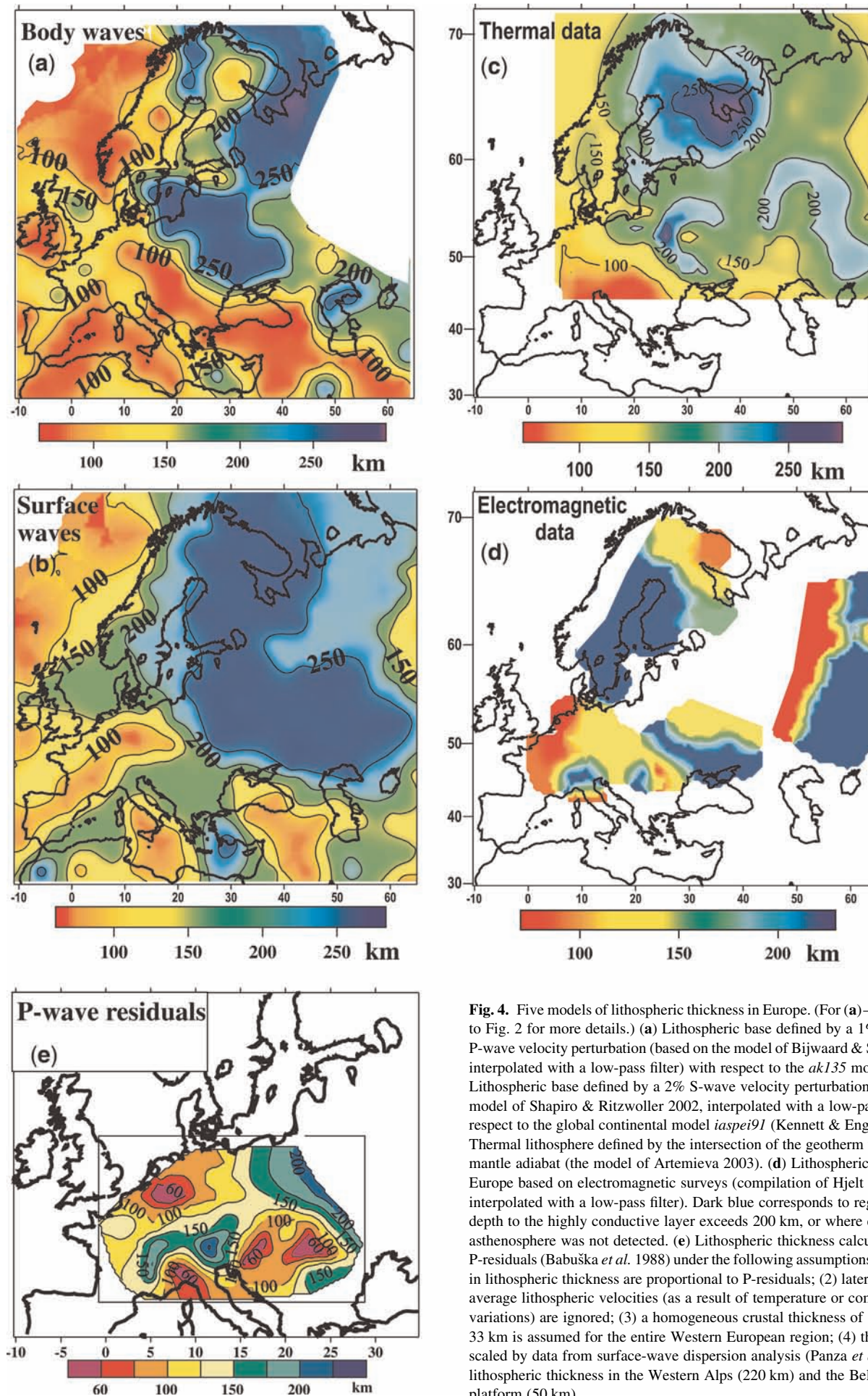


Fig. 4. Five models of lithospheric thickness in Europe. (For (a)–(c) see caption to Fig. 2 for more details.) (a) Lithospheric base defined by a 1% P-wave velocity perturbation (based on the model of Bijwaard & Spakman 2000, interpolated with a low-pass filter) with respect to the *ak135* model. (b) Lithospheric base defined by a 2% S-wave velocity perturbation (based on the model of Shapiro & Ritzwoller 2002, interpolated with a low-pass filter) with respect to the global continental model *iaspei91* (Kennett & Engdahl 1991). (c) Thermal lithosphere defined by the intersection of the geotherm with a 1300 °C mantle adiabat (the model of Artemieva 2003). (d) Lithospheric thickness in Europe based on electromagnetic surveys (compilation of Hjelt & Korja 1993, interpolated with a low-pass filter). Dark blue corresponds to regions where depth to the highly conductive layer exceeds 200 km, or where electrical asthenosphere was not detected. (e) Lithospheric thickness calculated from P-residuals (Babuška *et al.* 1988) under the following assumptions: (1) variations in lithospheric thickness are proportional to P-residuals; (2) lateral variations in average lithospheric velocities (as a result of temperature or compositional variations) are ignored; (3) a homogeneous crustal thickness of 33 km is assumed for the entire Western European region; (4) the results are scaled by data from surface-wave dispersion analysis (Panza *et al.* 1986) on lithospheric thickness in the Western Alps (220 km) and the Belgo-Dutch platform (50 km).

its formation. Giant mafic dyke swarms (the oldest known, in SW Greenland, is *c.* 3.25 Ga old), continental rifting (the oldest known, in the Kaapvaal and Slave cratons, is *c.* 3.0–3.3 Ga old), and break-up of supercontinents (the oldest known is *c.* 2.5–2.7 Ga old) are believed to be surface manifestations of ancient plume–lithosphere interactions (Nelson 1992). The ages of the known large-scale mantle–lithosphere interaction events within the EEC are much younger than in other cratons (Khain 1985). In the Baltic Shield, the Riphean (1.35–1.05 Ga) rifting affected the Baltic Sea region with the emplacement of rapakivi granites and a subsequent subsidence of the basin (Gaál & Gorbatshev 1987). Within the EEP, the fundamental trans-cratonic Central Russia Rift System (CRRS) formed at *c.* 1.3–1.0 Ga either by a large-scale rifting event or by amalgamation of three large terranes into the EEC (Gorbatshev & Bogdanova 1993) (Fig. 1). This process was followed by intensive intraplate volcanism at *c.* 1.0 Ga–650 Ma (Nikishin *et al.* 1996). However, there is otherwise little evidence for Precambrian rifting in the present-day structure of the deep lithosphere of the EEC, although this may be due to the sparse high-resolution geophysical data coverage of the upper mantle in this region (Figs 2–4); much of the knowledge comes from geological data. Nevertheless, joint interpretations of different geophysical datasets indicate significant compositional variations in the lithospheric mantle of the EEP, which may be related to Precambrian (as well as Phanerozoic) tectonomagmatic activity (see discussion below).

Gravity data. Density inhomogeneities in the upper mantle, related to variations in temperature and mineral composition, can provide significant driving forces of both vertical and horizontal motions of lithospheric blocks. As the gravity field contains effects of all density heterogeneities of the Earth, it is necessary to subtract all signals that do not originate from the mantle to extract the mantle component of the gravity field. These signals include the gravity effect of the crust, which is the largest, but can be approximated from independent *a priori* data. The resulting residual gravity anomalies reflect density anomalies in the mantle within the accuracy of the crustal model.

Although attempts to calculate mantle gravity anomalies were made since the first seismic sections became available, a reliable 3D gravity model of the lithosphere of most of Europe (Artemjev *et al.* 1993, 1994) could not be constructed until sufficient data on the crustal structure had been accumulated. The new model of mantle residual Bouguer gravity anomalies, based on updated data on the crustal structure of Europe (Fig. 5), shows a sharp change in the sign of anomalies across the TESZ, from positive values over the EEC to negative values over Western Europe. A strong positive anomaly over the Caucasus implies the presence of a subducting slab, which, so far, has not been resolved in tomographic models (Fig. 2). Near-zero values of mantle gravity anomalies over the Baltic Shield are in agreement with the isopycnic hypothesis (Jordan 1988) and suggest that low lithospheric densities caused by Fe depletion of the cratonic keel are well compensated by low mantle temperatures. The positive anomalies of the EEP suggest that compositional density anomalies in the lithospheric mantle of the EEP are not compensated by temperatures as a result of either a more fertile composition or very low mantle temperatures (Fig. 6). However, a strong positive anomaly in the southern part of the EEP, which has been affected by Palaeozoic rifting, rules out a temperature origin of the gravity anomaly. Spatial correlation of the strongest positive residual gravity anomaly with the position of the Central Russia Rift System (Fig. 5) also suggests a compositional rather than a thermal origin of the anomaly. Furthermore, this conclusion is supported by high average crustal velocities in the CRRS (Fig. 7), which may be caused by magmatic underplating; it implies that infiltration of basaltic magmas into the lithosphere played an important role in the tectonic evolution of the CRRS.

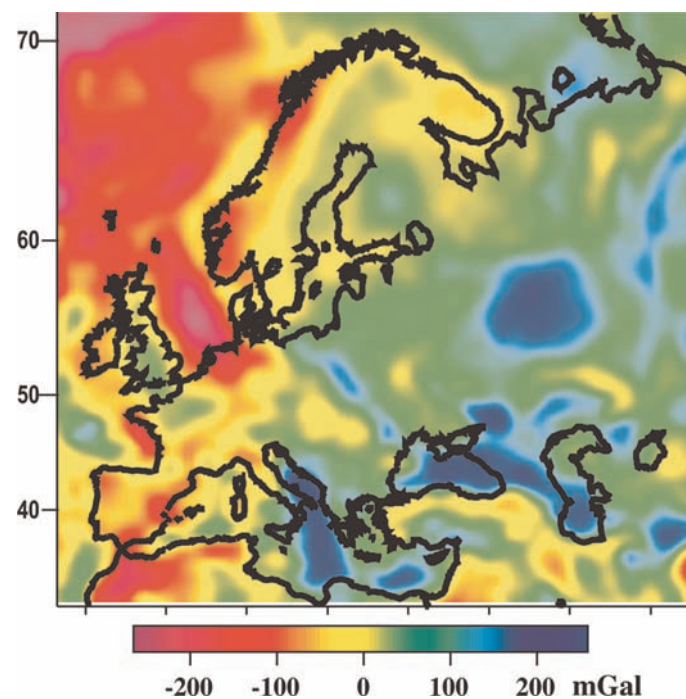


Fig. 5. Mantle residual gravity anomalies, which are a part of a 3D global model (Kaban *et al.* 1999, 2003; Kaban & Schwintzer 2001), supplemented by higher-resolution regional data (Kaban 2001). The anomalies reflect density variations produced by compositional or temperature variations, presumably in the upper 40–60 km of the subcrustal lithosphere. The model is calculated by subtracting: (1) the anomalous gravity field of the sedimentary cover and water; (2) the anomalies related to the Moho depth variations; (3) density variations within the crystalline crust from the observed gravity field (Bouguer anomalies on land and free-air anomalies offshore). The results depend critically on seismic data on the crustal structure, because during calculations seismic velocities are converted to densities. The predictions of the present model are higher by *c.* 50 mGal than residual gravity anomalies for the European continent based on older data on the crustal structure (Yegorova & Starostenko 2002), although the general pattern of the anomalies remains similar. Density excess in the mantle is typical for Precambrian terranes and regions of Phanerozoic subduction. Density deficit in the Phanerozoic mantle may be caused by high temperatures and partial melt.

Contrast in lithospheric properties across the Trans-European Suture Zone (TESZ)

The TESZ is a fundamental tectonic boundary within the European continent. It is formed by a broad complex zone of Palaeozoic terranes accreted to the southwestern margin of the East European Craton and marks the transition from the Precambrian cratonic lithosphere to the Neoproterozoic–Palaeozoic lithosphere of Western and Central Europe. The deep structure of the TESZ is characterized by a sharp change in lithospheric properties, well established by different geophysical methods (Thybo *et al.* 1999, 2002).

The transition from the cratonic to the Phanerozoic lithosphere is characterized by the following features.

(1) Crustal thickness changes sharply from 35–45 km in the EEP, to 40–55 km in the Teisseyre–Tornquist Zone, and to 28–32 km with a surprisingly flat Moho beneath the mosaics of Variscan and Caledonian terranes of Western and Central Europe (Guterch *et al.* 1986; Abramovitz *et al.* 1998; Grad *et al.* 2002) (Fig. 7). Furthermore, the magnetization of the crust of Central Europe is extremely weak compared with the upper and middle crust of the EEC (Banka *et al.* 2002). Thin crust with a flat Moho and a lack of seismic signature in the lithospheric mantle of the European Caledonides and Variscides suggests that a large portion of the lower crust and the lithospheric

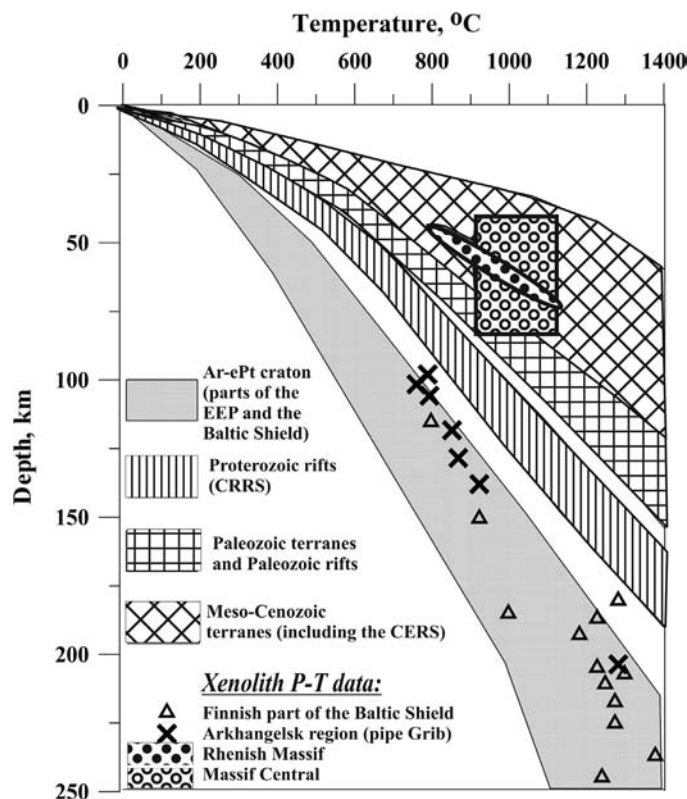


Fig. 6. Typical geotherms in different tectonic structures of Europe. For stable parts of the EEC the geotherms are constrained by surface heat-flow data assuming steady-state conductive regime (Artemieva 2003). Models of heat production distribution in the crust were constrained taking into account: (1) wavelength of surface heat-flow variations; (2) regional seismic models for the crustal velocity structure; (3) regional and global petrological models on the bounds on bulk crustal heat production (see details in Artemieva & Mooney 2001). For tectonically active regions of Western Europe, mantle temperatures are based on a nonsteady-state conductive model constrained by data on Cenozoic magmatism (Artemieva 1993) and on the conversion of regional seismic tomography models into temperatures (Sobolev *et al.* 1996). For comparison, P - T data on mantle xenoliths are shown (Coisy & Nicolas 1978; Seck & Wedepohl 1983; Nicolas *et al.* 1987; Werling & Altherr 1997; Kukkonen & Peltonen 1999; Malkovets *et al.* 2003). Ar-ePt, Archaean–Early Proterozoic.

mantle could have been delaminated as a result of the Palaeozoic orogenies (Ziegler *et al.* 2004).

(2) A pronounced and sharp decrease in seismic velocities (by 2–3%) down to the depth of 100–200 km is observed at the transition from fast cratonic lithosphere to Palaeozoic upper mantle (Zielhuis & Nolet 1994; Poupinet *et al.* 1997; Masson *et al.* 1999; Villaseñor *et al.* 2001; Cotte *et al.* 2002) (Fig. 2). This velocity contrast is caused by differences in lithospheric composition and mantle temperatures. Part of the velocity anomaly may possibly be attributed to palaeosubduction along the cratonic margin, which increased the fluid content in the upper mantle (Nolet & Zielhuis 1994).

(3) The transition zone between the lithospheric terranes of Precambrian and Palaeozoic ages dips at a steep angle to the vertical (*c.* 13–20°) in the Irish Caledonides and the Uralides, based on teleseismic studies (Masson *et al.* 1999; Poupinet *et al.* 1997). In comparison, the dip of the transition boundary across the Caledonian Deformation Front in the southern part of the Baltic Shield is shallow (*c.* 15–20° to the horizontal with a SW dip based on a seismic normal-incidence reflection profile) (MONA LISA Working Group 1997). A subhorizontal boundary between the cratonic and Phanerozoic lithospheres implies that high-velocity lower crust, or a part of the subcrustal lithosphere of

Fennoscandia, may extend far to the south (i.e. to the Elbe–Oder line), underlying Phanerozoic structures of Northern Europe (Thybo 1990; Cotte *et al.* 2002). This conclusion is supported by the results of a joint interpretation of seismic, gravity and magnetic data (Thybo 2001; Bayer *et al.* 2002) and by a likely compositional origin of the velocity anomalies observed in the TOR tomography experiment (see discussion below). A similar pattern of a non-vertical transition from Archaean to Proterozoic lithosphere has been documented by LITHOPROBE data at the margins of the Canadian Shield (Bostok 1999; Ludden & Hynes 2000).

(4) A strong subhorizontal upper mantle reflectivity has been documented beneath the Variscides and Caledonides at the depth range of 50–100 km (Masson *et al.* 1999; Abramovitz & Thybo 2000; Grad *et al.* 2002), as compared with a weak mantle reflectivity in the cratonic lithosphere of the EEC, where only one significant mantle reflector was found at *c.* 10 km below Moho (BABEL Working Group 1993; Grad *et al.* 2002).

(5) Surface heat flow changes abruptly by 20–30 mW m⁻² from cratonic to younger Europe (Fig. 3), and is accompanied by a significant rise in lithospheric temperatures (Cermak 1993; Artemieva 2003, 2006).

(6) Lithospheric thickness sharply changes from 150–200 km in the EEC to 80–120 km in Phanerozoic Europe (Figs 2, 4, 7 and 8, and Table 2) (e.g. Panza *et al.* 1986; Babuška *et al.* 1988; Zielhuis & Nolet 1994; Du *et al.* 1998; Artemieva & Mooney 2001).

(7) An abrupt change in the upper mantle density structure is reflected in a transition from near-zero or weakly positive isostatic gravity anomalies in the cratonic part to strongly negative anomalies in Western Europe (Fig. 5). Strong negative residual mantle anomalies suggest the presence of low-density masses within the upper mantle and provide indirect evidence for high mantle temperatures. Near-zero isostatic gravity anomalies in the cratonic part of the continent imply that the expected density increase caused by depleted composition of the cratonic lithosphere is entirely compensated by the density increase caused by low mantle temperatures, in agreement with the isopycnic hypothesis (Jordan 1988).

Palaeozoic structures of Europe

Palaeozoic orogens of Europe include the Uralides at the eastern margin of the EEP and the Caledonian and Variscan (Hercynian) structures in the western part of the continent (Fig. 1). The crustal structure of European Palaeozoic orogens has been studied in detail by numerous seismic profiles (including normal incidence and wide-angle reflection seismic profiles) in the North Sea (BIRPS, MONA LISA), Germany (DEKORP BASIN 96), France (ECORS), Poland (POLONAISE), Ireland (VARNET- 96), Spain (IBERSEIS, ILIHA, NARS), and in the Urals (ESRU, URSEIS). However, data on the properties of the mantle lithosphere of European Palaeozoic orogens still remain limited (Blundell *et al.* 1992) and, in the case of the Caledonides, are restricted mainly to the transitional regions from the cratonic to post-cratonic lithosphere (i.e. across the Caledonian Deformation Front) (Masson *et al.* 1999; Roberts 2003).

The Caledonides (named after Caledonia, the Latin name for Britain) and Variscides were formed during orogenic events involving a triple plate collision (Baltica, Laurentia and Avalonia) associated with the closure of the Iapetus Ocean and Tornquist Sea, and subsequent amalgamation of a series of terranes (Dewey 1969; McKerrow & Cocks 1976). Radiometric data on abundant granitoids and metamorphic rocks provide the ages of these Palaeozoic tectonic events, which included deformation, magmatism and metamorphism, as 500–400 Ma in the Caledonides and 430–300 Ma (possibly as late as 280 Ma) in the Variscan belt (e.g. Stille 1951; Emmermann 1977;

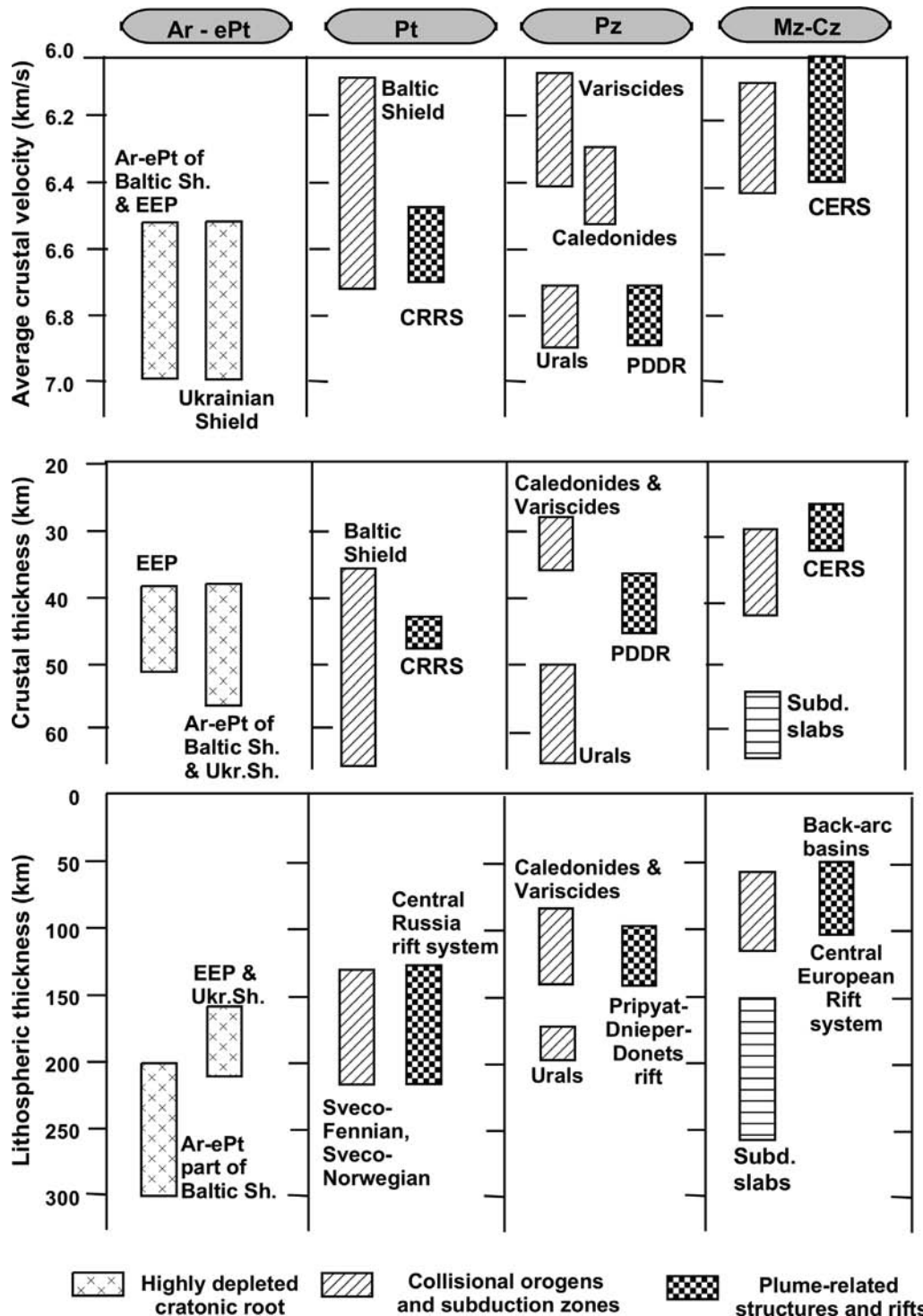


Fig. 7. Ranges of (a) average V_p seismic velocities in the crust, (b) crustal thickness, and (c) lithospheric thickness in different tectonic structures of Europe (based on Table 1). CRRS, Central Russia Rift System; CERS, Central European Rift System; PDDR, Pripjat–Dnieper–Donets rift; EEP, East European Platform. Ar-ePt, Archaean–Early proterozoic; Pt, Proterozoic; Pz, Phanerozoic; Mz-Cz, Mesozoic–Cenozoic.

Matte 1986). Opening of the North Atlantic Ocean disrupted the Caledonian orogenic belt into the European (Svalbard, Norwegian, Irish–British and Danish–Polish Caledonides) and the North American (the Appalachians and East Greenland) parts (Dewey 1969).

The Uralides orogen, a well-preserved arc–continent collision zone composed of a series of late Proterozoic–Palaeozoic fold belts formed at *c.* 400–250 Ma, following the closure of the Uralian palaeo-ocean at *c.* 470–400 Ma and the accretion of the Kazakh terrane at the eastern passive margin of the EEC at *c.* 400–320 Ma (Edwards & Wasserburg 1985; Savelieva 1987; Sengör *et al.* 1993; Bea *et al.* 1997; Puchkov 1997; Brown *et al.* 1998). This orogen is partly exposed in the Urals mountains, Severnaya Zemlya and the Taymyr Peninsula, whereas its

eastern part is buried under the West Siberian Basin. Further collisions of the EEC with the Siberian craton resulted in the formation of the Timan Ridge in Triassic–early Jurassic time. Compared with other Palaeozoic orogens, which have been essentially reworked during the late Palaeozoic and Meso-Cenozoic tectonomagmatic processes, the Uralides have remained intact since the Palaeozoic.

European Caledonides

A thin crust (Fig. 7), in places with a seismically laminated lower crust and a sharp subhorizontal Moho, that crosses pre-existing terrane boundaries, is typical of the Caledonides, Variscides and

Table 1. Summary of geophysical data for the crust and the upper mantle of tectonic structures of Europe

Region	Age	Crustal thickness (km)	V_p above/below Moho (km s^{-1})	Average crustal V_p (km s^{-1})	Reflectivity pattern		Bouguer anomalies (mGal)	Surface heat flow (mW m^{-2})	Moho temperatures ($^{\circ}\text{C}$)	Lithospheric thickness (km), based on different techniques and different definitions
					In the lower crust	In the upper mantle				
<i>Craton</i>										
Baltic Shield (Kola–Karelian Archaean nucleus)	3.1–2.5 Ga	37–51	6.9–7.4/8.0–8.4	6.5–7.0 (typical 6.6–6.8)	Weak reflectivity		0 to –20	20–40	500–600 (B), 350–600 (A)	>170 (1-Pz); 210–230 (1-Cc); ~220 (3-G); ~250 (3-Sa); ~200 (5-CB); >200 (5-P); 200–250 (5-B); >240 (5-KP); 250–300 (5-AM); 210 (6-J) ~200 (1-Pa); 200 (3-R); >200 (4-Bb); 150–170 (5-CB); 180–210 (5-A) >150 (5-K); 170–220 (5-AM)
East European Platform	2.1–1.8 Ga	38–52	7.0/8.0–8.5 (typical 8.2–8.3)	6.4–6.9 (typical 6.5–6.6)	No significant reflectors deeper than 10 km below Moho		–20 to +30	35–50	500–600 (A, AM)	
Ukrainian Shield	3.6–3.0 Ga	38–65	6.8–7.5/8.2–8.6	6.5–7.1	Some reflectivity		+10 to +30	25–40	500–700 (A)	
<i>Collisional orogens/subduction</i>										
Svecofennian Province	1.90–1.86 Ga; 1.84–1.77 Ga; 1.6–1.5 Ga	35–64	6.9–7.3/8.0–8.4	6.1–6.8 (6.8 in the region of the thick crust)			0 to –60	40–60	550–700 (CB) 600–700 (A, B)	130–160 (1-Pz); 160–220 (1-Cc); 170–220 (3-G); 100–140 (5-CB); 140–180 (5-B); 150–200 (5-A)
Variscides	430–300 Ma	Flat Moho, 28–32	6.2–7.0/7.8–8.1	6.0–6.4	Strong subhorizontal lamellae, truncated at Moho		0 to –40	50–70	550–650 (CB); 600–700 (C)	80–100 (1-Pz); 100–120 (2-Sp); ~100 (2-KS); 80–140 (4-Bb); 70–120 (5-CB)
Caledonides	500–415 Ma	28–38	6.2–6.5/7.8–8.2 (typical 8.1–8.2)	6.3–6.7 (typical 6.4–6.5)	High reflectivity, truncated at Moho		–40 to –100	50–70	600–650 (B, CB, A)	90–130 (1-Cc, Pz); 90–110 (5-CB); 90–140 (5-A, B)
Urals	450–250 Ma	45–60	7.6–7.8/8.2–8.4	6.7–6.9	Transparent; set of mantle reflectors at c. 175 km depth			25–50	~175 (3-K); ~200 (3-R)	
Alps	~40 Ma	35–60	6.2–6.5/8.2	6.1–6.4	S-dipping crustal reflectors; discontinuous reflection Moho		–50 to –100	60–100	800–1000 (CB); 700–1000 (Bq)	80–130 (1-Pz); 120–170 (2-Sp); down to ~200 (2-KS); 140–220 (4-Bb); 50–70 (5-CB) [Po plain ~60 (4-Bb)]; 80–130 (5-O)
Pyrenees	Cz	40–55	/8.0–8.1	6.2	The entire crust is reflective		–50 to –120	80–100	750–850 (ZF)	80 (1-MP), 80–100 (1-SG)
Carpathians	20 Ma	32–60	7.6–7.8/8.0	6.3				70–100		80–180 (4-Bb); 100 (5-C); 80–150 (5-Z); 150 (6-Pr); 60–80 (6-Ad)

(Continued)

Table 1. Continued

Region	Age	Crustal thickness (km)	V_p above/below Moho (km s^{-1})	Average crustal V_p (km s^{-1})	Reflectivity pattern		Bouguer anomalies (mGal)	Surface heat flow (mW m^{-2})	Moho temperatures ($^{\circ}\text{C}$)	Lithospheric thickness (km), based on different techniques and different definitions*
					In the lower crust	In the upper mantle				
Rifting and processes related to mantle plumes Svecofennian Province	1.25 Ga	30–55	6.9–7.3/8.0–8.3	6.1–6.8 (typical 6.4)			0 to –20	40–60	550–700 (CB)	130–160 (1-Pz); 160–220 (1-Cc); 170–220 (3-G); 100–140 (5-CB); 140–180 (5-B); 150–200 (5-A)
Central Russia	1.3 Ga–650 Ma	42–46 (min 32)	6.9–7.4/8.0–8.4	6.5–6.6				40–50	500–600 (A)	160–180 (5-A)
Rift System										
Dnieper–Donets–Pripjat rift	~350 Ma	35–45	7.2–7.5/8.0	6.7–6.8	The entire crust is reflective		–30 to +30	45–75	550–900 (A)	100–140 (5-A)
Pannonian Basin	20–0 Ma	25–30	6.6/	6.3			0 to +20	90–110		40 (3-Po); 60–80 (4-Bb); 60–80 (5-C); 75–100 (5-Z); 60–85 (6-Ad)
French Massif Central	~30 Ma	28–32		6.1–6.2			–120 to –140	80–120		60–100 (1-So), ~120 (1-Gr); 80–120 (4-Bb); 100–140 (4-Bb); 60–90 (5-Sb)
Rhenish Massif–Rhine graben	42–31 Ma, 25–20 Ma	28–32 (RM); 22–28 (RG)	6.2–6.6/8.1 (RM); 6.7–7.6/7.9–8.2 (RG)	6.0–6.1	Rhenish massif: transparent in the N part, strongly reflective in the S part		+10	80–140 ?	650 (CB)	60–80 (1-Pz); 50 (1-MP); 60–80 (4-Bb); 50–70 (5-CB)

*Lithospheric thickness calculated from: 1, surface waves; 2, P-wave seismic tomography; 3, seismic reflection or refraction data; 4, teleseismic V_p residuals; 5, thermal models; 6, electrical studies. Lithospheric definitions used in individual studies are given below with the corresponding sources.

Sources for the crustal structure are given in the text. Average crustal velocities are from Pavlenkova References (1996). Sources for thermal models: A, Artemieva & Mooney (2001); B, Balling (1995); Bq, Bousquet *et al.* (1997); C, Cermak (1994, 1995); CB, Cermak & Bodri (1995); K, Kutas *et al.* (1989); KP, Kukkonen & Peltonen (1999); O, Okaya *et al.* (1996); P, Pasquale *et al.* (1990, 1991); Sb, Sobolev *et al.* (1996); ZF, Zeyen & Fernandez (1994); Z, Zeyen *et al.* (2002). Lithospheric thermal thickness (5) is assumed to be at: $T = 1300^{\circ}\text{C}$ adiabat (A, AM, B, Z); $T = (1100 + z) \times 0.85$ (z is depth in km; CB, C); $T = 1100^{\circ}\text{C}$ (K, O, P); xenolith geotherm (KP). Sources for seismic studies of the upper mantle: Bb, Babuška *et al.* (1988, 2002); Cc, Calcagnile *et al.* (1990) and Calcagnile (1991); G, Guggisberg (1986); Gr, Granet *et al.* (1995a, b); K, Knapp *et al.* (1996); KS, Kissling & Spakman (1996); MP, Muteller & Panza (1984); Pa, Paulssen *et al.* (1999); Po, Posgay *et al.* (1995); Pz, Panza *et al.* (1980) and Calcagnile (1991); R, Ryberg *et al.* (1996); Sa, Sacks *et al.* (1979); Sp, Spakman (1990); EGT); So, Souriau *et al.* (1980); SG, Souriau & Granet (1995). Base of the seismic lithosphere (1–4) is defined: by mantle reflectors (K); as the seismological high-velocity region overlying the LVZ (Bb, Cc, G, Pa, Pz); as the top of the layer with zero or negative V_p gradient (KS, S). Sources for electrical and magnetotelluric studies of the upper mantle: Ad, Adam *et al.* (1982) and Adam (1996); J, Jones (1984); Pr, Praus *et al.* (1990). Base of the electric lithosphere (6) is defined by a strong decrease in upper mantle conductivity.

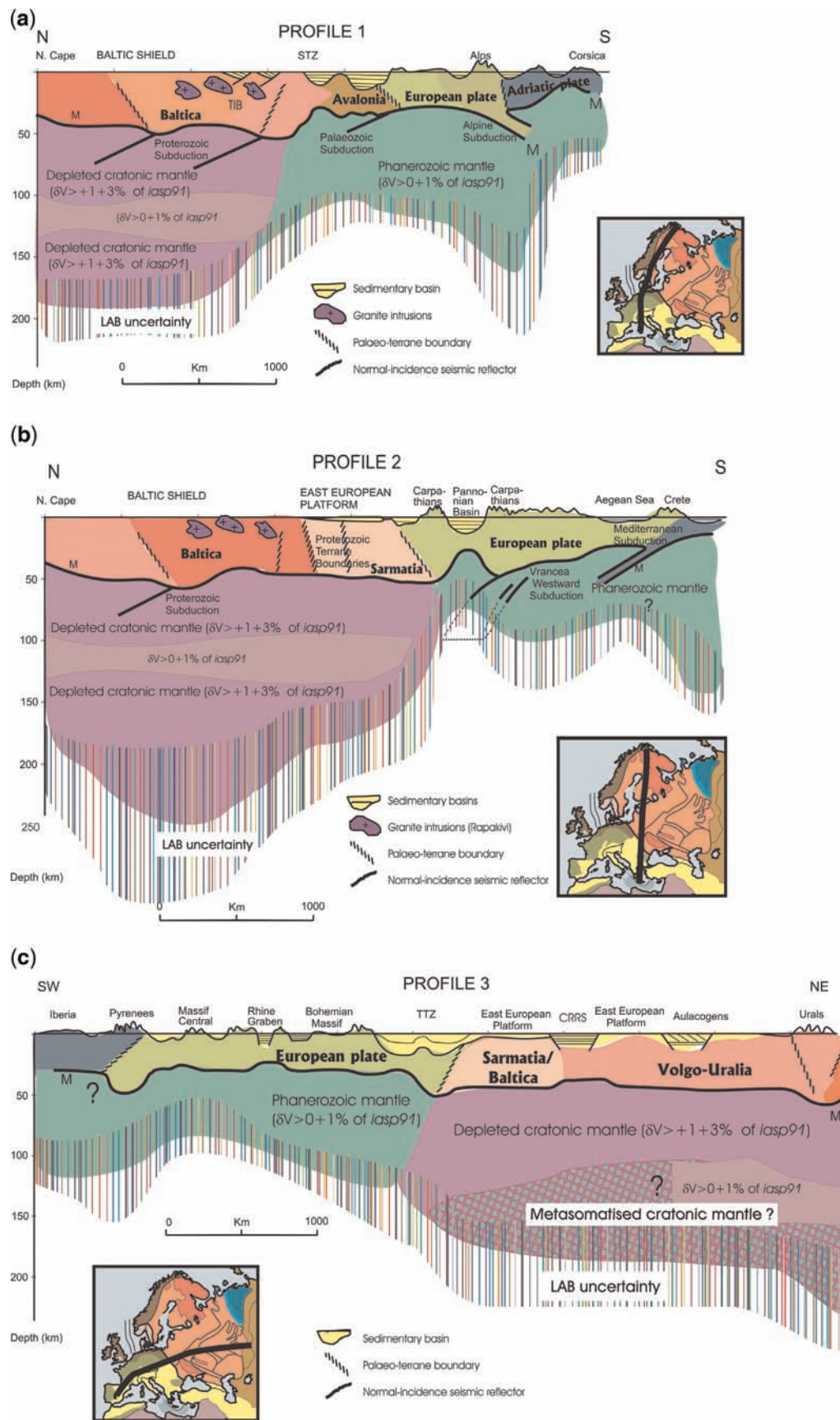


Fig. 8. Three profiles through the lithosphere of Europe: (a) north–south profile from the Baltic Shield to Corsica through the Alps; this profile follows the EGT profile (Blundell *et al.* 1992); (b) north–south profile from the Baltic Shield to Crete through the Pannonian Basin; (c) SW–NE profile from Iberia to the Urals through the Central European Rift System, the Carpathians, and the East European Platform. The pronounced differences in lithospheric thickness along the profiles should be noted; these are only partly coupled to variations in crustal thickness. The difference in wavelengths in crustal and lithospheric thickness variations may be caused by depth-dependent differences in resolution. Deep, normal-incidence reflection seismic data show traces of palaeo-subduction for all tectonic ages, independent of the lithospheric thickness. A reduced velocity zone, identified beneath some cratonic terranes (see the section on the Baltic Shield), has absolute seismic velocities slightly lower than in the surrounding high-velocity layers in the cratonic mantle, but still *c.* 1% higher than in global continental reference models (*ak135* or *iaspei*). The range of possible lithospheric thickness values is based on different methods (Table 2); the uncertainty is *c.* 50 km. M, Moho; STZ, Sorgenfrei–Tornquist Zone; TIB, Trans-Igneous Belt; LAB, lithosphere–asthenosphere boundary.

Table 2. Lithospheric thickness in Europe, based on different techniques and different definitions

Region	Lithospheric thickness (km)						Range of estimated lithospheric thickness (km)
	From surface waves (1)	From P-wave tomography (2)	From reflection or refraction data (3)	From V_p residuals (4)	From thermal models (5)	From electrical and MT studies (6)	
<i>Craton</i>							
Baltic Shield (Kola–Karelian Archean nucleus)	> 170 (Pz); 210–230 (Cc)	~220 (G)			~200 (CB); >200 (P); 200–250 (B); >240 (KP); 250–300 (AM)	210 (J)	200–300
East European Platform Ukrainian Shield	~200 (Pa)	200 (R)		>200 (Bb)	150–170 (CB); 180–210 (A) >150 (K); 170–220 (AM)		150–210 150–220
<i>Collisional orogens/subduction</i>							
Swecofennian Province	130–160 (Pz); 160–220 (Cc)	170–220 (G)			100–140 (CB); 140–180 (B); 150–200 (A)		100–220
Variscides	80–100 (Pz)	100–120 (Sp); ~100 (KS)		80–140 (Bb)	70–120 (CB)		70–140
Caledonides	90–130 (Cc); 90–130 (Pz)	~175 (Km); ~200 (R)			90–110 (CB); 90–140 (A, B)		90–140
Urals Alps	80–130 (Pz)	120–170 (Sp); slab down to 200–220 (KS)		140–220 (Bb); [Po plain ~60 (Bb)]	50–70 (CB); 80–130 (O)		175–200 50–150; slab down to 200–220
Pyrenees	80 (MP); slab down to 80–100 (SG)						80–100; slab down to 80–100
Carpathians		~40 Ma ~20 Ma		80–180 (Bb)	~100 (C); 80–130 (Z), slab down to 150 (Z)	150 (Pr); 60–80 (Ad)	60–150; slab down to 150–180
<i>Rifting and processes related to mantle</i>							
Swecofennian Province	130–160 (Pz); 160–220 (Cc)	Rapakivi 1.25 Ga	170–220 (G)		100–140 (CB); 140–180 (B); 150–200 (A)		100–220
Central Russia rift system Dnieper–Donets–Pripyat rift	1.3 Ga–650 Ma ~350 Ma				160–180 (A) 100–140 (A)		160–180 100–140
Pannonian Basin French Massif Central	20–0 Ma ~30 Ma		40 (Po)	60–80 (Bb); 100–140 (Bb); 80–120 (Bb)	60–80 (C); 75–100 (Z); 60–90 (Aa, Sb)	60–85 (Ad)	40–100 60–120
Rhenish Massif–Rhine graben	~30 Ma			60–80 (Bb)	50–70 (CB)		50–80

*Lithospheric thickness calculated from: 1, surface waves; 2, P-wave seismic tomography; 3, seismic reflection or refraction data; 4, teleseismic V_p residuals; 5, thermal models; 6, electrical studies. Lithospheric definitions used in individual studies are given below with the corresponding sources.

Sources for the crustal structure are given in the text. Sources for thermal models: A, Artemieva (2003); Aa, Artemieva (1993); AM, Artemieva & Mooney (2001); B, Balling (1995); C, Cermak (1994, 1995); CB, Cermak & Bodri (1995); K, Kutas *et al.* (1989); KP, Kukkonen & Peltonen (1999); O, Okaya *et al.* (1996); P, Pasquale *et al.* (1991); Sb, Sobolev *et al.* (1997); Z, Zeyen *et al.* (2002). Lithospheric thermal thickness (5) is assumed to be at: $T = 1300^\circ\text{C}$ adiabat (A, AM, B, Z); $T = (1100 + z) \times 0.85$ (z is depth in km; CB, C); $T = 1100^\circ\text{C}$ (K, O, P); xenolith geotherm (KP). Sources for seismic studies of the upper mantle: Bb, Babuška *et al.* (1988, 2002); Cc, Calcagnile *et al.* (1990) and Calcagnile (1991); G, Guggisberg (1986); Gr, Granet *et al.* (1995); Kn, Knapp *et al.* (1996); KS, Kissling & Spakman (1996); Pa, Paulissen *et al.* (1999); Po, Posgay *et al.* (1995); Pz, Panza *et al.* (1980); R, Ryberg *et al.* (1996); Sp, Spakman (1990, EGT); So, Souriau *et al.* (1980); SG, Souriau Granet (1995). Base of the seismic lithosphere (1–4) is defined: by mantle reflectors (Kn); as the seismological high-velocity region overlying the LVZ (Bb, Cc, G, Pa, Pz); as the top of the layer with zero or negative V_p gradient (KS, S). Source for electrical and magnetotelluric studies of the upper mantle: Ad, Adam *et al.* (1982) and Adam (1996); J, Jones (1983); Pr, Praus *et al.* (1990). Base of the electric lithosphere (6) is defined by a strong increase in upper mantle conductivity.

the northern Appalachians (Behr & Heinrichs 1987; Nelson 1992; Meissner 1996). This has long been believed to be typical for all Palaeozoic orogens. This crustal structure is often interpreted as an indication that a large part of the lower crust, and probably of the lithospheric mantle, has been delaminated during the Palaeozoic orogenies. However, seismic data from eastern East Avalonia shows no sign of lower crustal reflectivity (MONA LISA Working Group 1997). Nelson (1992) postulated another scenario of crustal modification during Palaeozoic orogenic events that includes: (1) post-compressional delamination of eclogitized lower crust and the uppermost mantle lithosphere resulting in crustal thinning (however, Abramovitz *et al.* (1998) interpreted low sub-Moho velocities at the northern edge of the former Caledonian orogeny in Denmark as being associated with the presence of lower crustal rocks of eclogite facies); (2) decompressional melting in upwelling asthenosphere tending to replace the foundering lithosphere; (3) ponding of mafic sills within the lower crust and at the crustal base, producing a sharp Moho and a laminated lower crust. As these processes took place after the main compressional events, the present crustal structure does not necessarily show any simple relationship to pre-existing terrane boundaries.

Estimates of lithospheric thickness in the Norwegian and Danish–Polish Caledonides, based on surface-wave dispersion analysis, S-wave seismic tomography (Calcagnile 1982, 1991; Panza *et al.* 1980; Pedersen & van der Beek 1994) and thermal modelling (Cermák 1994; Balling 1995; Zeyen *et al.* 2002), give values in the range of 90–130 km (see also Fig. 4). The MONA LISA Working Group (1997) detected subhorizontal seismic reflections at a depth of *c.* 80 km in the North Sea area, which can be interpreted as being close to the lithospheric base. In one case such reflectors are observed on two crossing profiles, thus ruling out side-swipes and other artefacts. Nevertheless, S-wave models may not have sufficient lateral resolution, such that an apparent lithospheric thinning in the Caledonides of Norway may result from smearing of a strong offshore low-velocity anomaly (e.g. Fig. 2d).

Little is known about the structure of the subcrustal lithosphere of the British and Irish Caledonides; most upper mantle studies are restricted to the Iapetus Suture separating the Laurentian and Avalonian continents. Across the Caledonian Deformation Front, P-wave seismic velocities in the upper mantle increase by *c.* 0.26 km s⁻¹ (Masson *et al.* 1999), and surface heat flow increases from 45–60 mW m⁻² in the cratonic lithosphere of Laurentia to 70–80 mW m⁻² in the Caledonides (Fig. 3). The latter values are significantly higher than in the Norwegian Caledonides (45–55 mW m⁻²); it is, however, unclear if high heat flow values in the British and Irish Caledonides are caused by reduced lithosphere thickness or by shallow effects (e.g. high crustal heat production, groundwater circulation).

The Variscides

Tectonics. The Variscan (Hercynian) orogeny has affected most of Central and Western Europe and forms a 700–1000 km wide and *c.* 3000 km long belt, extending from Poland and SE England to western Iberia (Franke 1986; Ziegler 1986; Fig. 1). The major tectonic features of the European Variscides are three NE–SW-striking subparallel sutures (e.g. Neugebauer 1989), often interpreted as related to oceanic closure. However, plate tectonic interpretations of the origin of the Variscan orogen remain controversial, mainly because of the lack of evidence for the position of an ocean inside the Variscides (e.g. Ziegler 1986; Neugebauer 1989; Ziegler *et al.* 2004). Some workers (e.g. Behr *et al.* 1984) have proposed convergent, southward-dipping, subduction zones in the entire Variscan Europe. Others (e.g. Lorenz & Nicholas 1984; Matte 1986) favoured two-sided, north- and south-dipping, subduction caused by the closure of two Palaeozoic oceans,

followed by obduction and collision of Europe and Africa. The total crustal shortening during the Variscan orogeny exceeds 600 km; the terranes of Proterozoic to Carboniferous ages (e.g. Armorican, Ardennes, Iberian, Bohemian, French Massif Central) were deformed and partly metamorphosed, and large volumes of granitoids were emplaced between 370 and 280 Ma (Matte 1986). A large part of the Variscides has been later reworked by Mesozoic–Cenozoic events, related to tectono-magmatic activity in the Central European Rift System and large relative movements of the Eurasian and African plates.

Seismic models. Seismic studies of Hercynian Europe indicate that, despite the strongly heterogeneous tectonic structures of the Variscan belt, the seismic velocity structure of the subcrustal lithosphere is rather uniform, with dominating subhorizontal wide-angle reflectors in the upper 90 km (Hirn *et al.* 1973; Faber & Bamford 1979; ILIHA DSS Group 1993). These data imply that the Hercynian structures in the European lithosphere have not been preserved since the Palaeozoic formation of the orogen. However, one should bear in mind that the resolution in these studies is relatively low because of the >3 km intervals between the seismic stations along the refraction profiles. Hence, it cannot be excluded that dipping orogenic structures, which could be ascribed to the Variscan orogeny, could exist in higher-resolution, normal-incidence reflection seismic sections.

A layered structure of the Variscan lithospheric mantle with a horizontal foliation of the upper layer and a vertical (or steeply dipping) layering in the lithospheric mantle below *c.* 45 km depth is supported by recent studies of spinel lherzolite xenoliths from the Bohemian Massif, which sample the Variscan lithosphere down to a depth of *c.* 70 km (Christensen *et al.* 2001). Data on Pn anisotropy and SKS shear-wave splitting provide further support for this conclusion (Fuchs & Wedepohl 1983). Christensen *et al.* (2001) argued that a horizontal olivine *a*-axis in the lower layer, with an approximately east–west strike, parallel to the observed fast shear-wave direction, has been inherited from the Variscan convergence. Strong seismic anisotropy (6.5–15% for P-wave velocities; Babuška & Plomerová 1992) in the lithospheric mantle of the Variscides provides evidence for palaeosubduction zones associated with the closure of the oceanic domains and the consequent Hercynian orogeny.

By the pattern of seismic anisotropy, the Variscides can be subdivided into two domains with NW- or SE-dipping anisotropic structures in the lithospheric mantle (Babuška & Plomerová 1992). The general SW–NE orientation of the suture between the lithospheric domains with different anisotropy patterns differs from the north–south trend suggested by Panza *et al.* (1986). The depth range of seismic anisotropy in the lithospheric mantle is largely unknown. However, the boundary between the two domains approximately corresponds to the suture between the Saxothuringian and Moldanubian terranes and correlates with two features: (1) a pronounced step in lithospheric thickness, which increases southeastwards from 80–100 km to 120–140 km over a distance of *c.* 150 km (Fig. 4d; Babuška & Plomerová 1992); (2) a dip of a highly conductive layer in the mantle (Paus *et al.* 1990). Based on P-wave residuals (Fig. 4d), the typical thickness of the Variscan lithosphere is estimated to be 80–120 km, with small values (60–80 km) in the Cenozoic Central European Rift system (see below), and large values (120–140 km) beneath the Proterozoic–early Palaeozoic terranes (e.g. the NE part of the Massif Central and the Bohemian Massif). Because the variation in the P-wave residuals in Central Europe does not correlate with the present stress field (Muller *et al.* 1992), NW- and SE-dipping anisotropic structures in the lithospheric mantle of the Variscides are interpreted as traces of two divergent systems of palaeosubduction zones with olivine orientations inherited from subducted ancient lithosphere (Babuška & Plomerová 1992).

Similarly, two distinct patterns of upper mantle S-wave seismic anisotropy have been distinguished in the Armorican massif; upper mantle of the southern domain exhibits orogen-related anisotropy with NW–SE orientation of Pn and SKS fast directions, parallel to the strike of the South Armorican shear zone, whereas in the northern domain SKS fast directions do not follow the strike of major Hercynian shear zones. Furthermore, at 90–150 km depth the upper mantle has +3% P-wave velocity anomaly in the southern domain and –3% P-wave velocity anomaly in the northern domain (Judenhert *et al.* 2002). This seismic pattern is interpreted as evidence for a pre-Hercynian subduction process, which welded together two parts of the Armorican massif.

Surface-wave tomography of Central Europe indicates low mantle velocities at depths below 150 km (Fig. 2b; Shapiro & Ritzwoller 2002); earlier estimations of lithospheric thickness, based on surface-wave dispersion analysis, are in the range of 70–100 km (Panza *et al.* 1986; Du *et al.* 1998). In the Iberian peninsula, mantle velocities in surface-wave tomography models reach asthenospheric values between 80 and 180 km depth (Badal *et al.* 1996). P-wave tomography, which has a much weaker vertical resolution (compare Fig. 2a and 2c), indicates that lithospheric thickness in Central Europe is less than 100 km (Bijwaard & Spakman 2000; Piromallo & Morelli 2003), except for the Armorican Massif, where lithospheric thickness may be as large as *c.* 150–200 km (Fig. 4a and d). A linear belt of large lithospheric thickness beneath SE Iberia, resolved by P-wave velocity models, is probably associated with a Cenozoic subduction zone (Blanco & Spakman 1993). Similar linear velocity anomalies are seen beneath other Cenozoic subduction systems (the Alps, the Hellenic arc; see Fig. 4a and d, and discussion below); but surprisingly, there is no seismic sign of a subducting slab beneath the Caucasus, despite the presence of a strong positive gravity anomaly (Fig. 5).

Thermal models. Surface heat flow in the Variscides is high, *c.* 70–100 mW m⁻² (Fig. 3), and locally it significantly exceeds these values (Cermak 1995). Strong negative isostatic gravity anomalies (–40 to –60 mGal; Fig. 5) indirectly imply high temperatures in the mantle of Hercynian Europe. However, the highly heterogeneous crustal structure as well as the transient thermal regime of the mantle induced by recent tectonic activity in many parts of the Variscan belt prevent reliable estimation of mantle geotherms from surface heat-flow data. Some attempts have been made by Cermak & Bodri (1995), who argued for a uniform lithospheric thermal thickness (70–80 km) in Hercynian Europe along the European Geotraverse with a slight southward decrease in thickness. Within the frame of this model, temperatures at 50 km depth were estimated to be in the range 700–900 °C (Cermak 1995). For the Bohemian Massif, a steady-state thermal model of the mantle interpreted jointly with gravity data (Pasquale *et al.* 1990; Zeyen *et al.* 2002) has led to the conclusion that the thermal lithosphere beneath this terrane is *c.* 90–120 km thick. A melilite–nephelinite composition of magmas, typical for early stages of Cenozoic magmatism in the Massif Central and Rhenish Massif, implies that the thickness of the Hercynian lithosphere was at least 80–100 km in the Tertiary (Artemieva 1993). In comparison, based on analysis of Hercynian mafic magmas, Lorenz & Nicholas (1984) argued that the regional lithospheric thickness during the Variscan orogeny was probably between 40 and 50 km, implying a *c.* 40–50 km growth of the lithosphere by thermal cooling over a period of 200–300 Ma.

Regional P- and S-wave tomographic models have been recently used to assess upper mantle temperatures in Western Europe (Goes *et al.* 2000). At present this work gives, probably, the best available constraints on the thermal regime of the European mantle, despite a significantly different lateral and vertical resolution of the two tomography models and inevitable weakly constrained assumptions on mantle composition and its fluid

regime. According to these estimates, mantle temperatures in Hercynian Europe along a 10°E profile may exceed 1000 °C at a depth of 100 km, whereas the lithospheric thermal thickness, defined as the depth to an isotherm of 1300 °C, is expected to be *c.* 120–140 km. These values are close to thermal estimates for Palaeozoic rifts within the EEP (Fig. 6) (Artemieva 1993), such that, within the accuracy of model constraints, the range of mantle temperatures should be similar for most of the tectonic structures of Europe with Palaeozoic tectonothermal ages.

The Uralides

Tectonics. The Uralian orogen, which is composed of a series of accreted island arcs, volcanic complexes and fold belts, is an unusual Palaeozoic orogen, as it has remained intact within the continental interior since its formation. Surface geology (in particular, the presence of ophiolite complexes), plate tectonic reconstructions and palaeomagnetic data have been used to argue that the formation of the Uralides began some time between the Early Ordovician and Early Carboniferous by accretion of late Proterozoic–Palaeozoic microcontinental fragments and island arcs formed at the active margin of the Kazakhstan plate to a passive continental margin of the EEC (Savelieva 1987; Zonenshain *et al.* 1990; Sengör *et al.* 1993). The Main Uralian Fault, a 20 km wide zone of sheared schists with a deformation age of 450–385 Ma, is a well-preserved plate boundary, which separates the former passive continental margin zone of the EEC in the west from the accreted Asian island arc, oceanic and continental terranes to the east. It appears in normal-incidence reflection seismic profiles as a 40° east-dipping reflectivity zone extending to a depth of at least 15 km (Knapp *et al.* 1998), and has been interpreted as an Ordovician subduction zone dipping beneath the Kazakhstan continent (Hamilton 1970). In Silurian–Early Devonian times (the ages of the oldest island-arc complexes of the Tagil and West Magnitogorsk zones), the eastern margin of the EEC could already have become an active continental margin, with a west-dipping subduction zone existing in the Devonian (Hamilton 1970; Degtiarev 2001). The formation of a subduction zone dipping beneath the EEC could have a strong influence on the Devonian tectonics of the EEP. Models of mantle convection that take into account the dynamic effect of a subducting slab provide a good explanation for a peak in sedimentation in the eastern part of the EEP, associated with a Devonian west-dipping subduction at the Urals (Mitrovica *et al.* 1996). At the final stages of the collision of the EEC and the Siberian–Kazakhstan plate (at *c.* 320–250 Ma) the remaining oceanic plate between the two cratons was subducted eastwards underneath the Kazakhstan continent, and the Urals fold belt was developed. However, the modern topography of the Urals came into existence only during the Tertiary–Quaternary (Lider 1976; Morozov 2001) and the recent uplift of the Urals is as enigmatic as Cenozoic uplift of the Caledonides of Norway and Greenland (Japsen & Chalmers 2000).

Seismic data. The Urals orogen has a well-preserved, more than 50 km thick, crustal root, reaching a depth of about 65 km in the Polar Urals and under the Tagil–Magnitogorsk block (Druzhinin *et al.* 1990; Egorkin & Mikhaltsev 1990; Carbonell *et al.* 1996), very high average crustal velocities as a result of magmatic intrusions, and a 175–200 km thick lithosphere (Mechie *et al.* 1993; Ryberg *et al.* 1996; Knapp *et al.* 1996; Fig. 7). The most recent summary of geochemical and seismic data on the crustal structure along the length of the orogen, as well as new tectonic and geodynamic constraints on the subduction-related and orogenic processes, have been presented by Brown *et al.* (2002). However, data on the subcrustal lithosphere of the Uralides remain limited.

The results of teleseismic tomography across the Middle Urals (Poupinet *et al.* 1997) show that, down to 100 km depth, the sub-crustal lithosphere beneath the Western Urals has seismic velocities 2–3% higher than beneath the accreted island arc complex to the east of the Main Uralian Fault. This result suggests that the fast lithosphere of the EEC dips underneath the low-velocity lithosphere of the Uralides. These results are consistent with seismic refraction interpretations along the PNE profile Quartz (Mechie *et al.* 1993; Ryberg *et al.* 1996), which show that the Urals are underlain by an eastward-dipping high-velocity block with compressional velocities of *c.* 8.7 km s^{-1} down to a 100 km depth. Such high velocities may correspond to the palaeosubduction-related preferred mineral orientation in the underthrust lithosphere of the East European continental margin. However, modern tectonic models reject the idea that the Uralides are entirely underlain by lithosphere of EEC affinity (Morozov 2001). Along the URALSEIS seismic profile in the Southern Urals, the cratonic lithosphere down to depths of 60–220 km extends no further than 200–250 km to the east of the ‘geological’ edge of the EEC (Savelyev *et al.* 2001). Correlation of the seismic structure of the upper mantle down to 100–200 km depth with the surface geology in the Urals suggests that orogenic processes have affected most of the lithosphere and that their signature has been preserved in the upper mantle for hundreds of millions of years.

Seismic models of the crustal structure along the ESRU profile in the Middle Urals indicate that the Uralides extend beneath the sedimentary cover of the West Siberian Basin (Friberg *et al.* 2001). Based on an analysis of magnetic anomalies, Hamilton (1970) placed the eastern margin of the Uralides beneath the central part of the West Siberian Basin. This is consistent with seismic models of the upper mantle of northern Eurasia based on refraction data along the PNE profile Quartz (Ryberg *et al.* 1996), which show that the lithospheric thickness changes from *c.* 200 km, typical for the EEP and probably for the Uralides, to *c.* 150 km at a distance of 500 km eastwards from the Urals. Thus, it is likely that the high-velocity block beneath the western part of the West Siberian Basin is the extension of the Uralides.

Similar to the northern EEP, a pronounced reduced-velocity zone is observed beneath the Uralides along the Quartz profile in the depth interval of 105–130 km (Ryberg *et al.* 1996; Morozova *et al.* 2000; Fig. 8c). This highly reflective layer with reduced seismic velocities extends for 3000 km further eastwards (Thybo & Perchuc 1997) and is underlain by a high-velocity layer at *c.* 200–250 km depth (Nielsen *et al.* 1999; Kuzin 2001). Seismic reflection profiling of the Southern Urals (Knapp *et al.* 1996) revealed mantle reflections at depths of *c.* 80 km and 175 km; the lower reflector was interpreted as possibly imaging the base of the lithosphere.

Thermal data. The lithospheric thermal thickness at the eastern margin of the EEC, adjacent to the Ural mountains, is similar to estimates based on seismic interpretations for the Urals, *c.* 170–200 km (Artemieva & Mooney 2001). However, there is no reliable constraint of lithospheric temperatures beneath the Uralides, as anomalously low heat-flow values have been reported for the Southern Urals (Salnikov 1984; Kukkonen *et al.* 1997): *c.* 25 mW m^{-2} in the 1500 km long Magnitogorsk block, compared with 40–50 mW m^{-2} in the EEP and in the eastern part of the Southern Urals (Fig. 3). Possible explanations for this thermal anomaly include palaeoclimatic variations, low crustal heat production, lateral groundwater heat transfer, or anomalously low mantle heat flow beneath the central part of the Southern Urals, perhaps associated with Palaeozoic subduction zones. For models with a low crustal heat production in island arc complexes of the crust, Moho temperatures (at a depth of *c.* 60 km) are estimated to be *c.* 550–600 °C (Kukkonen *et al.* 1997). Downward continuation of this conductive geotherm would imply a lithospheric thermal thickness of *c.* 200 km.

Gravity data. The short wavelength of gravity anomalies in the Uralides (less than 100–200 km) suggests their crustal origin. Gravity studies across the Middle and Southern Urals show a +50 mGal linear high of Bouguer anomalies above the Magnitogorsk block flanked by two negative gravity anomalies spatially limited to the area of the Pre-Uralian Foredeep, and the Western and Central Uralian zones (–75 to –50 mGal) to the west from the Main Uralian Fault and to the Eastern Uralian Zone (–65 to –40 mGal) in the Eastern Urals. The negative Bouguer anomaly in the Pre-Uralian Foredeep is attributed to thick sediments at the edge of the EEC; as the positive free-air anomaly in the Western and Central Uralian Zones is well correlated with the topography, the Bouguer gravity minimum in these tectonic zones is well explained by a superposition of low-density sediments and the nearby crustal root beneath the Tagil–Magnitogorsk block (Döring *et al.* 1997). Similarly, the negative anomaly in the Eastern Zone has been explained by a joint effect of intruded granites and the nearby crustal root.

Surprisingly, the crustal root beneath the Tagil–Magnitogorsk block is not reflected in the topography and produces a positive Bouguer gravity anomaly. 2D gravity modelling shows that gravity maximum can be explained by the joint effect of a subsurface load of mafic–ultramafic material superimposed on the negative gravity effect of a crustal root (Döring *et al.* 1997). Seismic modelling supports this conclusion and indicates the presence of the crustal high-velocity body within the island arc material of the Magnitogorsk Zone (Carbonell *et al.* 2000).

Palaeozoic rifts

The Precambrian part of Europe comprises extensional structures, the development of which may have involved deep mantle processes. The most important (and the most well-studied) Palaeozoic rifts include the Oslo rift in the southern part of the Baltic Shield (considered as a classical example of a ‘passive rift’) and the Pripyat–Dniepr–Donets rift in the southern part of the EEP (which is considered to be an ‘active rift’). However, the amount of data on the structure of their subcrustal lithosphere is limited.

Pripyat–Dniepr–Donets rift (PDDR). Geophysical models of the lithosphere of the PDDR and the adjacent structures have been the goal of the GEORIFT project of EUROPROBE (Stephenson 2004), in the frame of which new regional gravity models of mantle anomalies (Yegorova *et al.* 1999) and geodynamic models of tectonic evolution of the region (Kuszniir *et al.* 1996; Starostenko *et al.* 1999) were developed. However, seismic data on the deep lithospheric structure of the Palaeozoic rifts within the EEP are not available, as the deepest reaching reflection and refraction data of the DOBRE experiments provide seismic images to depths of only a few kilometres below Moho (DOBREFraction’99 Working Group 2003).

Geodynamic models of the formation of continental rifts are traditionally divided into models of ‘passive’ and ‘active’ rifting (Sengör & Burke 1978); however, the validity of this approach is debated, as rifting activity is probably also governed by forces related to plate tectonics and thus many active continental rifts can be caused by stress-induced lithospheric extension (Ziegler & Cloetingh 2004). Traditionally, active models are based on the hypothesis that crustal extension results from a (plume-related?) thermal anomaly in the upper mantle. In these models, an uplift of hot mantle material to lithospheric depths (sometimes up to the crust) produces lithospheric extension and thinning. Indirect evidence for the presence of mantle plumes beneath some of the rift zones is provided by isotope data and the large volumes of magmas generated simultaneously with rifting. In particular, the model of active rifting is proposed for the Palaeozoic rifts in the southern part of the EEP

(Chekunov *et al.* 1992) based on a large volume of Devonian magmas (with a peak at *c.* 350 Ma) in the PDDR (Lyashkevitch 1987) and on geochemical data for the Dniepr graben (Wilson & Lyashkevitch 1996). A gravity maximum over the PDDR is interpreted to be caused by a large volume (*c.* 60%) of high-density mantle intrusive rocks in the crust (Yegorova *et al.* 1999), although a similar effect perhaps can be produced by eclogitization of the lower crust.

The thermal regime of the lithosphere of the PDDR can be constrained from surface heat-flow data as the lithosphere has relaxed to a stationary thermal regime since the Devonian rifting. The PDDR is characterized by a linear, *c.* 200 km wide, anomaly of a slightly elevated surface heat flow (45–55 mW m⁻², reaching locally 70–90 mW m⁻² in the Pripyat Depression), which separates the Ukrainian Shield (25–40 mW m⁻²) and the Voronezh Massif (Fig. 3). However, typical heat-flow values within the PDDR are similar to the values measured within most of the EEP, and a relatively short wavelength of the zone with higher heat flow suggests a chiefly shallow origin for heat-flow variations.

Steady-state thermal models (i.e. Kutas 1979; Artemieva 2003) imply that the lithospheric thermal thickness in the southern part of the EEP, including the PDDR, is *c.* 120–150 km, which, within the model accuracy, is similar to estimates for the Palaeozoic structures of Western and Central Europe (the Armorican and Bohemian massifs, in particular; see above and Fig. 6). It implies that the lower part of the cratonic lithosphere (*c.* 50–100 km) could have been thermally eroded or delaminated during the Devonian rifting. Alternatively, models of the transient thermal evolution since the impact of a presumed mantle plume (at 369 Ma) (Galushkin & Kutas 1995; Starostenko *et al.* 1999) result in lithospheric temperatures significantly lower than in steady-state models. In these interpretations, geotherms are similar to the EEP geotherms, implying a lithospheric thermal thickness of *c.* 180–200 km as in other Archaean–early Proterozoic cratons of the world (Jaupart & Mareschal 1999; Artemieva & Mooney 2001).

Oslo rift. The Oslo rift, which includes a chain of rift structures and grabens, extending from southern Norway to the TTZ or the Caledonian suture over a distance of *c.* 400–600 km, is considered to be a classical example of a passive rift (Pedersen & van der Beek 1994). Models of passive rifting assume that lithospheric extension is caused by tensional stresses at plate boundaries. If the stress is high (or the lithosphere is hot and thin), stress-induced lithosphere extension may cause rifting (Kuznir & Park 1984), accompanied by a passive upwelling of mantle material along weak lithospheric zones and its adiabatic melting. Because in this case the source of magmas is within the upper mantle, geochemical methods cannot reliably distinguish the models of passive from active rifting caused by small-scale mantle convection. Despite a large volume of basaltic magmas emplaced at *c.* 240–300 Ma (Neumann *et al.* 1995), the *P–T* analysis of their composition indicates that the magmatism was not caused by a high-temperature anomaly in the mantle (Neumann 1994). Numerical modelling of thermo-mechanical processes of rifting has shown that a step-like increase in lithospheric thickness at the eastern margin of the rift could have led to a passive diapirism and consequent rifting (Pascal *et al.* 2002). This explanation is close to the model by King & Anderson (1995) for the formation of large igneous provinces at cratonic margins by small-scale convection initiated by a step-like change in lithospheric thickness at the transition from a thick cratonic root to a thin younger lithosphere. Alternatively, based on analyses of the lateral distribution of seismic crustal velocities over the whole area to the south of the Oslo rift, Thybo (1997) proposed that the primary driving force for formation of the rift structures throughout the area could be related to deformation caused by far-field forces from the distant Variscan orogeny.

Because of the relatively small size of the Oslo rift, the structure of its lithospheric mantle cannot be resolved in large-scale geophysical models. Dispersion analysis of long-period Rayleigh waves implies that the thickness of the seismic lithosphere in southern Fennoscandia is *c.* 110–120 km (Calcagnile 1982). Despite a low lateral and insufficient vertical (50–100 km) resolution of this model, these estimates agree with the depth at which strong, almost horizontal reflectors are continuously seen in the upper mantle; that is, 80–100 km over distances of 5–20 km (Lie *et al.* 1990). By analogy with lower crustal reflectors, they are interpreted as a transition from brittle to plastic deformation and thus can be considered to be the base of the rheological lithosphere. Similar estimates of lithospheric thickness in the southern part of the Baltic Shield in the vicinity of the Oslo rift were obtained by regional P-wave seismic tomography (Plomerová *et al.* 2001).

The Oslo rift is characterized by positive Bouguer anomalies (0 to +50 mGal) compared with negative anomalies (less than –50 mGal) in the adjacent southern Fennoscandia (Ramberg 1976). Despite the inherent non-uniqueness of gravity models, most researchers interpret positive anomalies to indicate large volumes of mantle intrusions in the crust (e.g. Neumann *et al.* 1995). Surface heat flow in the Oslo rift is similar to the values measured in the Proterozoic terranes of Fennoscandia (40–50 mW m⁻²), suggesting that a stationary thermal regime has been re-established in the rift zone. Short-wavelength, slightly increased heat-flow values along the rift axis are likely to be produced by higher crustal heat production in the areas of Palaeozoic magmatism. Estimates of Moho temperatures (at a depth of *c.* 29–34 km; Kinck *et al.* 1991) differ strongly: *P–T* petrological estimates give values of 250–350 °C (Neumann *et al.* 1995), whereas lithospheric geotherms constrained by surface heat flow suggest temperatures of 550–650 °C (Balling 1995; Cermak & Bodri 1995). Values of 450–550 °C, as for other Palaeozoic structures of Europe (Fig. 6), probably provide the most conservative estimate.

Lithosphere of Mesozoic–Cenozoic structures of Europe

Most of the Hercynian orogen has been significantly reworked and overprinted as the result of plate tectonic processes related to the collision of the Eurasian and the African lithospheric plates, as well as by tectonomagmatic events associated with the formation and development of the Central European Rift System.

Regions of Cenozoic subduction and Alpine orogeny

Tectonics of the region. The huge volume of geological–geophysical information on the tectonic evolution and lithospheric structure of the Alps and the Mediterranean prevents even a simple listing of major results within the framework of the present review. For detailed information the reader is addressed to other publications (e.g. Mueller 1989, 1997; Blundell *et al.* 1992; Kissling & Spakman 1996; Pfiffner *et al.* 1997; Cavazza *et al.* 2004). The convergence of the Eurasian and African plates began at *c.* 120 Ma. It resulted in plate collision and subduction at *c.* 65 Ma and uplift of the Alpine orogenic belt after *c.* 23 Ma (Schmid *et al.* 1996; Castellarin & Cantelli 2000). The present convergence velocity is *c.* 9 mm a⁻¹ (De Mets *et al.* 1994). These tectonic processes have led to the formation of a highly complex and heterogeneous structure of the crust (Hirn *et al.* 1980; Giese 1985; Pfiffner 1990; Ye *et al.* 1995; Bleibinhaus & TRANSALP Working Group 2001; TRANSALP Working Group 2001, 2002) and the upper mantle of the region (Hirn *et al.* 1984; Panza *et al.* 1986; Pfiffner *et al.* 1988; Kissling 1993; Lippitsch *et al.* 2003).

Numerical models of mantle convection indicate that subduction of a lithospheric plate beneath continental lithosphere

causes a dynamic down-flexure of the lithospheric plate as a result of the down-pull by the dense cold subducting slab, leading to fast basement subsidence and basin formation (Gurnis 1992; Stern & Holt 1994; Pysklywec & Mitrovica 1998). This mechanism was used to explain the formation of the Po basin as the result of subduction beneath the Alps (Bott 1990), and can explain (at least partly) the formation of the Tyrrhenian, Aegean and Pannonian basins. It is likely that subduction-induced basin subsidence can explain one of the stages in the formation of the Northern Caucasus foredeep as the result of subduction of the Arabic (Turkish) plate under the Scythian plate. However, the existing geodynamic models attribute the formation of this basin chiefly to crustal processes (e.g. eclogitization or viscous flow in the lower crust) (Artyushkov 1993; Mikhailov *et al.* 1999; Ershov *et al.* 2003).

Geophysical models for the Alps and the Mediterranean. Regional P-wave (Hirn *et al.* 1984; Spakman 1986, 1990; Blanco & Spakman 1993; Souriau & Granet 1995; Kissling & Spakman 1996; Piromallo *et al.* 2001; Lippitsch *et al.* 2003) and S-wave (Panza *et al.* 1986; Snieder 1988; Pasyanos & Walter 2002) refraction and tomography models provide the bulk of the available information on the structure of the crust and upper mantle of the Alps and the Mediterranean. They indicate the presence of several subduction zones in the region and pronounced lithospheric thickening associated with them, especially underneath the Alps (e.g. Figs 2a, e, g and 4a, d). The maximal crustal thickness (crustal root) beneath the western and central Alps is found in a block where high upper mantle velocities extend to a depth of 200–250 km (Cavazza *et al.* 2004), interpreted as a lithospheric plate (presumably continental European lower lithosphere) steeply subducting southeastwards beneath the Adriatic microplate (Lippitsch *et al.* 2003; Fig. 8). This high-resolution teleseismic P-wave tomography of the Alps further suggests the existence of the second NE-dipping subduction zone in the eastern Alps, interpreted as the continental Adriatic lower lithosphere subducting beneath the European plate (Lippitsch *et al.* 2003). Similarly, P-wave residuals models for Southern Europe (Babuška *et al.* 1990) advocate the existence of two regions, beneath the western and central Alps and beneath the eastern Alps, with high values of lithospheric thickness (>200 km) with a sharp decrease in lithospheric thickness to *c.* 60 km beneath the Po basin (Fig. 4d). Similar lithospheric structures, with localized high-velocity blocks in the upper mantle interpreted as subducting slabs, have been identified in seismic tomography models for the Ligurian–Tuscany region of Italy (Panza *et al.* 1986) and southern Spain, where a detached subducted slab is identified in the regional tomographic images of the upper mantle (Spakman 1991; Blanco & Spakman 1993).

Regional P-wave tomography models indicate the existence of a 30 km wide block with 2% lower velocities extending to a depth of *c.* 80–100 km beneath the central and eastern Pyrenees (Souriau & Granet 1995). This velocity anomaly has been interpreted as lower crust of Iberia subducted as the result of convergence of the Eurasian and the African plates (Vacher & Souriau 2001). By analogy to a model proposed earlier for the Alps (Austheim 1991), weak negative residual gravity anomalies calculated for the Pyrenees are explained by eclogitization of the lower crust during its subduction (Vacher & Souriau 2001). Other zones of Cenozoic subduction (including the Hellenic arc, the Carpathians and the Caucasus) are characterized by linear belts of positive residual gravity anomalies (Fig. 5), ascribed to cold dense subducting lithospheric slabs in the underlying mantle. These gravity anomalies spatially correlate with linear high-velocity upper mantle structures resolved in regional P-wave seismic tomography models. Similarly, the presence of an ancient subducting slab beneath the western margin of the EEP as indicated by a regional S-wave tomography model (Nolet & Zielhuis 1994; Zielhuis & Nolet 1994) is supported by a linear belt of positive residual gravity anomalies along the TESZ (Fig. 5).

Estimates of mantle temperatures for the tectonically active regions of Europe are scarce, as steady-state models constrained by surface heat-flow measurements (e.g. Della Vedova *et al.* 1990; Cermák 1994; Zeyen *et al.* 2002) are not applicable. Thermo-kinematic models (e.g. Werner 1981; Royden *et al.* 1983*b*; Davy & Gillet 1986; Zeyen & Fernandez 1994; Bousquet *et al.* 1997) require detailed information on dynamic processes in the mantle, which are usually not completely understood, and, as a result, such models are poorly constrained. An advanced 2D thermo-mechanical model of the lithosphere of the Alps takes into account the processes of crustal shortening and formation of crustal and lithospheric roots during subduction (Okaya *et al.* 1996). According to this model, the Moho is an almost isothermal boundary with a temperature of *c.* 500–600 °C, although crustal thickness across the orogen changes from *c.* 30 km beneath the Variscides in the north to *c.* 55–60 km beneath the Alps and to *c.* 30–34 km beneath the Po basin in the south (Giese & Bunes 1992; Pfiffner *et al.* 1997; Waldhauser *et al.* 1998; TRANSALP Working Group 2002); lithospheric thermal thickness gradually increases from north to south from *c.* 80 km beneath the Variscides to *c.* 120–150 km beneath the southern Alps–northern Apennines (Okaya *et al.* 1996). Steady-state thermal models for the lithosphere of Southern Europe give overestimated values of mantle temperatures and, thus, lithospheric thicknesses that are too small (70–80 km) (Della Vedova *et al.* 1990; Cermák 1993). Although regional magnetotelluric (MT) studies indicate the presence of a highly conducting upper mantle layer at a depth of $>90 \pm 10$ km (ÉREGT Group 1990; Fig. 4e), its origin can be ascribed not only to the presence of melt, but also to fluids or graphite (although the presence of fluids would cause the dissolution of the pyroxenes of the rocks into partial melt as interpreted in some places of the EEP and in central France; Thybo & Perchuc 1997).

The Carpathians and the Pannonian Basin. A large number of geodynamic models for the Cenozoic evolution of the Pannonian Basin propose either an ‘active’ (e.g. Bergerat 1989) or a ‘passive’ role (Royden *et al.* 1983*a, b*; Le Pichon & Alvarez 1984; Horvath 1993; Huisman *et al.* 2001; Huisman & Bertotti 2002; Sperner *et al.* 2002) of the asthenospheric mantle in its formation and tectonic evolution. The large variety of passive models is probably due to a lack of detailed information on the interaction of the subducting slab with the asthenosphere–lithosphere system at different stages of subduction, especially when the continuous formation of the Alps affects the stress regime in the adjacent tectonic regions (Cloetingh *et al.* 2004). Seismic models based on P-wave residuals (Babuška *et al.* 1988) (Fig. 4d), MT and electromagnetic studies (Adam *et al.* 1982; Adam 1996; Adam & Bielik 1998), and geothermal (mostly steady-state) models (Bielik *et al.* 1991; Cermák 1994; Cranganu & Deming 1996; Bojar *et al.* 1998; Andreescu *et al.* 2002; Zeyen *et al.* 2002) reveal an anomalously thin (60–80 km) lithosphere of the Pannonian Basin, with local values as small as *c.* 40 km (Posgay *et al.* 1995). Negative residual isostatic anomalies (Fig. 5 and Yegorova *et al.* 1998) indicate the presence of anomalous low-density asthenospheric material and support the hypothesis that an earlier passive stage of basin formation may have been replaced at present by an active mantle (Huisman *et al.* 2001).

Low values of lithospheric thickness beneath the Pannonian Basin contrast with a thick lithosphere beneath the western Carpathians, where the thickness has been estimated to be 150 km by MT studies (Prau *et al.* 1990; Fig. 4e), 130–150 km by joint interpretation of surface heat-flow and gravity data (Zeyen *et al.* 2002) and seismic and MT data (Horvath 1993), and *c.* 100 km by steady-state thermal modelling (Cermák 1994), although the steady-state thermal models are physically inadequate for Cenozoic tectonic structures. The thick lithosphere beneath the Carpathians is ascribed to westward subduction of the Eurasian slab (Wortel & Spakman 2000). The existence of a

subduction zone beneath the southern Carpathians is well established from seismic data, with the main seismicity localized in the depth range 60–180 km along a steeply dipping plane of the Vrancea zone.

Regions of Mesozoic–Cenozoic tectonomagmatic activity

Rift system of the North Sea (RSNS). The rift system of the North Sea, deeply buried under thick Tertiary sediments, is one of the most prominent Mesozoic rifts of Europe and includes the Viking Graben in the north and the Central Graben in the south. Although its formation probably began during the late stages of the Caledonian orogeny, the major phase was related to Mesozoic rifting at the Atlantic passive continental margin; some researchers consider the RSNS as an unopened ocean or a failed arm of a broad Mesozoic rifting along the North Atlantic margins (Bott 1995). Mesozoic rifting started in Triassic–Early Jurassic times, continued for an unusually long time (*c.* 175 Ma; Bott 1995), and may have been affected by a mantle plume. The subsequent post-rift thermal subsidence occurred during the Tertiary (Ziegler 1992), and may be partly ascribed to delayed thermal reactions caused by late metamorphic reactions in the uppermost mantle (Vejbaek 1990).

Despite a huge geological–geophysical database on the crustal structure of the RSNS, data on its upper mantle structure are very limited. Regional S-wave seismic tomography models (Fig. 2), which have better vertical resolution than P-wave tomography models, show high velocities in the mantle down to 100–150 km depth. As it is unlikely that mantle temperatures in the Mesozoic rift are low, it is possible that high mantle velocities originate from compositional anomalies. Furthermore, residual gravity anomalies have strong negative values in the North Sea region (Fig. 5), implying a low-density (hot?) upper mantle beneath the RSNS, in agreement with a strong attenuation anomaly at a depth of 150 km (Fig. 2h). As seismic velocity and gravity models for the RSNS apparently contradict each other, the origin of the anomaly remains unclear.

Central European Rift System (CERS). The CERS is formed by a continuous chain of Cenozoic rift structures that extend from the Atlas Mountains in northern Africa to the North Sea. Various geodynamic models, including plume-related active rifting, passive rifting in response to collisional processes in the Alps and Pyrenees, back-arc rifting, or slab pull associated with Alpine subduction, have been proposed to explain geological and geological data available for the CERS: a thin crust, high surface heat flow, weak seismicity, Cenozoic magmatism and anomalous properties of the upper mantle (for reviews see Ziegler 1992; Prodehl *et al.* 1995; Merle & Michon 2001; Dezes *et al.* 2004; Michon & Merle 2005). However, because of the narrow structures of the CERS, one cannot expect to resolve upper mantle anomalies in large-scale geophysical models (e.g. Figs 2, 4 and 6). Below we discuss in detail the lithospheric structure of three major tectonic provinces within the CERS: the Rhine Graben, the Rhenish Massif, and the French Massif Central.

Rhine Graben. Intensive magmatism in the Rhine Graben began at 80 Ma and continued until 7–15 Ma; however, rifting began only at 45 Ma in the southern part of the Rhine Graben, from where it gradually extended northwards. The crustal structure of the Rhine Graben is well known, although data on the properties of the upper mantle are non-unique. The surface expression of the rift zone does not exceed 36 km, whereas the width of the lithospheric zone with anomalous properties is estimated to be 200 km (Prodehl *et al.* 1995). Recent teleseismic surface-wave studies indicate that the region with low mantle velocities is localized to the Rhine Graben itself, whereas the regional value of lithospheric thickness is *c.* 80 km (Glahn *et al.* 1993). Absolute P-wave velocities estimated by tomography models do not reveal a low-

velocity anomaly in the upper mantle beneath the Rhine Graben down to a depth of *c.* 280 km (Achauer & Masson 2002). Furthermore, regional P-wave tomography indicates high mantle velocities beneath the Rhine Graben (Ansorge *et al.* 1979; Spakman 1986; Babuška *et al.* 1988).

The Rhine Graben is characterized by weak negative Bouguer anomalies (less than -30 mGal). They are explained either by an anomalous crustal structure without any significant thermal anomaly in the mantle (Grosse *et al.* 1990) or by the presence of anomalously low-density material in the upper mantle as required by strong negative mantle residual anomalies (-150 to -200 mGal) (Yegorova *et al.* 1998). However, the latter conclusion is not supported by thermal data. High values of surface heat flow in the Rhine Graben (ranging from 70 to 140 mW m^{-2} with an average around 100 mW m^{-2}) were measured in shallow boreholes (Cermak 1995). They have a strong short-wavelength component, which implies that a large part of the heat-flow anomaly has a shallow origin and is probably caused by groundwater circulation. Thus, geophysical data on the upper mantle structure do not provide evidence for a presence of a ‘baby-plume’ beneath the Rhine Graben, but favour a passive mechanism of rifting, caused by lithospheric extension, which resulted from a complex stress field associated with the convergence of the Eurasian and the African plates.

Rhenish Massif (RM). The intensive volcanism of the RM began in the Eocene with an eruption of nephelinitic magma (Wilson *et al.* 2004), which implies a lithospheric thickness of at least 80–100 km. At *c.* 25 Ma the composition of magmas changed to basalts and trachytes with a depth of generation <60 –80 km. The youngest volcanic areas in the western part of the RM have an age of *c.* 700 ka (Lippolt 1983). Uplift of the RM began in the late Oligocene and still continues. The upper mantle structure beneath the RM is asymmetric according to different geophysical data. Contrasting Bouguer anomalies with weakly negative values (-10 to -20 mGal) to the west of the Rhine and weakly positive anomalies ($+10$ to $+20$ mGal) in the eastern part are well explained by a heterogeneous crustal structure (Jacoby *et al.* 1983). However, low velocities in the upper mantle of the RM were found both in P-wave and S-wave models (Panza *et al.* 1986; Spakman 1986; Babuška *et al.* 1988; Ritter *et al.* 2001). Teleseismic studies of the RM reveal a zone with a 3–5% low-velocity anomaly at a depth of 50–200 km, which is shallowest in the western part of the RM (Raikes & Bonjer 1983). A recent P-wave tomography experiment in the Eifel area supports earlier interpretations and shows a narrow (with a radius of about 100 km) low P-velocity anomaly in the upper mantle down to at least 400 km depth (Ritter *et al.* 2001). A lateral velocity contrast of up to 2% (with respect to the *iasp91* model) within this columnar velocity anomaly can be explained by about 150–200 K excess temperature, which was attributed to the Rhenish plume.

Nevertheless, the origin of Cenozoic tectonic and magmatic activity in the RM is still debated. The RM has high values of surface heat flow (*c.* 80 mW m^{-2}) with slightly higher values in its eastern part. Downward continuation of geotherms, constrained by upper mantle xenoliths from the RM (Seck & Wedepohl 1983), gives lithospheric thermal thickness estimates of *c.* 80–90 km (Fig. 6). Shallowing of the mantle transition zone beneath the western part of the RM is interpreted as an indicator of a possible upper mantle plume (Grunewald *et al.* 2001). Alternatively, partial melting in the upper mantle beneath the RM may be caused by passive adiabatic decompression (Schmincke *et al.* 1983) as a result of lithospheric extension during rifting (Ziegler & Cloetingh 2004).

Massif Central (MC). Volcanic activity in the MC began in the Oligocene and was accompanied by uplift of the entire massif. The main phase of volcanism was at 2–5 Ma; but there is no correlation between the age of volcanism and its geographical distribution (Werling & Altherr 1997). Similar to the RM, *P–T* analysis of lower crustal and mantle xenoliths of different ages

and from different locations (Coisy & Nicolas 1978; Werling & Altherr 1997) indicates that all of them approximately follow the 85–90 mW m⁻² reference geotherm of Pollack & Chapman (1977; Fig. 6), implying a lithospheric thermal thickness of *c.* 70–80 km at the time of eruption.

Three-dimensional regional P-wave tomography models reveal a low-velocity zone in the upper mantle of the MC at a depth of 60–100 km (Granet *et al.* 1995a), which is interpreted as the top of the mantle upwelling (plume?) (Granet *et al.* 1995b). Estimates of lithospheric thickness from P-wave residuals (Fig. 4d; Babuška *et al.* 1988, 1992) and surface waves (Souriau *et al.* 1980) also give a depth of *c.* 60–100 km. The region with a 3% velocity decrease in the upper mantle correlates spatially with both the area of recent volcanism and a local long-wavelength minimum of Bouguer anomalies (–45 mGal, Autran *et al.* 1976). However, the entire MC is characterized by the same range of residual mantle gravity anomalies (–50 to –150 mGal) as other terranes of Proterozoic to early Palaeozoic ages within the Variscides (e.g. the Bohemian and the Armorican massifs; Fig. 5).

P-wave tomography models for the MC (Granet *et al.* 1995a) have been used to constrain density and temperature of the upper mantle. Both gravity (Stoll *et al.* 1994) and temperature (Sobolev *et al.* 1996) models do not require the presence of large percentages of melt in the upper mantle of the MC, although the latter model assumes the presence of a mantle plume beneath the MC as responsible for a regional (50–70 km wide) lithospheric thinning to 70 km depth. Lucazeau *et al.* (1984) have modelled the thermal anomaly beneath the MC (where surface heat-flow values are 105 ± 13 mW m⁻²) by upwelling of a 40 km wide mantle diapir, and concluded that *c.* 50% of the anomaly can be attributed, to the crustal heat production and the rest should be ascribed to the combined effect of the mantle diapir and the Hercynian orogeny.

Petrological studies of mantle xenoliths from the MC have revealed a significant difference in the upper mantle properties beneath its southern and northern blocks (Lenoir *et al.* 2000). Mantle peridotites from the northern domain have geochemical signatures similar to peridotites from Archaean cratons (though with low Mg#; Mg# = MgO/(MgO + FeO)). Such difference in the composition of mantle peridotites may reflect a block structure of the Hercynian lithosphere formed by Palaeozoic accretion of continental terranes of different ages. Heterogeneous lithospheric structure of accreted terranes could have favoured the location of the Cenozoic mantle thermal anomaly beneath the young and thin lithosphere of the southern block of the MC.

The existence of a hidden Hercynian suture zone in the lithosphere of the MC is indicated by seismic anisotropy models (Babuška *et al.* 2002), which suggest the existence of a Cenozoic asthenospheric flow from the Western Mediterranean to beneath the MC, channelled along a boundary between different lithospheric blocks (Barruol & Granet 2002). This model does not require the presence of a mantle plume (or diapir) to explain the mantle thermal anomaly beneath the part of the MC where the strongest seismic velocity anomaly is observed in tomography models.

Synthesis: an integrated model of the European upper mantle structure and compositional variations

Comparison of different seismic models of the upper mantle of the continent (including P- and S-wave tomography, P-wave residuals, reflection and refraction profiles) with MT, electromagnetic, thermal and gravity models and mantle xenolith data is used here to constrain an integrated model of the lithosphere of Europe. A change in physical properties of the upper mantle at the lithospheric base, as reflected in different geophysical models, is temperature dependent and may be caused by high-temperature relaxation or by partial melting. The lithospheric base as

determined by different geophysical techniques may approximately correspond to the transition from the lithosphere to a zone of partial melt (see above for a detailed discussion). A diffuse character of the base of the seismic lithosphere together with a substantial thickness of the transition zone between purely conductive and purely convective heat transfer limits vertical resolution of any integrated model of lithospheric thickness to 50 km (Fig. 9).

The integrated model of the lithospheric thickness in Europe (Fig. 9) is based on P-wave seismic tomography models (Spakman 1990; Bijwaard & Spakman 2000; Piromallo & Morelli 2003), surface-wave tomography models (Panza *et al.* 1986; Du *et al.* 1998; Shapiro & Ritzwoller 2002), P-wave residuals (Babuška & Plomerová 1992), thermal models (Balling 1995; Cermak & Bodri 1995; Artemieva 2003), and *P–T* data for mantle xenoliths (Coisy & Nicolas 1978; Seck & Wedepohl 1983; Nicolas *et al.* 1987; Werling & Altherr 1997; Kukkonen & Peltonen 1999; Malkovets *et al.* 2003). Taking the limitations of different interpretation techniques into account, we compare and combine these models into a consistent map, to identify the bulk features of the lithospheric structure of Europe. Inevitably, the model smears some small-scale details; they can be found in corresponding publications of regional surveys (e.g. see the subsequent papers of this book). Our interpretation reveals continent-scale differences in both thickness (Table 2) and composition of the lithospheric mantle. These major differences reflect the tectonic history of the continent over *c.* 3.5 Ga and the effects of mantle processes on lithosphere modification. Thus, this integrated model provides a reference frame for comparing tectonic structures of Europe and their world analogues, and it forms the basis for a better understanding of geodynamic evolution of the European continent in space and time.

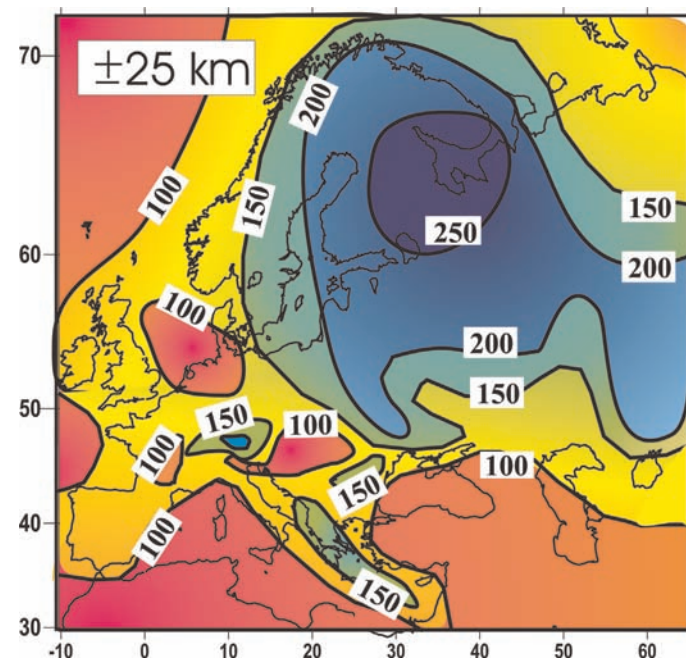


Fig. 9. Integrated model of lithospheric thickness in Europe, based on seismic, thermal, MT, electromagnetic and gravity interpretations. In general, a direct comparison of lithospheric thickness values, constrained by different techniques, is not valid, as they are based on measurements of diverse physical parameters. The difference between the thicknesses of ‘seismic’ and ‘thermal’ lithosphere can be up to 40–50 km (Jaupart & Mareschal 1999), which approximately corresponds to the thickness of the transition zone between pure conductive and pure convective heat transfer. For this reason the isolines are drawn with a 50 km interval. North Africa, Central Asia and regions with the oceanic crust are excluded.

Compositional variations within European lithospheric mantle

Compositional variations within the cratonic roots (as a result of depletion in basaltic components) result in density and seismic velocity anomalies, which may be significantly masked by temperature variations in the upper mantle. As the V_p/V_s ratio is thought to be more sensitive to variation in composition than temperature (e.g. Lee 2003), we constrain maps of V_p/V_s ratio from smoothed and filtered P- and S-wave tomography models (Bijwaard & Spakman 2000; Shapiro & Ritzwoller 2002) at depths of 150 km and 250 km and interpret them as reflecting compositional variations in the subcrustal lithosphere of Europe (Fig. 10). Teleseismic P-wave tomography has the best lateral resolution, but poorly resolves the vertical extent of velocity anomalies (see Fig. 2a and c, where the shape of the velocity anomalies has basically the same pattern at all depths in the interval 100–265 km), whereas surface-wave tomography has the best vertical resolution. These differences reduce the obtainable resolution from straightforward comparison of S-wave and P-wave tomography results. It is, however, obvious that the cratonic and Phanerozoic parts of the European mantle at depths to 150–250 km have significantly different composition. The lack of resolution in the P-wave tomography models for the northeastern part of the EEP does not permit interpretation of this part of the craton. However, a pronounced anomaly is detectable over the EEC at *c.* 250 km depth, which suggests that the lithosphere extends at least to this depth in the Finnish part of the Baltic Shield and the central–western part of the EEP.

We supplement the data on variations in V_p/V_s ratio by data on the lateral variation of mantle residual gravity anomalies, which have a good lateral resolution and almost no vertical resolution. To separate the effects of temperature and composition on density anomalies, mantle residual gravity anomalies (Fig. 5) were corrected for thermal expansion using data on lithospheric temperatures (Figs 4c and 5) and following the approach of Kaban *et al.* (2003). The gravity effect of temperature variations in the upper mantle was estimated down to 225 km depth and removed from the total mantle gravity field; the resulting ‘compositional’ density variations are shown in Figure 11a.

Another approach to separate the contributions of temperature from composition is based on independent free-board constraints (Fig. 11b; Artemieva 2003). There is a striking similarity between the two maps of density heterogeneities constrained by gravity and buoyancy (Fig. 11). However, both density maps lose resolution in the Caledonides (as a result of smearing of off-shore gravity anomalies and unaccounted dynamic topography in free-board constraints). The strongest low-density anomalies, probably caused by a highly depleted lithospheric composition, are observed in the upper mantle of the Baltic Shield. A gradual increase of average (i.e. integral for the entire lithospheric column) lithospheric density in the EEP from north to south as a result of lateral variations of the composition is evident in both maps. The average density of the lithospheric mantle of the southern parts of the EEP is similar to the density of the Phanerozoic mantle of Western Europe. This density increase in the cratonic root can be related to metasomatic reworking of the cratonic lithosphere during large-scale intensive Devonian rift-related magmatism, when infiltration of Fe-enriched basaltic magmas may have increased the average lithospheric density (Artemieva 2003). Subduction zones of the Mediterranean and the Caucasus are marked by pronounced high-density anomalies (Fig. 11a).

Because gravity anomalies do not provide constraints on the depth distribution of anomalous masses in the upper mantle, a comparison of Figure 11 with maps of V_p/V_s at different depths (Fig. 10) permits us to speculate on their vertical distribution. There is a general overall agreement between the mantle density anomalies and the seismic compositional anomalies at

150–250 km depth. In agreement with mantle xenolith data from craton and off-craton settings (e.g. Griffin *et al.* 1998), at these depths the transition from Archaean–early Proterozoic lithosphere of the Baltic Shield and the East European Platform to younger upper mantle of the Variscides, Caledonides and the Sveco-Norwegian province of the Baltic Shield is clearly seen in compositional variations (Figs 10 and 11). This finding supports the conclusion that, except for the subduction zones beneath the Western and Eastern Mediterranean, the Alps and the Carpathians, the lithosphere of Phanerozoic Europe does not reach 150 km depth. The high V_p/V_s ratio most likely results from the presence of partial melts at this depth in the upper mantle.

Compositional origin of velocity contrast in the TOR tomography

The transition from depleted to non-depleted cratonic composition is clearly imaged in the TOR seismic tomography interpretations (e.g. Arlitt 1999; Gregersen *et al.* 2002; Shomali & Roberts 2002). As thermal models do not indicate any significant change in mantle temperatures across the transition zone from the Baltic Shield to the Danish Caledonides (Balling 1995; Cermak & Bodri 1995; Artemieva 2003), the sharp P-wave velocity contrast in the TOR tomography images across the Teisseyre–Tornquist Zone (TTZ) should be attributed to a purely compositional change. Moreover, if the entire velocity anomaly observed in the TOR models is caused by compositional variations in the upper mantle, it provides additional support to an earlier hypothesis that the lower crust–uppermost mantle of Fennoscandia extends much further south than the geological boundary between the Baltic Shield and Danish Caledonides (Thybo 1990, 2001; Bayer *et al.* 2002).

Interpretations of the TOR tomography model suggest a V_p contrast between the cratonic lithosphere of the Baltic Shield and the Caledonian lithosphere as large as *c.* 3% (δV_p *c.* +1% beneath the Sveconorwegian province and δV_p *c.* –2% in the Phanerozoic mantle; e.g. Arlitt 1999). Experimental studies indicate that V_p is more sensitive to temperature variations than is V_s , which is more sensitive to variations in composition (primarily, to the iron content) (e.g. Lee 2003). As a 1% V_s anomaly can be explained by a *c.* 4% anomaly in Fe content (e.g. Deschamps *et al.* 2002), probably most of the δV_p anomaly beneath the Sveconorwegian province can be attributed to Fe depletion, although the required degree of depletion is about twice that expected for Proterozoic terranes (Griffin *et al.* 1998). The negative seismic velocity anomaly beneath Phanerozoic Europe cannot be explained in terms of iron-content variations and requires the presence of fluids or a strong mineralogical/compositional anomaly. The presence of fluids along the accreted cratonic margin, probably associated with ancient subduction zones, has been proposed earlier for the central segment of the TESZ (Nolet & Zielhuis 1994) and cannot be ruled out as a cause of a negative velocity anomaly on the Phanerozoic side of the TOR profile.

Summary

Integrated analysis of the available geophysical, petrological and tectonic data for Europe reveals the major characteristics of its lithospheric structure and tectonic evolution.

(1) Precambrian areas of Europe have a thick lithosphere, typically 150–220 km. Lithospheric thickness in the mid- and late Proterozoic provinces of the Baltic Shield is *c.* 120–180 km. There is no obvious correlation between lithospheric thickness and the geological age of the crust (i.e. the absolute age of the oldest rocks determined from Re–Os isotope data) or the tectonic age (i.e. the age of the last major thermo-tectonic event) as proposed earlier (e.g. Poudjom Djomani *et al.* 1999).

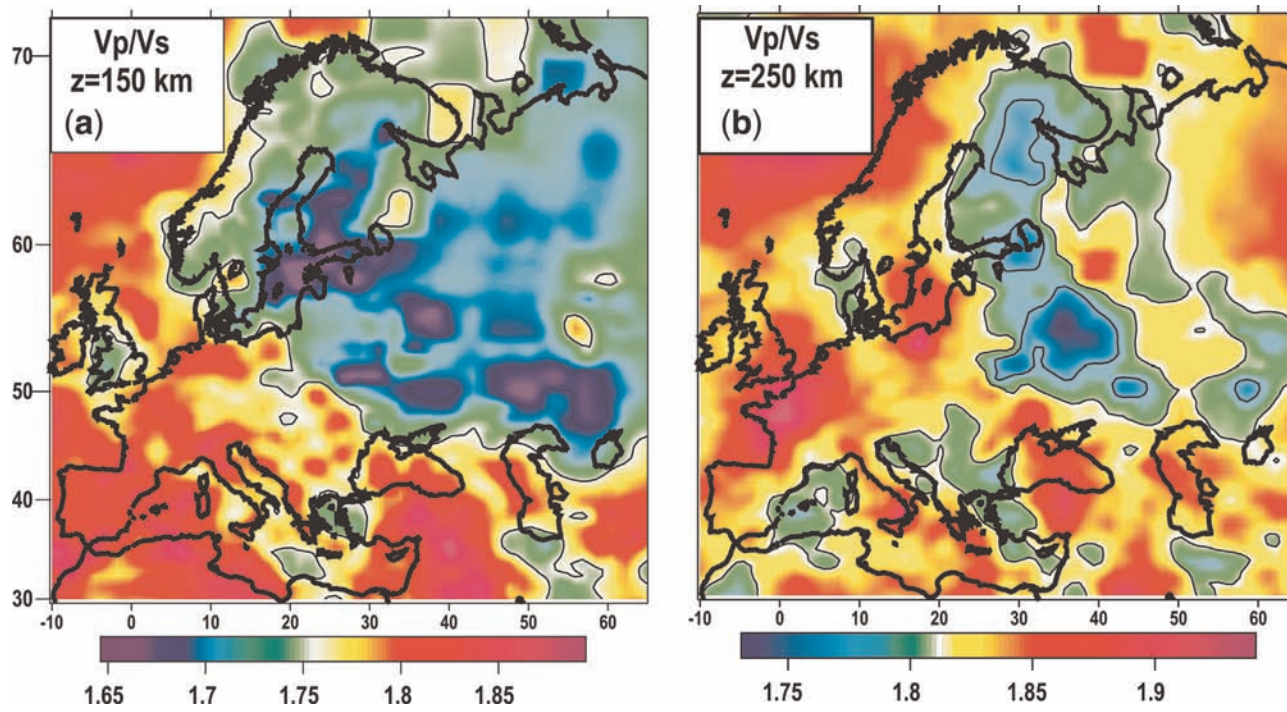


Fig. 10. Compositional anomalies in the lithosphere of Europe, represented by anomalies of V_p/V_s ratio at depths of 150 km (a) and 250 km (b) calculated from smoothed and filtered P-wave tomography model by Bijwaard & Spakman (2000) recalculated to absolute velocity by scaling by *ak135* model values and S-wave tomography model by Shapiro & Ritzwoller (2002). V_p/V_s ratio is thought to be more sensitive to compositional than temperature variations (e.g. Lee 2003). Low lateral resolution for the northeastern parts of the maps is due to low resolution of the P-wave tomography model (compare with Fig. 2a and c).

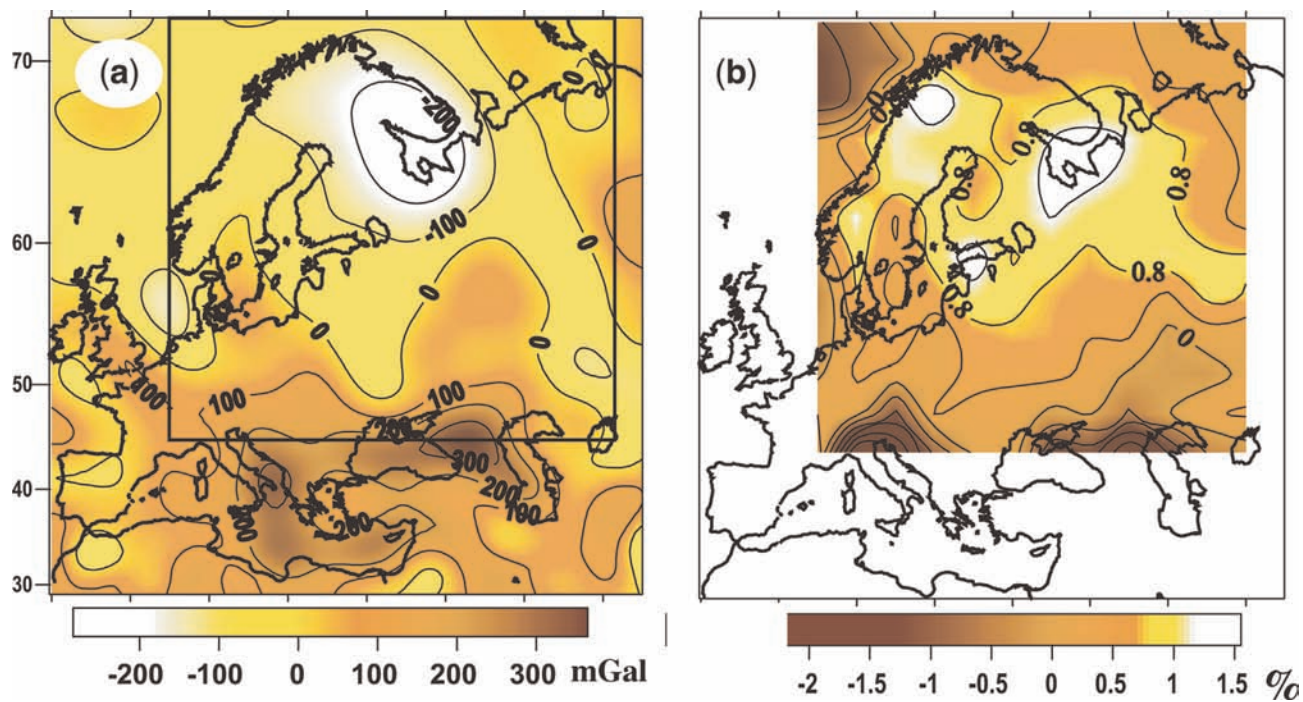


Fig. 11. Density anomalies in the upper mantle of Eurasia of a non-thermal origin. (a) Mantle residual gravity anomalies (Fig. 5) corrected for temperature (Figs 2 g and 5). The resolution of this map is limited to approximately $3^\circ \times 3^\circ$, which corresponds to a homogeneous resolution of thermal data in the study area. Conservative estimates of possible uncertainties of the residual anomalies are up to 75–100 mGal (Kaban *et al.* 2003). Amplitudes of the residual compositional anomaly significantly exceed this level (c. 600 mGal). (b) Density deficit in the subcrustal lithosphere calculated on a $5^\circ \times 5^\circ$ grid from buoyancy (using data on the topography, crustal structure, lithospheric thickness and mantle temperatures) (from Artemieva 2003). A low-density anomaly over the Caledonides may result from a non-accounted dynamic topography. The general agreement of the zero-contour of gravity anomalies (a) and 0.8% contour of density anomalies from buoyancy (b) should be noted. The maps suggest a high degree of density deficit of a non-thermal origin in the northern parts of the EEP and the Baltic Shield. This anomaly can probably be associated with an Iron depletion of the cratonic lithospheric root. The pronounced difference in the gravity field from high (west) to low (east) across the TESZ correlates with the change in V_p/V_s (Fig. 10) from low values in Western Europe to high values in the Precambrian part. In contrast, the high densities in Southern Europe (corresponding to the subduction systems in the Eastern Mediterranean Sea) correspond to very high V_p/V_s ratios.

An exceptionally thick lithospheric root is revealed by seismic, thermal and xenolith data for the Karelian part of the Baltic Shield, where it locally reaches a depth of *c.* 250–300 km. The region of thick lithosphere correlates spatially with the region of locally thick crust (>60 km) that formed during the Proterozoic orogenic event (Korja *et al.* 1993). Mantle xenoliths from the same region (at the edge of the Archaean terrane), brought to the surface by late Proterozoic (*c.* 600 Ma) kimberlite magmatism from depths as great as 240 km, sample a fluid-free mantle; this conclusion is supported by regional MT data (Kukkonen *et al.* 2003). Gravity and buoyancy constraints on mantle density (Artemieva 2003; Kaban *et al.* 2003) reveal a strong density anomaly of compositional origin in this part of the Baltic Shield, which can be attributed to a highly depleted lithosphere. We speculate that local thickening of the lithosphere could have been produced during the same tectonic (orogenic) event as the formation of the crustal root; and that the depleted and devolatilized composition of a thick cratonic root prevented its later destruction by mantle convection (Ballard & Pollack 1987). Thus, the lithospheric structure of the Karelian province may preserve evidence of tectonic processes that operated during the Proterozoic. Moreover, dipping and subhorizontal seismic reflectors at depths of 40–110 km at the margins of the Svecofennian and Sveconorwegian provinces, which are traced over distances of up to 100 km and correlate with a 5–7 km step on the Moho, are interpreted as evidence for Proterozoic subduction.

Geophysical data reveal that the lithospheric structure of the Ukrainian Shield, which was formed by amalgamation of several Archaean–early Proterozoic terranes, is highly heterogeneous and different from that of the Baltic Shield: crustal thickness varies from 38 to 58 km and lithospheric thickness is in the range of 170–220 km. Similar values of lithospheric thickness are also typical for the north–central parts of the EEP. Southern parts of the EEP, affected by Palaeozoic rifting, have thin lithosphere (100–150 km), and it is likely that the cratonic lithospheric root has been thermally eroded (and/or delaminated) and metasomatized during the Devonian rifting.

Seismic interpretations of refraction profiles (i.e. the PNE profile Quartz and FENNOLORA) and regional tomography models (i.e. SVEKALAPKO) suggest the existence of a layer at depths of 100–150 km with 1–2% lower seismic velocities than in the surrounding high-velocity cratonic upper mantle. It is important to note that seismic velocities in this reduced velocity layer within the cratonic lithosphere are *c.* 1% higher than average seismic velocities in the global continental models *ak135* or *iaspei*. The nature of the reduced velocities is debated. Alternative models suggest high subsolidus temperatures (with a possible presence of small pockets of a partially molten material), the presence of fluids or compositional anomalies (i.e. a transition from a depleted upper layer to a non-depleted lower layer within the lithospheric root).

(2) The Palaeozoic Variscan and Caledonian orogens of Western Europe were significantly reworked and overprinted by late Palaeozoic and Mesozoic–Cenozoic tectonic processes associated with the convergence of the Eurasian and the African plates (Ziegler & Dèzes 2006). They have a uniform crustal thickness (typically 28–32 km), and the lithospheric thickness is in the range of 80–140 km, with the larger values beneath the Proterozoic–early Palaeozoic terranes (the Armorican, Bohemian and Brabant massifs, and the northern part of the Massif Central). The subcrustal lithosphere has a subhorizontal layering in the upper 90 km, revealed by seismic refraction studies and mantle xenolith data. Zones of strong seismic anisotropy in the upper mantle of the Variscides are interpreted as relict subduction zones.

Compared with the Palaeozoic orogens of Western Europe, the Uralides, which remained intact within the continental interior and have not been reworked by later tectonic processes, have an

atypical structure of the crust (50–55 km thick with local roots reaching *c.* 65 km) and of the lithosphere (probably 170–200 km thick). Palaeozoic rifts within the Precambrian part of Europe (the Oslo rift and the Pripyat–Dnieper–Donets rift) have lithospheric thickness, similar to the Variscan belt, of 100–140 km.

(3) The lithospheric structure of tectonically active parts of Western Europe is highly heterogeneous. Several Cenozoic orogens formed during closure of Tethyan ocean domains and subsequent continental subduction (the Alps, Carpathians, Caucasus, Apennines), followed by the development of back-arc basins (e.g. the Tyrrhenian, Aegean and Pannonian depressions). Crustal thickness in these orogens locally reaches 60–65 km in the convergence zone of lithospheric plates, where lithospheric thickness can exceed 150–200 km. The back-arc basins have thin crust (25–30 km) and thin lithosphere (60–80 km).

In the Central European Rift System, lithospheric thickness is similar to that of the adjacent Palaeozoic Variscan structures (80–120 km), although in some parts it can be as thin as 70–80 km. Available geophysical data do not provide distinctive evidence for a plume-related origin of the CERS. Instead, they suggest a passive mechanism of rifting, so that most of tectono-magmatic activity within the CERS was caused by a complicated stress regime associated with the convergence of the Eurasian and the African lithospheric plates.

The authors are grateful to W. Spakman, C. Piromallo, N. Shapiro, M. Ritzwoller, G. Panza, Zhijun Du, M. Granet, M. Billien, J. Trampert, T. Yegorova and V. Starostenko for kindly providing their seismic tomography and gravity models and for permitting us to use them in this review. Special thanks are due to M. Cara, J. Ritsema, J. Trampert and E. Debayle for valuable discussions on the resolution of seismic tomography models. We are grateful to J. Ansorge, P. Ziegler and K. Fuchs for thoughtful, helpful and constructive reviews. The manuscript benefited from their valuable suggestions; the text, however, reflects the point of view of the authors, which does not always agree with that of the reviewers. The comments of M. Coble are appreciated. The research of I.M.A. is funded by a personal grant from Carlsbergfondet, Denmark, which is gratefully acknowledged. Economical support from the Danish Natural Science Research Council and the Carlsberg Foundation to H.T. is acknowledged.

References

- ABRAMOVITZ, T. & THYBO, H. 2000. Seismic images of Caledonian, lithosphere-scale collision structures in the southeastern North Sea along MONA LISA Profile 2. *Tectonophysics*, **317**, 27–54.
- ABRAMOVITZ, T., THYBO, H. & BERTHELTSEN, A. 1997. Proterozoic sutures and terranes in the southeastern Baltic Shield interpreted from BABEL deep seismic data. *Tectonophysics*, **270**, 259–277.
- ABRAMOVITZ, T., THYBO, H. & MONA LISA WORKING GROUP 1998. Seismic structure across the Caledonian Deformation Front along MONA LISA profile 1 in the southeastern North Sea. *Tectonophysics*, **288**, 153–176.
- ABRAMOVITZ, T., THYBO, H. & PERCHUC, E. 2002. Tomographic inversion of seismic P- and S-wave velocities from the Baltic Shield based on FENNOLORA data. *Tectonophysics*, **358**, 151–174.
- ACHAUER, U. & MASSON, F. 2002. Seismic tomography of continental rifts revisited: from relative to absolute heterogeneities. *Tectonophysics*, **358**, 17–38.
- ADAM, A. 1996. Regional magnetotelluric (MT) anisotropy in the Pannonian Basin (Hungary). *Acta Geodaetica of Geophysica Hungaricae*, **31**, 191–216.
- ADAM, A. & BIELIK, M., 1998. The crustal and upper-mantle geophysical signature of narrow continental rifts in the Pannonian basin. *Geophysical Journal International*, **134**, 157–166.
- ADAM, A., VANYAN, L. L., VARLAMOV, D. A., YEGOROV, I. V., SHILOVSKY, A. P. & SHILOVSKY, P. P. 1982. Depth of crustal conducting layer and asthenosphere in the Pannonian Basin determined by magnetotellurics. *Physics of the Earth and Planetary Interiors*, **28**, 251–260.
- ANDERSON, D. L. 1989. *Theory of the Earth*. Blackwell Scientific, Boston, MA.

- ANDREESCU, M., NIELSEN, S. B., POLONIC, G. & DEMETRESCU, C. 2002. Thermal budget of the Transylvanian lithosphere. Reasons for a low surface heat-flux anomaly in a Neogene intra-Carpathian basin. *Geophysical Journal International*, **150**, 494–505.
- ANSORGE, J., BONJER, K.-P. & EMTER, D. 1979. Structure of the uppermost mantle from long-range seismic observations in southern Germany and the Rhinegraben area. *Tectonophysics*, **56**, 31–48.
- ARLITT, R. 1999. *Teleseismic body wave tomography across the trans-European suture zone between Sweden and Denmark*. PhD thesis, ETH, Zurich.
- ARTEMIEVA, I. M. 1993. Petrochemical data as an indicator of a deep heat regime of intraplate continental areas of magmatic activity. *Journal of the Society of Resource Geology*, **B16**, 82–93.
- ARTEMIEVA, I. M. 2003. Lithospheric structure, composition, and thermal regime of the East European craton: implications for the subsidence of the Russian Platform. *Earth and Planetary Science Letters*, **213**, 429–444.
- ARTEMIEVA, I. M. 2006. Global $1^\circ \times 1^\circ$ thermal model TC1 for the continental lithosphere: Implications for lithosphere secular evolution. *Tectonophysics*, **416**, 245–277.
- ARTEMIEVA, I. M. & MOONEY, W. D. 2001. Thermal structure and evolution of Precambrian lithosphere: a global study. *Journal of Geophysical Research*, **106**, 16387–16414.
- ARTEMIEVA, I. M. & MOONEY, W. D. 2002. On the relation between cratonic lithosphere thickness, plate motions, and basal drag. *Tectonophysics*, **358**, 211–231.
- ARTEMIEVA, I. M., MOONEY, W. D., PERCHUC, E. & THYBO, H. 2002. Processes of lithosphere evolution: new evidence on the structure of the continental crust and upper mantle. *Tectonophysics*, **358**, 1–15.
- ARTEMJEV, M. E., DEMJANOV, G. V., KABAN, M. K. & KUCHERINENKO, V. A. 1993. Gravity field of the lithosphere density inhomogeneities of Northern Eurasia. *Physics of the Solid Earth*, **5**, 12–22.
- ARTEMJEV, M. E., KABAN, M. K., KUCHERINENKO, V. A., DEMYANOV, G. V. & TARANOV, V. A. 1994. Subcrustal density inhomogeneities of northern Eurasia as derived from the gravity data and models of the lithosphere. *Tectonophysics*, **240**, 249–280.
- ARTYUSHKOV, E. V. 1993. *Physical Tectonics*. Nauka, Moscow (in Russian).
- AULBACH, S., GRIFFIN, W. L., PEARSON, N. J., O'REILLY, S. Y., DOYLE, B. J. & KIVI, K. 2001. Re-Os Isotope Evidence for Meso-Archaean Mantle Beneath 2.7 Ga Contwoyto Terrane, Slave Craton, Canada: Implications for the Tectonic History of the Slave Craton. In: *Proc. Slave-Kaapvaal Workshop, Merrickville, Canada, Sept. 5–9, 2001*; <http://www.cg.nrcan.gc.ca/slave-kaapvaal-workshop/>.
- AUSTRHEIM, H. 1991. Eclogite formation and dynamics of crustal roots under continental collision zones. *Terra Nova*, **3**(5), 492–499.
- AUTRAN, A., GERARD, A. & WEBER, C. 1976. La carte gravimétrique de la France, exemples d'utilisation géologique. *Bulletin de la Société Géologique de France*, **18**, 1119–1132.
- BABEL WORKING GROUP 1990. Evidence for early Proterozoic plate tectonics from seismic reflection profiles in the Baltic Shield. *Nature*, **348**, 34–38.
- BABEL WORKING GROUP 1993. Deep seismic reflection/refraction interpretation of crustal structure along BABEL profiles A and B in the southern Baltic Sea. *Geophysical Journal International*, **112**, 325–343.
- BABUŠKA, V. & PLOMEROVÁ, J. 1992. The lithosphere in central Europe—seismological and petrological aspects. *Tectonophysics*, **207**, 141–163.
- BABUŠKA, V., PLOMEROVÁ, J. & PAJDUSAK, P. 1988. Lithosphere–asthenosphere in central Europe: models derived from P residuals. In: NOLET, G. & DOST, B. (eds) *Proceedings of the 4th EGT Workshop: The Upper Mantle*. ESF, Strasbourg, 37–48.
- BABUŠKA, V., PLOMEROVA, J. & GRANET, M. 1990. The deep lithosphere in the Alps: a model inferred from P residuals. *Tectonophysics*, **176**, 137–165.
- BABUŠKA, V., PLOMEROVA, J., VECSEY, L., GRANET, M. & ACHAUER, U. 2002. Seismic anisotropy of the French Massif Central and predisposition of Cenozoic rifting and volcanism by Variscan suture hidden in the mantle lithosphere. *Tectonics*, **21**(4), doi 10.1029/2001TC901035.
- BADAL, J., CORCHETE, V., PAYO, G., CANAS, J. A. & PUJADES, L. 1996. Imaging of shear wave velocity structure beneath Iberia. *Geophysical Journal International*, **124**, 591–611.
- BALLARD, S. & POLLACK, H. N. 1987. Diversion of heat by Archaean cratons: a model for southern Africa. *Earth and Planetary Science Letters*, **85**, 253–264.
- BALLING, N. 1995. Heat flow and thermal structure of the lithosphere across the Baltic Shield and northern Tornquist Zone. *Tectonophysics*, **244**, 13–50.
- BANKA, D., PHARAOH, T. C., WILLIAMSON, J. P. & TESZ PROJECT POTENTIAL FIELD CORE GROUP 2002. Potential field imaging of Palaeozoic orogenic structure in northern and central Europe. *Tectonophysics*, **360**, 23–45.
- BARRUOL, G. & GRANET, M. 2002. A Tertiary asthenospheric flow beneath the southern French Massif Central indicated by upper mantle seismic anisotropy and related to the west Mediterranean extension. *Earth and Planetary Science Letters*, **202**, 31–47.
- BAYER, U., GRAD, M., PHARAOH, T. C., ET AL. 2002. The southern margin of the East European Craton: new results from seismic sounding and potential field between the North Sea and Poland. *Tectonophysics*, **360**, 301–314.
- BEA, F., FERSHTATER, G., MONTERO, P., SMIRNOV, V. & ZINKOVA, E. 1997. Generation and evolution of subduction-related batholiths from the central Urals: constraints on the P–T history of the Uralian orogen. *Tectonophysics*, **276**, 103–116.
- BEHR, H. J. & HEINRICH, T. 1987. Geological interpretation of DEKORP 2-5: a deep seismic reflection profile across the Saxo-Thuringian and possible implications for the late Variscan structural evolution of Central Europe. *Tectonophysics*, **142**, 173–202.
- BEHR, H. J., ENGEL, W., FRANKE, W., GIESE, P. & WEBER, K. 1984. The Variscan belt in central Europe—main structures, geodynamic implications, open questions. *Tectonophysics*, **109**, 15–40.
- BERGERAT, F. 1989. From pull-apart to the rifting process: the formation of the Pannonian basin. *Tectonophysics*, **157**, 271–280.
- BIELIK, M., MAJČIN, D., FUSAN, O., BURDA, M., VYSKOCIL, V. & TRESL, J. 1991. Density and geothermal modelling of the Western Carpathian Earth's crust. *Geologica Carpathica*, **42**, 315–322.
- BIJWAARD, H. & SPAKMAN, W. 2000. Non-linear global P-wave tomography by iterated linearized inversion. *Geophysical Journal International*, **141**, 71–82.
- BILLIEN, M., LÉVÊQUE, J.-J. & TRAMPERT, J. 2000. Global maps of Rayleigh wave attenuation for periods between 40 and 150 seconds. *Geophysical Research Letters*, **27**, 3619–3622.
- BLANCO, M. J. & SPAKMAN, W. 1993. The P-wave velocity structure of the mantle below the Iberian Peninsula: evidence for subducted lithosphere below southern Spain. *Tectonophysics*, **221**, 13–34.
- BLEIBINHAUS, F. & TRANSALP WORKING GROUP 2001. Velocity structure in the Eastern Alps along the TRANSALP profile. *Geophysical Research Abstracts*, **3**, 620.
- BLUNDELL, D., FREEMAN, R. & MUELLER, S. (eds) 1992. *A Continent Revealed. The European Geotraverse*. Cambridge University Press, Cambridge.
- BOCK, G., ACHAUER, U., ALINAGHI, A., ET AL. 2001. Seismic probing of Fennoscandian lithosphere. *EOS Transactions, American Geophysical Union*, **82**, 621, 628–629.
- BOJAR, A. V., NEUBAUER, F. & FRITZ, H. 1998. Cretaceous to Cenozoic thermal evolution of the southwestern South Carpathians: evidence from fission-track thermochronology. *Tectonophysics*, **297**, 229–249.
- BOSCHI, L., EKSTROM, G. & KUSTOWSKI, B. 2004. Multiple resolution surface wave tomography: the Mediterranean basin. *Geophysical Journal International*, **157**, 293–304.
- BOSTOCK, M. G. 1999. Seismic imaging of lithospheric discontinuities and continental evolution. *Lithos*, **48**, 1–16.
- BOTT, M. P. H. 1990. Stress-distribution and plate boundary force associated with collision mountain-ranges. *Tectonophysics*, **182**, 193–209.
- BOTT, M. P. H. 1995. Rifted passive margins. In: OLSEN, K. H. (ed) *Continental Rifts: Evolution, Structure, Tectonics. Developments in Geotectonics*, **25**, 409–426.
- BOUSQUET, R., GOFFE, B., HENRY, P., LE PICHON, X. & CHOPIN, C. 1997. Kinematic, thermal and petrological model of the Central Alps:

- Lepontine metamorphism in the upper crust and eclogitisation of the lower crust. *Tectonophysics*, **273**, 105–128.
- BROWN, D., JUHLIN, C., ALVAREZ-MARRON, J., PEREZ-ESTAUN, A. & OSLIANSKI, A. 1998. Crustal-scale structure and evolution of an arc–continent collision zone in the southern Urals, Russia. *Tectonics*, **17**, 158–171.
- BROWN, D., JUHLIN, C. & PUCHKOV, V. (eds) 2002. *Mountain Building in the Uralides*. Geophysical Monograph. American Geophysical Union, **132**.
- BRUNETON, M., PEDERSEN, H., FARRA, V., ARNDT, N., KUKKONEN, I., VACHER, P. & SSTWG 2004. Evolution of Precambrian lithosphere in Finland as inferred from seismic surface waves and mantle xenoliths. *Geophysical Research Abstracts*, **6**, 03477.
- CALCAGNILE, G. 1982. The lithosphere–asthenosphere system in Fennoscandia. *Tectonophysics*, **90**, 19–35.
- CALCAGNILE, G. 1991. Deep structure of Fennoscandia from fundamental and higher mode dispersion of Rayleigh waves. In: MUELLER, S. (ed.) *The European Geotraverse, Part 7*. Elsevier, Amsterdam, 139–149.
- CALCAGNILE, G., PERRI, P., DEL GAUDIO, V. & MULLER, S. 1990. A two-dimensional velocity model for the upper mantle beneath FENNO-LORA from seismic surface waves and body waves. In: FREEMAN, R., GIESE, P. & MULLER, S. (eds) *The European Geotraverse: Integrative Studies*. ESF, Strasbourg, 49–66.
- CALVERT, A. J., SAWYER, E. W., DAVIS, W. J. & LUDDEN, J. N. 1995. Archean subduction inferred from seismic images of a mantle suture in the Superior province. *Nature*, **375**, 670–674.
- CARBONELL, R., PEREZ-ESTAUN, A., GALLART, J., ET AL., 1996. A crustal root beneath the Urals: wide-angle seismic evidence. *Science*, **274**, 222–224.
- CARBONELL, R., GALLART, J., PEREZ-ESTAUN, A., ET AL. 2000. Seismic wide-angle constraints on the crust of the southern Urals, *Journal of Geophysical Research*, **105**(B6), 13755–13777.
- CARLSON, R. W., SHIREY, S. B., PEARSON, D. G. & BOYD, F. R. 1994. The mantle beneath continents. *Carnegie Institution of Washington Yearbook*, **93**, 109–117.
- CASTELLARIN, A. & CANTELLI, L. 2000. Neo-Alpine evolution of the Southern Eastern Alps. *Journal of Geodynamics*, **30**, 251–274.
- CAVAZZA, W., ROURE, F., SPAKMAN, W., STAMPFLI, G. M. & ZIEGLER, P. A. (eds) 2004. *The TRANSMED Atlas—The Mediterranean Region from Crust to Mantle*. Springer, Berlin.
- CERMAK, V. 1982. Geothermal model of the lithosphere and the map of the lithosphere thickness for the USSR territory. *Izvestiya AN SSSR, Fizika Zemli*, **11**, 25–38 [In Russian].
- CERMAK, V. 1993. Lithospheric thermal regimes in Europe. *Physics of the Earth Planetary Interiors*, **79**, 179–193.
- CERMAK, V. 1994. Results of heat flow studies in Czechoslovakia. In: BUCHA, V. & BLIŽKOVSKY, M. (eds) *Crustal Structure of the Bohemian Massif and the West Carpathians*. Springer, Berlin, 85–118.
- CERMAK, V. & BODRI, L. 1995. Three-dimensional deep temperature modeling along the European Geotraverse. *Tectonophysics*, **244**, 1–12.
- CERMAK, V. 1995. A geothermal model of the Central Segment of the European Geotraverse. *Tectonophysics*, **244**, 51–56.
- CHEKUNOV, A. V., GAVRISH, V. K., KUTAS, R. I. & RYABCHUN, L. I. 1992. Dnieper–Donets paleorift. *Tectonophysics*, **208**, 257–272.
- CHRISTENSEN, N. I., MEDARIS, L. G., WANG, H. F. & JELINEK, E. 2001. Depth variation of seismic anisotropy and petrology in central European lithosphere: a tectonothermal synthesis from spinel lherzolite. *Journal of Geophysical Research*, **106**, 645–664.
- CLOETINGH, S. A. P. L., BUROV, E. & MATENCO, L. 2004. Thermo-mechanical controls on the mode of continental collision in the SE Carpathians (Romania). *Earth and Planetary Science Letters*, **218**, 57–76.
- CLOWES, R. M., COOK, F. A. & LUDDEN, J. N. 1998. LITHOPROBE leads to new perspectives on continental evolution. *GSA Today*, **8**, 1–7.
- COISY, P. & NICOLAS, A. 1978. Regional structure and geodynamics of the upper mantle beneath the Massif Central. *Nature*, **274**, 429–432.
- COOK, F. A., VAN DER VELDEN, A. J., HAL, K. W. ET AL. 1998. Tectonic delamination and subcrustal imbrication of the Precambrian lithosphere in northwestern Canada mapped by LITHOPROBE. *Geology*, **26**, 839–842.
- COOK F. A., VAN DER VELDEN A. J., HALL K. W. & ROBERTS, B. J. 1999. Frozen subduction in Canada's Northwest Territories: Lithoprobe deep lithospheric reflection profiling of the western Canadian Shield. *Tectonics*, **18**, 1–26.
- COTTE, N., PEDERSEN, H. A. & TOR WORKING GROUP 2002. Sharp contrast in lithospheric structure across the Sorgenfrei–Tornquist Zone as inferred by Rayleigh wave analysis of TOR1 project data. *Tectonophysics*, **360**, 75–88.
- CRANGANU, C. & DEMING, D. 1996. Heat flow and hydrocarbon generation in the Transylvanian basin, Romania. *AAPG Bulliten*, **80**, 1641–1653.
- DARBYSHIRE, F. A. 2005. Upper mantle structure of Arctic Canada from Rayleigh wave dispersion. *Tectonophysics* **405**, 1–23.
- DAVY, P. & GILLET, P. 1986. The stacking of thrust slices in collision zones and its thermal consequences. *Tectonics*, **5**, 913–929.
- DEGTIAREV, K. E. 2001. Major stages in Palaeozoic evolution of the Southern Urals. In: MOROZOV, A. F. (ed.) *Deep Structure and Geodynamics of the Southern Urals (the URALSEIS Project)*. Ministry of Natural Resources of Russia, Tver, 270–274 (in Russian).
- DELLA VEDOVA, B., LUCAZEAU, F., PELLIS, G. & PASQUALE, V. 1990. Heat flow and tectonics along the EGT southern segment. In: FREEMAN, R. & MUELLER, S. (eds) *Proceedings of the 6th EGT Workshop*. ESF, Strasbourg, 431–440.
- DE METS, C., GORDON, R. G., ARGUS, D. F. & STEIN, S. 1994. Effect of recent revisions to the geomagnetic reversal time scale on estimates of current plate motions. *Geophysical Research Letters*, **21**, 2191–2194.
- DESCHAMPS, F., TRAMPERT, J. & SNIEDER, R. 2002. Anomalies of temperature and iron in the uppermost mantle inferred from gravity data and tomographic models. *Physics of the Earth and Planetary Interiors*, **129**, 245–264.
- DEZES, P., SCHMID, S. M. & ZIEGLER, P. A. 2004. Evolution of the European Cenozoic Rift System: interaction of the Alpine and Pyrenean orogens with their foreland lithosphere. *Tectonophysics*, **389**, 1–33.
- DEWEY, J. F. 1969. Evolution of the Caledonian/Appalachian orogen. *Nature*, **222**, 124–129.
- DOBREFRACTION'99 WORKING GROUP 2003. 'DOBREFRACTION'99'-velocity model of the crust and upper mantle beneath the Donbas Foldbelt (East Ukraine). *Tectonophysics*, **371**, 81–110.
- DÖRING, J., GÖTZE, H. J. & KABAN, M. K. 1997. Preliminary study of the gravity field of the southern Urals along the URSEIS 95 seismic profile. *Tectonophysics*, **276**, 49–62.
- DRUZHININ, V. S., EGORKIN, A. V. & KASHUBIN, S. N. 1990. New data on the deep structure of the Urals and adjacent regions from DSS studies. *Doklady Akademii Nauk SSSR*, **315**(5), 1086–1090 (in Russian).
- DU, Z. J., MICHELINI, A. & PANZA, G. F. 1998. EurID: a regionalized 3-D seismological model of Europe. *Physics of the Earth and Planetary Interiors*, **106**, 31–62.
- EDWARDS, R. L. & WASSERBURG, G. J. 1985. The age and emplacement of obducted oceanic crust in the Urals from Sm–Nd and Rb–Sr systematics. *Earth and Planetary Science Letters*, **72**, 389–404.
- EGORKIN, A. V. & MIKHALTSEV, A. V. 1990. The result of seismic investigations along geotraverses. In: FUCHS, K., KOZLOVSKY, YE. A., KRIVTSOV, A. I. & ZOBACK M. D. (eds) *Super-deep Continental Drilling and Deep Geophysical Sounding*. Springer, Berlin, 111–119.
- EMMERMANN, R. 1977. A petrogenetic model for the origin and evolution of the Hercynian granite series of the Schwarzwald. *Neues Jahrbuch für Mineralogie, Abhandlungen*, **128**, 219–253.
- EREGT GROUP 1990. An electrical resistivity crustal section from the Alps to the Baltic Sea (central segment of the EGT). *Tectonophysics*, **207**, 123–139.
- ERSHOV, A. V., BRUNET, M.-F., NIKISHIN, A. M., BOLOTOV, S. N., NAZAREVICH, B. P. & KOROTAEV, M. V. 2003. Northern Caucasus basin: thermal history and synthesis of subsidence models. *Sedimentary Geology*, **156**, 95–118.
- EUROBRIDGE WORKING GROUP & EUROBRIDGE'95 2001. Deep seismic profiling within the East European Craton. *Tectonophysics*, **339**, 153–175.
- FABER, S. & BAMFORD, D. 1979. Lithospheric structural contrasts across the Caledonides of Northern Britain. *Tectonophysics*, **56**, 17–30.

- FRANKE, W. 1986. Development of the central European Variscides—a review. In: FREEMAN, R. & MUELLER, S. (eds) *Proceedings of the 3rd EGT Workshop*, ESF, Strasbourg, 65–72.
- FRIBERG, M., JUHLIN, C., ROTH, J., HORSTMAYER, H., RYBALKA, A. & BLIZNETSOV, M. 2001. Europrobe seismic reflection profiling across the eastern Middle Urals and West Siberian Basin. *Terra Nova*, **14**, 7–13.
- FUCHS, K. & WEDEPOHL, K. H. 1983. Relation of geophysical and petrological models of upper mantle structure of the Rhenish massif. In: FUCHS, K., VON GEHLEN, K., MÄLZER, H., MURAWSKI, H. & SEMMEL, A. (eds) *Plateau Uplift—the Rhenish Shield—a Case History*. Springer, Berlin, 352–363.
- GAAL, R. & GORBATSCHEV, R. 1987. An outline of the Precambrian evolution of the Baltic shield. *Precambrian Research*, **35**, 15–52.
- GALUSHKIN, YU. I. & KUTAS, R. I. 1995. Dnieper–Donets paleorift: evolution of thermal regime and oil and gas potential. *Geophysical Journal (Kiev)*, **15**, 335–352 [in Russian].
- GARETSKII, R. G., BOBORYKIN, A. M., BOGINO, V. A., GERMAN, V. A., VERES, S. A., KLUSHIN, S. V. & SHAFARUK, V. G. 1990. Deep seismic sounding on the territory of Belorussia. *Geophysical Journal International*, **8**, 439–448.
- GEE, D. & ARTEMIEVA, I. M. (eds) 2001. *EUROPROBE 1992–2001*. Uppsala University, Uppsala.
- GEE, D. & ZEYEN, H. (eds) 1996. *EUROPROBE*. Uppsala University, Uppsala.
- GIESE, P. 1985. The structure of the upper lithosphere between the Ligurian Sea and the Southern Alps. Part B: the consolidated crust and the uppermost mantle. In: GALSON, D. A. & MUELLER, S. (eds) *Proceedings of the 2nd EGT Workshop: the Southern Segment*. ESF, Strasbourg, 143–154.
- GIESE, P. & BUNESS, H. 1992. Moho depth. In: BLUNDELL, D., FREEMAN, R., & MUELLER, S. (eds) *A Continent Revealed: The European Geotraverse*. Cambridge University Press, Cambridge.
- GLAHN, A., GRANET, M. & THE RHINE GRABEN TELESEISMIC GROUP 1993. Southern Rhine Graben: small wavelength tomographic study and its implication for the dynamic evolution of the graben. *Geophysical Journal International*, **113**, 399–418.
- GOES, S., GOVERS, R. & VACHER, P. 2000. Shallow mantle temperatures under Europe from P and S wave tomography. *Journal of Geophysical Research*, **105**, 11,153–11,169.
- GOODWIN, A. M. 1996. *Principles of Precambrian Geology*. Academic Press, London.
- GORBATSCHEV, R. & BOGDANOVA, S. 1993. Frontiers in the Baltic Shield. *Precambrian Research*, **64**, 3–21.
- GRAD, M. & TRIPOLSKY, A. 1995. Crustal structure from P and S seismic waves and petrological model of the Ukrainian shield. *Tectonophysics*, **250**, 89–112.
- GRAD, M., KELLER, G. R., THYBO, H., GUTERCH, A. & POLONAISE WORKING GROUP 2002. Lower lithospheric structure beneath the Trans-European Suture Zone from POLONAISE'97 seismic profiles. *Tectonophysics*, **360**, 153–168.
- GRAND, S. P. & HELMBERGER, D. V. 1984. Upper mantle shear structure of North America. *Geophysical Journal of the Royal Astronomical Society*, **76**, 399–438.
- GRANET, M., STOLL, G., DOREL, J., ACHAUER, U., POUPINET, G. & FUCHS, K. 1995a. Massif Central (France): new constraints on the geodynamical evolution from teleseismic tomography. *Geophysical Journal International*, **121**, 33–48.
- GRANET, M., WILSON, M. & ACHAUER, U. 1995b. Imaging a mantle plume beneath the French Massif Central. *Earth and Planetary Science Letters*, **136**, 281–296.
- GREGERSEN, S., VOSS, P. & TOR WORKING GROUP 2002. Summary of project TOR: delineation of a stepwise, sharp, deep lithosphere transition across Germany–Denmark–Sweden. *Tectonophysics*, **360**, 61–73.
- GRIFFIN, W. L., O'REILLY, S. Y., RYAN, C. G., GAUL, O. & IONOV, D. 1998. Secular variation in the composition of subcontinental lithospheric mantle. In: BRAUN, J., DOOLEY, J., GOLEBY, B., VAN DER HILST, R. & KLOOTWIJK, C. (eds) *Structure and Evolution of the Australian Continent*. American Geophysical Union, Geodynamics Series, **26**, 1–25.
- GROSSE, S., CONRAD, W., BEHR, H. J., & HEINRICHS, T. 1990. Major gravity axes and anomalies in Central Europe. In: FREEMAN, R., GIESE, P. & MUELLER, S. (eds) *The European Geotraverse: Integrative Studies*. ESF, Strasbourg, 135–146.
- GRUNEWALD, S., WEBER, M. & KIND, R. 2001. The upper mantle under Central Europe: indications for the Eifel plume. *Geophysical Journal International*, **147**, 590–601.
- GUGGISBERG, B. 1986. *Eine zweidimensionale refraktionsseismische Interpretation der geschwindigkeits-Tiefenstruktur des oberen Mantels unter dem Fennoskandischen Schild (Projekt FENNO-LORA)*. PhD Thesis, ETH Zurich.
- GUGGISBERG, B. & BERTHELSEN, A. 1987. A two-dimensional velocity model for the lithosphere beneath the Baltic Shield and its possible tectonic significance. *Terra Cognita*, **7**, 631–638.
- GURNIS, M. 1992. Rapid continental subsidence following the initiation and evolution of subduction. *Science*, **255**, 1556–1558.
- GUTERCH, A., GRAD, M., MATERZOK, R. & PERCHUC, E. 1986. Deep structure of the Earth's crust in the contact zone of the Palaeozoic and Precambrian platforms in Poland (Tornquist–Teisseyre Zone). *Tectonophysics*, **128**, 251–279.
- HAMILTON, W. 1970. The Uralides and the motion of the Russian and Siberian platforms. *Geological Society of American Bulletin*, **81**, 2553–2576.
- HIRN, A., STEINMETZ, L., KIND, R. & FUCHS, K. 1973. Long-range profiles in western Europe. II. Fine structure of the lower lithosphere in France (southern Bretagne). *Zeitschrift für Geophysik*, **39**, 363–381.
- HIRN, A., DAIGNIERES, M., GALLART, J. & VADELL, M. 1980. Explosion seismic sounding of throws and dips in the continental Moho. *Geophysical Research Letters*, **7**, 263–266.
- HIRN, A., POUPINET, G., WITTLINGER, G., GALLART, J. & THOUVENOT, F. 1984. Pyrenees and Alps: teleseismic prospecting of lithospheric contrasts. *Nature*, **308**, 531–533.
- HJELT, S.-E. & KORJA, T. 1993. Lithospheric and upper-mantle structures, results of electromagnetic soundings in Europe. *Physics of the Earth Planetary Interiors*, **79**, 137–177.
- HORVATH, F. 1993. Towards a mechanical model for the formation of the Pannonian Basin. *Tectonophysics*, **226**, 333–357.
- HUISMANS, R. S. & BERTOTTI, G. 2002. The Transylvanian basin, transfer zone between coeval extending and contracting regions: inferences on the relative importance of slab pull and rift push in arc–back arc systems. *Tectonics*, **21**(2), DOI: 10.1029/2001TC900026.
- HUISMANS, R. S., PODLADCHIKOV, Y. Y. & CLOETINGH, S. A. P. L. 2001. Dynamic modeling of the transition from passive to active rifting, application to the Pannonian basin. *Tectonics*, **20**, 1021–1039.
- ILIHA DSS GROUP 1993. A deep seismic sounding investigation of lithospheric heterogeneity and anisotropy beneath the Iberian Peninsula. *Tectonophysics*, **221**, 35–51.
- JACOBY, W. R., JOACHIMI, H. & GERSTENECKER, C. 1983. The gravity field of the Rhenish massif. In: FUCHS, K., VON GEHLEN, K., MÄLZER, H., MURAWSKI, H. & SEMMEL, A. (eds) *Plateau Uplift—the Rhenish Shield: a Case History*. Springer, Berlin, 247–258.
- JAPSEN, P. & CHALMERS, J. A. 2000. Neogene uplift and tectonics around the North Atlantic: Overview. *Global Planetary Change*, **24**, 165–173.
- JAUPART, C. & MARESCHAL, J.-C. 1999. The thermal structure and thickness of continental roots. *Lithos*, **48**, 93–114.
- JONES, A. G. 1982. On the electrical crust–mantle structure in Fennoscandia: no Moho and the asthenosphere revealed? *Geophysical Journal of the Royal Astronomical Society*, **68**, 371–388.
- JONES, A. G. 1984. The electrical structure of the lithosphere and asthenosphere beneath the Fennoscandian shield. *Journal of Geomagnetism and Geoelectricity*, **35**, 811–827.
- JORDAN, T. H. 1988. Structure and formation of the continental tectosphere. *Journal of Petrology, Special Lithosphere Issue*, 11–37.
- JUDENHERC, S., GRANET, M., BRUN, J.-P., POUPINET, G., PLOMEROVÁ, J., MOCQUET, A. & ACHAUER, U. 2002. Images of lithospheric heterogeneities in the Armorican segment of the Hercynian Range in France. *Tectonophysics*, **358**, 121–134.
- KABAN, M. 2001. A gravity model of the North Eurasia crust and upper mantle: 1. Mantle and isostatic residual gravity anomalies. *Russian Journal of Earth Science*, **3**(2), 143–163.

- KABAN, M. K. & SCHWINTZER, P. 2001. Oceanic upper mantle structure from experimental scaling of Vs and density at different depths. *Geophysical Journal International*, **147**, 199–214.
- KABAN, M. K., SCHWINTZER, P. & TIKHOTSKY, S. A. 1999. Global isostatic residual geoid and isostatic gravity anomalies. *Geophysical Journal International*, **136**, 519–536.
- KABAN, M. K., SCHWINTZER, P., ARTEMIEVA, I. M. & MOONEY, W. D., 2003. Density of the continental roots: compositional and thermal effects. *Earth and Planetary Science Letters*, **209**, 53–69.
- KENNETT, B. L. N. & ENGDAHL, E. R. 1991. Traveltimes for global earthquake location and estimation. *Geophysical Journal International*, **105**, 429–465.
- KHAIN, V. E. 1985. *Geology of the USSR. First Part. Old Cratons and Palaeozoic Fold Belts*. Borntraeger, Berlin.
- KINCK, J. J., HUSEBYE, E. S. & LUND, C.-E. 1991. The Scandinavian crust—structural complexities from seismic reflection and refraction profiling. *Tectonophysics*, **189**, 117–133.
- KING, S. D. & ANDERSON, D. L. 1995. An alternative mechanism of flood basalt formation. *Earth and Planetary Science Letters*, **136**, 269–279.
- KISSLING, E. 1993. Deep structures of the Alps—what do we really know? *Physics of the Earth and Planetary Interiors*, **79**, 87–112.
- KISSLING, E. & SPAKMAN, W. 1996. Interpretation of tomographic images of uppermost mantle structure: examples from the Western and Central Alps. *Journal of Geodynamics*, **21**, 97–111.
- KNAPP, J. H., STEER, D. N., BROWN, L. D., ET AL. 1996. Lithosphere-scale seismic image of the Southern Urals from explosion-source reflection profiling. *Science*, **274**, 226–228.
- KNAPP, J. H., DIACONESCU, C. C., BADER, M. A., SOKOLOV, V. B., KASHUBIN, S. N. & RYBALKA, A. V. 1998. Seismic reflection fabrics of continental collision and post-orogenic extension in the Middle Urals, central Russia. *Tectonophysics*, **288**, 115–126.
- KORJA, A., KORJA, T., LUOSTO, U. & HEIKKINEN, P. 1993. Seismic and geoelectric evidence for collisional and extensional events in the Fennoscandian shield—implications for Precambrian crustal evolution. *Tectonophysics*, **219**, 129–152.
- KORJA, T. 1990. *Electrical conductivity of the lithosphere. Magnetotelluric studies in the Fennoscandian Shield, Finland*. PhD thesis, University of Oulu.
- KOSTYUCHENKO, S. L., EGORKIN, A. V. & SOLODILOV, L. N. 1999. Structure and genetic mechanisms of the Precambrian rifts of the East European Platform in Russia by integrated study of seismic, gravity, and magnetic data. *Tectonophysics*, **313**, 9–28.
- KUKKONEN, I. T. 1998. Temperature and heat flow density in a thick cratonic lithosphere: the Sveka transect, central Fennoscandian Shield. *Journal of Geodynamics*, **26**, 111–136.
- KUKKONEN, I. T. & JOELEHT, A. 1996. Geothermal modelling of the lithosphere in the central Baltic Shield and its southern slope. *Tectonophysics* **255**, 24–45.
- KUKKONEN, I. T. & PELTONEN, P. 1999. Xenolith-controlled geotherm for the central Fennoscandian Shield: implications for lithosphere–asthenosphere relations. *Tectonophysics*, **304**, 301–315.
- KUKKONEN, I. T., GOLOVANOVA, I. V., KHACHAY, YU. V., DRUZHININ, V. S., KASAREV, A. M. & SCHAPOV, V. A. 1997. Low geothermal heat flow of the Urals fold belt—implications of low heat production, fluid circulation or paleoclimate? *Tectonophysics*, **276**, 63–85.
- KUKKONEN, I. T., KINNUNEN, K. A. & PELTONEN, P. 2003. Mantle xenoliths and thick lithosphere in the Fennoscandian Shield. *Physics and chemistry of the Earth*, **28**, 349–360.
- KUSZNIR, N. I., STOVBA, S., STEPHENSON, R. A. & POPLAVSKY, K. N. 1996. The formation of the NW Dnieper–Donets basin, 2D forward and reverse syn-rift and post-rift modeling. *Tectonophysics*, **268**, 237–255.
- KUTAS, R. I. 1979. Geothermal model of the crust of the Ukrainian Shield. In: CERMAK, V. & RYBACH, L. (eds) *Terrestrial Heat Flow in Europe*. Springer, Berlin, 269–304.
- KUTAS, R. I., TSVIASCHENKO, V. A. & KORCHAGIN, I. N. 1989. *Modelling thermal field of the continental lithosphere*. Naukova Dumka, Kiev [In Russian].
- KUZIN, A. M. 2001. [Study of the lithosphere velocity model along the URALSEIS profile using CDP seismic prospecting data.] In: MOROZOV, A. F. (ed.) *Deep structure and geodynamics of the southern Urals (the URALSEIS project)*. Ministry of Natural Resources of Russia, Tver, 106–113 [In Russian].
- KUZNIR, N. J. & PARK, R. G. 1984. Intraplate lithosphere deformation and the strength of the lithosphere. *Geophysical Journal of the Royal Astronomical Society*, **79**, 513–538.
- LEE, C. T. A. 2003. Compositional variation of density and seismic velocities in natural peridotites at STP conditions: implications for seismic imaging of compositional heterogeneities in the upper mantle. *Journal of Geophysical Research*, **108**(B9), article numbers 2441.
- LEFEVRE, L. V. & HELMBERGER, D. V. 1989. Upper mantle P-velocity structure of the Canadian Shield. *Journal of Geophysical Research*, **94**, 17749–17765.
- LENOIR, X., GARRIDO, C. J., BODINIER, J.-L. & DAUTRIA, J.-M. 2000. Contrasting lithospheric mantle domains beneath the Massif Central (France) revealed by geochemistry of peridotite xenoliths. *Earth and Planetary Science Letters*, **181**, 359–375.
- LE PICHON, X. & ALVAREZ, F. 1984. From stretching to subduction in back arc regions: dynamic considerations, *Tectonophysics*, **102**, 343–357.
- LIDER, V. A. 1976. *Quaternary Deposits of the Urals*. Nedra, Moscow, [in Russian].
- LIE, J. E., PEDERSEN, T. & HUSEBYE, E. S. 1990. Observations of seismic reflectors in the lower lithosphere beneath the Skagerrak. *Nature*, **345**, 165–168.
- LIPPITSCH, R., KISSLING, E. & ANSORGE, J. 2003. Upper mantle structure beneath the Alpine orogen from high-resolution teleseismic tomography. *Journal of Geophysical Research*, **108**(B8), 2376, DOI: 10.1029/2002JB002016.
- LIPPOLT, H. J. 1983. Distribution of volcanic activity in space and time. In: FUCHS, K., VON GEHLEN, K., MALZER, H., MURAWSKI, H., & SEMMEL, A. (eds). *Plateau Uplift—the Rhenish Shield: a Case History*. Springer, Berlin, 112–120.
- LOBKOVSKY, L. I., CLOETINGH, S., NIKISHIN, A. M., ET AL. 1996. Extensional basins of the former Soviet Union—structure, basin formation mechanisms and subsidence history. *Tectonophysics*, **266**, 251–285.
- LORENZ, V. & NICHOLAS, I. A. 1984. Plate and intraplate processes of Hercynian Europe during the Late Palaeozoic. *Tectonophysics*, **107**, 25–56.
- LUCAZEAU, F., VASSEUR, G. & BAYER, R. 1984. Interpretation of heat flow data in the French Massif Central. *Tectonophysics*, **103**, 99–119.
- LUDDEN, J. & HYNES, A. 2000. The Abitibi–Grenville Lithoprobe transect part III: introduction. *Canadian Journal of Earth Sciences*, **37**, 115–116.
- LYASHKEVITCH, Z. M. 1987. *Magmatism of the Pripyat–Dnieper–Donets Paleorift*. Naukova Dumka, Kiev [in Russian].
- MAJOROWICZ, J., CERMAK, V., SAFANDA, J., KRZYWIEC, P., WROBLEWSKA, M., GUTERCH, A. & GRAD, M. 2003. Heat flow models across the Trans-European Suture Zone in the area of the Polonaise’97 seismic experiment. *Physics and Chemistry of the Earth*, **28**, 375–391.
- MALKOVETS, V., TAYLOR, L., GRIFFIN, W., ET AL. 2003. Cratonic conditions beneath Archangelsk, Russia: garnet peridotites from the Grib kimberlite. *Proceedings of the 8th International Kimberlite Conference, Victoria, BC, Canada*, June 2003, FLA-0220.
- MASSON, F., HAUSER, F. & JACOB, A. W. B. 1999. The lithospheric trace of the Iapetus Suture in SW Ireland from teleseismic data. *Tectonophysics*, **302**, 83–98.
- MATTE, P. 1986. Tectonics and plate tectonics model for the Variscan Belt of Europe. *Tectonophysics*, **126**, 329–374.
- MATZEL, E. & GRAND, S. P. 2004. The anisotropic structure of the East European platform. *Journal of Geophysical Research*, **109**, B01302, DOI: 10.1029/2001JB000623.
- MCKERROW, W. S. & COCKS, L. R. M. 1976. Progressive faunal migration across the Iapetus Ocean. *Nature*, **263**, 304–306.
- MECHIE, J., EGORKIN, A. V., FUCHS, K., RYBERG, T., SOLODILOV, L. & WENZEL, F. 1993. P-wave mantle velocity structure beneath northern Eurasia from long-range recordings along the profile Quartz. *Physics of the Earth and Planetary Interiors*, **79**, 269–286.

- MEISSNER, R. 1996. *The continental crust: A geophysical approach*. Academic Press, London.
- MERLE, O. & MICHON, L. 2001. The formation of the West European rift: a new model as exemplified by the Massif Central area. *Bulletin de la Société Géologique de France*, **172**, 81–89.
- MICHON, L. & MERLE, O. 2005. Discussion on 'Evolution of the European Cenozoic Rift System: interaction of the Alpine and Pyrenean orogens with their foreland lithosphere'. *Tectonophysics*, **401**, 251–256.
- MIKHAILOV, V. O., TIMOSHKINA, E. P. & POLINO, R. 1999. Foredeep basins: the main features and model of formation. *Tectonophysics*, **307**, 345–359.
- MITROVICA, J. X., PYSKLYWEC, R. N., BEAUMONT, C. & RUTTY, A. 1996. The Devonian to Permian sedimentation of the Russian platform; an example of subduction-controlled long-wavelength tilting of continents. *Journal of Geodynamics*, **22**, 79–96.
- MONA LISA WORKING GROUP 1997. MONA LISA—deep seismic investigations of the lithosphere in the southeastern North Sea. *Tectonophysics*, **269**, 1–19.
- MOROZOV, A. F. (ed.) 2001. *Deep Structure and Geodynamics of the Southern Urals (the URALSEIS Project)*. Ministry of Natural Resources of Russia, Tver [in Russian].
- MOROZOVA, E. A., MOROZOV, I. B., SMITHSON, S. B. & SOLODILOV, L. 2000. Lithospheric boundaries and upper mantle heterogeneity beneath Russian Eurasia: evidence from the DSS profile Quartz. *Tectonophysics*, **329**, 333–344.
- MUELLER, S. 1989. Deep-reaching geodynamic processes in the Alps. In: COWARD, M. P., DIETRICH, D. & PARK, R. G. (eds) *Alpine Tectonics*. Geological Society, London Special Publications, **45**, 303–328.
- MUELLER, S. 1997. The lithosphere–asthenosphere system of the Alps. In: PFIFFNER, O. A., LEHNER, P., HEITZMANN, P., MUELLER, S. & STECK, A. (eds) *Deep Structure of the Swiss Alps. Results of NFP 20*. Birkhauser, Basel, 338–347.
- MULLER, B., ZOBACK, M. L., FUCHS, K. ET AL. 1992. Regional patterns of tectonic stress in Europe. *Journal of Geophysical Research*, **97** (B8), 11783–11803.
- NALIVKIN, V. D. 1976. Dynamics of the development of the Russian platform structures. *Tectonophysics*, **36**, 247–262.
- NELSON, K. D. 1992. Are crustal thickness variations in old mountain belts like the Appalachians a consequence of lithospheric delamination? *Geology*, **20**, 498–502.
- NEUGEBAUER, J. 1989. The Lapetus model—a plate tectonic concept for the Variscan belt of Europe. *Tectonophysics*, **169**(4), 229–256.
- NEUMANN, E.-R. 1994. The Oslo Rift: *P–T* relations and lithospheric structure. *Tectonophysics*, **240**, 159–172.
- NEUMANN, E.-R., OLSEN, K. H. & BALDRIDGE, W. S. 1995. The Oslo rift. In: OLSEN, K. H. (ed.) *Continental Rifts: Evolution, Structure, Tectonics*. Developments in Geotectonics, **25**, 345–374.
- NICOLAS, A., LUCAZEAU, F. & BAYER, R. 1987. Peridotite xenoliths in Massif Central basalts (France): textural and geophysical evidence for asthenospheric diapirism. In: NIXON, P. H. (ed) *Mantle Xenoliths*. Wiley, New York, 563–573.
- NIELSEN, L., THYBO, H. & SOLODILOV, L. 1999. Seismic tomographic inversion of Russian PNE data along profile Kraton. *Geophysical Research Letters*, **26**, 3413–3416.
- NIKISHIN, A. M., ZIEGLER, P. A., STEPHENSON, R. A., ET AL. 1996. Late Precambrian to Triassic history of the East European Craton: dynamics of sedimentary basin evolution. *Tectonophysics*, **268**, 23–64.
- NOLET, G. & ZIELHUIS, A. 1994. Low S velocities under the Tornquist–Teisseyre zone: evidence from water injection into the transition zone by subduction. *Journal of Geophysical Research*, **99**, 15813–15820.
- NYBLADE, A. A. & POLLACK, H. N. 1993. A global analysis of heat flow from Precambrian terrains: implications for the thermal structure of Archean and Proterozoic lithosphere. *Journal of Geophysical Research*, **98**, 12207–12218.
- OHLANDER, B., SKIOLD, T., ELMING, S. ET AL., 1993. Delineation and character of the Archean-Proterozoic boundary in northern Sweden. *Precambrian Research*, **64**, 67–84.
- OKAYA, N., FREEMAN, R., KISSLING, E. & MUELLER, S. 1996. A lithospheric cross-section through the Swiss Alps—I. Thermokinematic modelling of the Nealpine orogeny. *Geophysical Journal International*, **125**, 504–518.
- OSIPOVA, I. L., HIJELT, S.-E. & VANYAN, L. L. 1989. Source field problems in northern parts of the Baltic shield. *Physics of the Earth and Planetary Interiors*, **53**, 337–342.
- PANZA, G. F., MUELLER, S. & CALCAGNILE, G. 1986. The gross features of the lithosphere–asthenosphere system in Europe from seismic surface waves and body waves. *Pure and Applied Geophysics*, **118**, 1209–1213.
- PASCAL, C., WIJK, J. W., CLOETINGH, S. A. P. L. & DAVIES, G. R. 2002. Effect of lithosphere thickness heterogeneities in controlling rift localization: numerical modeling of the Oslo graben. *Geophysical Research Letters*, **29**(9), DOI: 10.1029/2001GL014354.
- PASQUALE, V., CABELLA, C. & VERDOYA, M. 1990. Deep temperatures and lithospheric thickness along the European Geotraverse. *Tectonophysics*, **176**, 1–11.
- PASQUALE, V., VERDOYA, M. & CHIOZZI, P. 1991. Lithospheric thermal structure in the Baltic Shield. *Geophysical Journal International*, **106**, 611–620.
- PASQUALE, V., VERDOYA, M. & CHIOZZI, P. 2001. Heat flux and seismicity in the Fennoscandian Shield. *Physics of the Earth and Planetary Interiors*, **126**, 147–162.
- PASYANOS, M. E. & WALTER, W. R. 2002. Crust and upper-mantle structure of North Africa, Europe and the Middle East from inversion of surface waves. *Geophysical Journal International*, **149**, 463–481.
- PAULSEN, H., BUKCHIN, B. G., EMELIANOV, A. P., LAZARENKO, M., MUZZERT, E., SNIEDER, R. & YANOVSKAYA, T. B. 1999. The NARS-DEEP project. *Tectonophysics*, **313**, 1–8.
- PAVLENKOVA, N. I. 1996. Crust and upper mantle structure in Northern Eurasia from seismic data. *Advances in Geophysics*, **37**, 1–133.
- PAVLENKOVA, N. I., PAVLENKOVA, G. A. & SOLODILOV, L. N. 1996. High velocities in the uppermost mantle of the Siberian craton. *Tectonophysics*, **262**, 51–65.
- PEARSON, D. G. 1999. The age of continental roots. *Lithos*, **48**, 171–194.
- PEDERSEN, T. & VAN DER BEEK, P. A. 1994. Extension and magmatism in the Oslo Graben, SE Norway: no sign of a mantle plume. *Earth and Planetary Science Letters*, **123**, 317–329.
- PELTONEN, P., HUUMA, H., TYNI, M. & SHIMIZU, N. 1999. Garnet peridotite xenoliths from kimberlites of Finland: nature of the continental mantle at an Archean craton–Proterozoic mobile belt transition. In: GURNEY, J. J., PASCOE, M. D. & RICHARDSON, S. H. (eds) *Proceedings of the 7th International Kimberlite Conference. Volume 2*, National Book Printers, Cape Town, 664–676.
- PERCHUC, E. & THYBO, H. 1996. A new model of upper mantle P-wave velocity below the Baltic Shield: indication of partial melt in the 95 to 160 km depth range. *Tectonophysics*, **253**, 227–245.
- PFIFFNER, O. A. 1990. Crustal shortening of the Alps along the EGT profile. In: FREEMAN, R., GIESE, P. & MUELLER, S. (eds) *The European Geotraverse: Integrative Studies*. ESF, Strasbourg, 255–262.
- PFIFFNER, O. A., FREI, W., FINCKH, P. & VALASEK, P. 1988. Deep seismic reflection profiling in the Swiss Alps; explosion seismology results for line NFP 20-EAST. *Geology*, **16**(11), 987–990.
- PFIFFNER, O. A., LEHNER, P., HEITZMANN, P., MUELLER, S. & STECK, A. (eds) 1997. *Deep Structure of the Swiss Alps. Results of NRP, Volume 20*. Birkhauser, Basel.
- PINET, C. & JAUPART, C. 1987. The vertical distribution of radiogenic heat production in the Precambrian crust of Norway and Sweden: geothermal implications. *Geophysical Research Letters*, **14**, 260–263.
- PIROMALLO, C. & MORELLI, A. 2003. P-wave tomography of the mantle under the Alpine–Mediterranean area. *Journal of Geophysical Research*, **108**(B2), article number 2065.
- PIROMALLO, C., VINCENT, A. P., YUEN, D. A. & MORELLI, A. 2001. Dynamics of the transition zone under Europe inferred from wavelet cross-spectra of seismic tomography. *Physics of the Earth and Planetary Interiors*, **125**, 125–139.
- PLOMEROVÁ, J., ARVIDSSON, R., BABUSKA, V., GRANET, M., KULHANEK, O., POUPINET, G. & SILENY, J. 2001. An array study of lithospheric structure across the Protogine zone, Värmland, south–central Sweden—signs of a paleocontinental collision. *Tectonophysics*, **332**, 1–21.

- POLLACK, H. N. & CHAPMAN, D. S. 1977. On the regional variation of heat flow, geotherms and lithospheric thickness. *Tectonophysics*, **38**, 279–296.
- POLLACK, H. N., HURTER, S. J. & JOHNSON, J. R. 1993. Heat flow from the Earth's interior: analysis of the global data set. *Reviews of Geophysics*, **31**, 267–280.
- POSGAY, K., BODOGY, T., HEGEDÜS, E., ET AL. 1995. Asthenospheric structure beneath a Neogene basin in SE Hungary. *Tectonophysics*, **252**, 467–484.
- POUDJOM DJOMANI, Y. H. P., FAIRHEAD, J. D. & GRIFFIN, W. L. 1999. The flexural rigidity of Fennoscandia: reflection of the tectonothermal age of the lithospheric mantle. *Earth and Planetary Science Letters*, **174**, 139–154.
- POUDJOM DJOMANI, Y. H., O'REILLY, S. Y., GRIFFIN, W. L. & MORGAN, P. 2001. The density structure of subcontinental lithosphere through time. *Earth and Planetary Science Letters*, **184**, 605–621.
- POUPINET, G., THOUVENOT, F., ZOLOTOV, E. E., MATTE, P., EGORKIN, A. V. & RACKITOV, V. A. 1997. Teleseismic tomography across the middle Urals: lithospheric trace of an ancient continental collision. *Tectonophysics*, **276**, 19–33.
- PRAUS, O., PECOVÁ, J., PETR, V., BABUŠKA, V. & PLOMEROVÁ, J. 1990. Magnetotelluric and seismological determination of lithosphere–asthenosphere transition in Central Europe. *Physics of the Earth and Planetary Interiors*, **60**, 212–228.
- PRODEHL, C., MUELLER, S. & HAAK, V. 1995. The European Cenozoic Rift System. In: OLSEN, K. H. (ed.) *Continental Rifts: Evolution, Structure, Tectonics*. Developments in Geotectonics, 25, 133–212.
- PUCHKOV, V. N. 1997. Tectonics of the Urals: modern concepts. *Geotectonics*, **31**, 294–312 [in Russian].
- PYSKLYWEC, R. N. & MITROVICICA, J. X. 1998. Mantle flow mechanisms for the large-scale subsidence of continental interiors. *Geology*, **26**, 687–690.
- RAIKES, S. A. & BONJER, K.-P. 1983. Large-scale mantle heterogeneity beneath the Rhenish massif and its vicinity from teleseismic P-residuals measurements. In: FUCHS, K., VON GEHLEN, K., MALZER, H., MURAWSKI, H. & SEMMEL, A. (eds) *Plateau Uplift—the Rhenish Shield: a Case History*. Springer, Berlin, 315–331.
- RAMBERG, I. B. 1976. Gravity interpretation of the Oslo Graben and associated igneous rocks. *Norges Geologiske Undersøkelse*, **325**, 1–194.
- RICHARDSON, S. H., HARRIS, J. W. & GURNEY, J. J. 1993. Three generations of diamonds from old continental mantle. *Nature*, **366**, 256–258.
- RITTER, J. R. R., JORDAN, M., CHRISTENSEN, U. R. & ACHAUER, U. 2001. A mantle plume below the Eifel volcanic fields, Germany. *Earth and Planetary Science Letters*, **186**(1), 7–14.
- ROBERTS, D. 2003. The Scandinavian Caledonides: event chronology, palaeogeographic settings and likely modern analogues. *Tectonophysics*, **365**, 283–299.
- RODGERS, A. & BHATTACHARYYA, J. 2001. Upper mantle shear and compressional velocity structure of the central US craton: shear wave low-velocity zone and anisotropy. *Geophysical Research Letters*, **28**, 383–386.
- ROYDEN, L., HORVATH, F. & RUMPLER, J. 1983a. Evolution of the Pannonian Basin system, 1, Tectonics. *Tectonics*, **2**, 63–90.
- ROYDEN, L., HORVATH, F., NAGYMAROSY, A. & STEGENA, L. 1983b. Evolution of the Pannonian Basin system, 2, Subsidence and thermal history. *Tectonics*, **2**, 91–137.
- RYBERG, T., WENZEL, F., MECHIE, J., EGORKIN, A., FUCHS, K. & SOLODILOV, L. 1996. Two-dimensional velocity structure beneath Northern Eurasia derived from the super long-range seismic profile Quartz. *Bulletin of the Seismological Society of America*, **86**, 857–867.
- SALNIKOV, V. E. 1984. *Geothermal Regime of the Southern Urals*. Nauka, Moscow [in Russian].
- SANDOVAL, S., KISSLING, E., ANSORGE, J. & SVEKALAPKO SEISMIC TOMOGRAPHY WORKING GROUP 2004. High-resolution body wave tomography beneath the SVEKALAPKO array—II. Anomalous upper mantle structure beneath the central Baltic shield. *Geophysical Journal International*, **157**, 200–214.
- SAVELIEVA, G. N. 1987. *Gabbro–Ultrabasite Complexes in Ophiolites of the Urals and their Analogues in the Modern Oceanic Crust*. Moscow, Nauka [in Russian].
- SAVELYEV, A. A., BERZIN, R. G., SULEIMANOV, A. K., DEGTYAREV, K. E., VOLOZH, YU. A. & ERMOLAEVA, G. M. 2001. Main features of the Phanerozoic structure along the URALSEIS profile. In: MOROZOV, A. F. (ed.) *Deep Structure and Geodynamics of the Southern Urals (the URALSEIS Project)*. Ministry of Natural Resources of Russia, Tver, 249–261 [in Russian].
- SCHMID, S. M., PFIFFNER, O. A., FROITZHEIM, N., SCHOENBORN, G. & KISSLING, E. 1996. Geophysical–geological transect and tectonic evolution of the Swiss–Italian Alps. *Tectonics*, **15**, 1036–1064.
- SCHMINCKE, H. U., LORENZ, V. & SECK, H. A. 1983. The Quaternary Eifel volcanic fields. In: FUCHS, K., VON GEHLEN, K., MALZER, H., MURAWSKI, H. & SEMMEL, A. (eds) *Plateau Uplift—the Rhenish Shield: a Case History*. Springer, Berlin, 139–151.
- SECK, H. A. & WEDEPOHL, K. H. 1983. Mantle xenoliths in the Rhenish Massif and the Northern Hessian depression. In: FUCHS, K., VON GEHLEN, K., MALZER, H., MURAWSKI, H. & SEMMEL, A. (eds) *Plateau Uplift: the Rhenish Shield: a Case History*. Springer, Berlin, 344–351.
- SENGÖR, A. M. C. & BURKE, K. 1978. Relative timing of rifting and volcanism on Earth and its tectonic implications. *Geophysical Research Letters*, **5**, 419–421.
- SENGÖR, A. M. C., NATAL'IN, B. A. & BURTMAN, V. S. 1993. Evolution of the Altaid tectonic collage and Palaeozoic crustal growth in Eurasia. *Nature*, **364**, 299–307.
- SHAPIRO, N. M. & RITZWOLLER, M. H. 2002. Monte-Carlo inversion for a global shear velocity model of the crust and upper mantle. *Geophysical Journal International*, **151**, 1–18.
- SHOMALI, Z. H. & ROBERTS, R. G. 2002. Non-linear body-wave teleseismic tomography along the TOR array. *Geophysical Journal International*, **148**, 562–574.
- SNIEDER, R. 1988. The S-velocity under Europe and the Mediterranean. In: NOLET, G. & DOST, B. (eds) *Proceedings of the 4th EGT Workshop: the Upper Mantle*. ESF, Strasbourg, 133–138.
- SNYDER, D. B. 2002. Lithospheric growth at margins of cratons. *Tectonophysics*, **355**, 7–22.
- SOBOLEV, S. V., ZEYEN, H., STOLL, G., WERLING, F., ALTHERR, R. & FUCHS, K. 1996. Upper mantle temperatures from teleseismic tomography of French Massif Central including effects of composition, mineral reactions, anharmonicity, anelasticity and partial melt. *Earth and Planetary Science Letters*, **139**, 147–164.
- SOL, S., THOMSON, C. J. & KENDALL, J. M. 2002. Seismic tomographic images of the cratonic upper mantle beneath the Western Superior Province of the Canadian Shield—a remnant Archaean slab? *Physics of the Earth and Planetary Interiors*, **134**(1–2), 53–69.
- SOURIAU, A. & GRANET, M. 1995. A tomographic study of the lithosphere beneath the Pyrenees from local and teleseismic data. *Journal of Geophysical Research*, **100**, 18117–18134.
- SOURIAU, A., CORREIG, A. M. & SOURIAU, M. 1980. Attenuation of Rayleigh wave across the volcanic area of the Massif Central, France. *Physics of the Earth and Planetary Interiors*, **23**, 62–71.
- SPAKMAN, W. 1986. The upper mantle structure in the central European–Mediterranean region. In: FREEMAN, R. & GIESE, P. (eds) *Proceedings of the 3rd EGT Workshop: the Central Segment*. ESF, Strasbourg, 215–221.
- SPAKMAN, W. 1990. The structure of the lithosphere and mantle beneath the Alps as mapped by delay time tomography. In: FREEMAN, R., GIESE, P. & MUELLER, S. (eds) *The European Geotraverse: Integrative Studies*. ESF, Strasbourg, 213–220.
- SPAKMAN, W. 1991. Delay-time tomography of the upper mantle below Europe, the Mediterranean, and Asia Minor. *Geophysical Journal International*, **107**, 309–332.
- SPERNER, B., RATSCHBACHER, L. & NEMCOK, M. 2002. Interplay between subduction retreat and lateral extrusion: tectonics of the Western Carpathians. *Tectonics*, **21**(6), 1051, DOI: 10.1029/2001TC901028.
- SRODA, P., CZUBA, W., GUTERCH, A., ET AL. 1999. P- and S-wave velocity model of the southwestern margin of the Precambrian East European Craton; POLONAISE '97, Profile P3. *Tectonophysics*, **314**, 175–192.
- STAROSTENKO, V. I., DANILENKO, V. A., VENGROVITCH, D. B., KUTAS, R. I., STOVBA, S. M., STEPHENSON, R. A. & KHARITONOV, O. M.

1999. A new geodynamical–thermal model of rift evolution, with application to the Dnieper–Donets basin, Ukraine. *Tectonophysics*, **313**, 29–40.
- STEPANYUK, L., CLAESSEON, S., BIBIKOVA, E. & BOGDANOVA, S. 1998. Sm–Nd crustal ages along the EUROBRIDGE Transect in the Western Ukrainian Shield. *Ukrainian Geophysical Journal*, **20**(4), 118–120.
- STEPHENSON, R. A. (ed.) 2004. EUROPROBE, GeoRift 3: intraplate tectonics and basin dynamics. The lithosphere of the southern Eastern European Craton and its margin. *Tectonophysics*, **381**.
- STERN, T. A. & HOLT, W. E. 1994. Platform subsidence behind an active subduction zone. *Nature*, **368**, 233–236.
- STILLE, H. 1951. Das mitteleuropäische variszische Grundgebirge im Bilde des gesamteuropäischen. *Geologisches Jahrbuch, Beihefte*, **8**.
- STOLL, G., FUCHS, K., GRANET, M., ACHAUER, U. & BAYER, R. 1994. The structure beneath Massif Central from teleseismic tomography and Bouguer gravity. *Annals of Geophysics*, **12**, c33.
- TEISSEYRE, W. 1903. *Der Paleozoische Horst von Podolien und die ihn umgehenden Senkungsfelder*. Beiträge zur Paleontologie und Geologie Österreichs–Ungarn und d. Orients, **XV**.
- THYBO, H. 1990. A seismic velocity model along the EGT profile—from the North German Basin into the Baltic Shield. In: FREEMAN, R., GIESE, P., & MULLER, S. (eds) *The European Geotraverse. Integrative Studies*. European Science Foundation, Strasbourg, 99–108.
- THYBO, H. 1997. Geophysical characteristics of the Tornquist Fan area, northwest TESZ: indication of Late Carboniferous to Early Permian dextral transtension. *Geological Magazine*, **134**, 597–606.
- THYBO, H. 2001. Crustal structure along the EGT profile across the Tornquist Fan interpreted from seismic, gravity and magnetic data. *Tectonophysics*, **334**, 155–190.
- THYBO, H. 2006. The heterogeneous Upper Mantle Low Velocity Zone. *Tectonophysics*, **416**, 53–79.
- THYBO, H. & PERCHUC, E. 1997. The seismic 8° discontinuity and partial melting in continental mantle. *Science*, **275**, 1626–1629.
- THYBO, H., PHARAOH, T. & GUTERCH, A. (eds) 1999. Geophysical investigations of the Trans-European Suture Zone. *Tectonophysics*, **314**.
- THYBO, H., PHARAOH, T. & GUTERCH, A. (eds) 2002. The Trans European Suture Zone II. *Tectonophysics*, **360**.
- THYBO, H., JANIK, T., OMELCHENKO, V. D. ET AL. 2003. Upper lithospheric seismic velocity structure across the Pripjat Trough and the Ukrainian Shield along the EUROBRIDGE'97 profile. *Tectonophysics*, **371**, 41–79.
- TORNQUIST, A. J. H. 1908. *Die Feststellung des Südwestrandes des Baltisch Russischen Schildes*. Schriften der Physikalisch-Ökonomische Gesellschaft zu Königsberg, **XLIX**.
- TRANSALP WORKING GROUP 2001. European orogenic processes research transects the Eastern Alps. *EOS Transactions, American Geophysical Union*, **82**(40), 453, 460–461.
- TRANSALP WORKING GROUP 2002. First deep seismic reflection images of the Eastern Alps reveal giant crustal wedges and transcrustal ramps. *Geophysical Research Letters*, **29**(10), DOI: 10.1029/2002GRL014911.
- VACHER, P. & SOURIAU, A. 2001. A three-dimensional model of the Pyrenean deep structure based on gravity modelling, seismic images and petrological constraints. *Geophysical Journal International*, **145**, 460–470.
- VAN DER VELDEN, A. J. & COOK, F. A. 1999. Proterozoic and Cenozoic subduction complexes: A comparison of geometric features. *Tectonics*, **18**, 575–581.
- VAN DER VOO, R., SPAKMAN, W. & BIJWAARD, H. 1999. Mesozoic subducted slabs under Siberia. *Nature*, **397**, 246–249.
- VEJBAEK, O. V. 1990. The Horn Graben, and its relationship to the Oslo Graben and the Danish Basin. *Tectonophysics*, **178**, 29–49.
- VILLASEÑOR, A., RITZWOLLER, M. H., LEVSHIN, A. L., BARMIN, M. P., ENGD AHL, E. R., SPAKMAN, W. & TRAMPERT, J. 2001. Shear velocity structure of central Eurasia from inversion of surface wave velocities. *Physics of the Earth and Planetary Interiors*, **123**, 169–184.
- VINNIK, L. P. & RYABOY, V. Z. 1981. Deep structure of the East European platform according to seismic data. *Physics of the Earth and Planetary Interiors*, **25**, 27–37.
- WALDHAUSER, F. E., KISSLING, E., ANSORGE, J. & MUELLER, S. 1998. Three-dimensional interface modelling with two-dimensional seismic data: the Alpine crust–mantle boundary. *Geophysical Journal International*, **135**, 264–278.
- WERLING, F. & ALTHERR, R. 1997. Thermal evolution of the lithosphere beneath the French Massif Central as deduced from geothermobarometry on mantle xenoliths. *Tectonophysics*, **275**, 119–141.
- WERNER, D. 1981. A geothermic method for the reconstruction of the uplift history of a mountain range, applied to the Central Alps. *Geologische Rundschau*, **70**, 296–301.
- WILSON, M. & LYASHKEVITCH, Z. 1996. Magmatic evolution and the geodynamics of rifting in the Pripjat–Dnieper–Donets rift. *Tectonophysics*, **268**, 65–82.
- WILSON, M., NEUMANN, E.-R., DAVIES, G. R., TIMMERMAN, M. J., HEEREMANS, M., & LARSEN, B. T. (eds) 2004. *Permo-Carboniferous Magmatism and Rifting in Europe*. Geological Society, London, Special Publications, **223**.
- WORTEL, R. & SPAKMAN, W. 2000. Subduction and slab detachment in the Mediterranean–Carpathian region. *Science*, **290**, 1910–1917.
- YE, S., ANSORGE, J., KISSLING, E., ET AL. 1995. Crustal structure beneath the eastern Swiss Alps derived from seismic-refraction data. *Tectonophysics*, **242**(3–4), 199–221.
- YEGOROVA, T. P. & STAROSTENKO, V. I. 2002. Lithosphere structure of Europe and Northern Atlantic from regional three-dimensional gravity modeling. *Geophysical Journal International*, **151**, 11–31.
- YEGOROVA, T. P., STAROSTENKO, V. I. & KOZLENKO, V. G. 1998. Large-scale gravity analysis of the inhomogeneities in the European–Mediterranean upper mantle. *Pure and Applied Geophysics*, **151**, 549–561.
- YEGOROVA, T. P., STEPHENSON, R. A., KOZLENKO, V. G., STAROSTENKO, V. I. & LEGOSTAEVA, O. V. 1999. 3-D gravity analysis of the Dniepr–Donets Basin and Donbas Foldbelt, Ukraine. *Tectonophysics*, **313**, 41–58.
- ZEYEN, H. & FERNANDEZ, M. 1994. Integrated lithospheric modelling combining thermal, gravity, and local isostasy analysis: application to the NE Spanish Geotranssect *Journal of Geophysical Research*, **99**, 18089–18102.
- ZEYEN, H., DEREROVA, J. & BIELIK, M. 2002. Determination of the continental lithospheric thermal structure in the Western Carpathians: integrated modelling of surface heat flow, gravity anomalies and topography. *Physics of the Earth and Planetary Interiors*, **134**, 89–104.
- ZIEGLER, P. 1986. Geodynamic model for the Palaeozoic crustal consolidation of western and central Europe. *Tectonophysics*, **126**, 303–328.
- ZIEGLER, P. A. 1992. European Cenozoic Rift System. *Tectonophysics*, **208**, 91–111.
- ZIEGLER, P. A. & CLOETINGH, S. 2004. Dynamic processes controlling evolution of rifted basins. *Earth-Science Reviews*, **64**, 1–50.
- ZIEGLER, P. A., SCHUMACHER, M. E., DEZES, P., VAN WEES, J.-D. & CLOETINGH, S. 2004. Post-Variscan evolution of the lithosphere in the Rhine Graben area: constraints from subsidence modeling. In: WILSON, M. (ed.) *Permo-Carboniferous Magmatism and Rifting in Europe*. Geological Society, London, Special Publications, **223**, 289–317.
- ZIELHUIS, A. & NOLET, G. 1994. Deep seismic expression of an ancient plate boundary in Europe. *Science*, **265**(5168), 79–81.
- ZONENSHAIN, L. P., KUZMIN, M. I. & NATAPOV, L. M. (eds) 1990. *Geology of the USSR; a plate-tectonic synthesis*. American Geophysical Union Geodynamics Series, **21**.

